

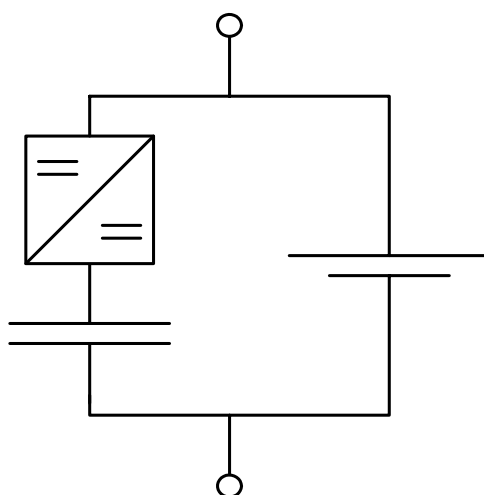
**CHALMERS**

**VOLVO**

# Alternative Energy Storage System for Hybrid Electric Vehicles

*-Master Thesis in Electrical Engineering-*

October 2003



Tobias Andersson  
Jens Groot

ISSN 1401-6184  
Master of Science Thesis No. 76E



DEPARTMENT OF ELECTRIC POWER ENGINEERING  
SCHOOL OF ELECTRICAL ENGINEERING  
CHALMERS UNIVERSITY OF TECHNOLOGY  
GÖTEBORG, SWEDEN

Copyright © 2003 Tobias Andersson and Jens Groot

**Title**

Alternative Energy Storage System for Hybrid Electric Vehicles

**Titel**

Alternativt energilager för elhybridfordon

**Author / Författare**

Andersson Tobias, Groot Jens

**Publisher / Utgivare**

Department of Electric Power Engineering  
Chalmers University of Technology  
412 58 Göteborg, Sweden

**ISSN**

1401-6184

**M.Sc. Thesis No. / Examensarbete nr.**

76E

**Subject / Ämne**

Power Electronics / Kraftelektronik

**Examiner / Examinator**

Thiringer Torbjörn

**Supervisors /Handledare**

Berg Helena, Lindström Joachim (Volvo Technology Corporation)

**Date / Datum**

2003-10-17

## **Abstract**

In this thesis an alternative energy storage system in the drive train of a hybrid electric vehicle is investigated. In particular, it concentrates on the potential reduction of the stresses of the battery when electrochemical capacitors, a.k.a supercapacitors, are added as a high power energy storage. The energy storage system is described and a simplified drive train is simulated in the simulation software *MATLAB*<sup>®</sup>/*SIMULINK*<sup>®</sup>. Different control strategies are tested and an estimation of the performance is given. With the simulation results at hand, a downscaled HEV drive train consisting of NiMH batteries, electrochemical capacitors, a DC/DC converter and an external load, is built and tested.

A comparison between simulated and experimental results is made, in terms of estimated battery stresses and efficiency. The results show a significantly reduction in battery stresses and a good agreement between the models used in simulations and the laboratory system. To further investigate the potential of a battery-electrochemical capacitor system, a full-scale system for a city bus is dimensioned and simulated. This simulation shows that the total weight of the energy storage system could be reduced significantly when batteries are combined with a bank of electrochemical capacitors. Moreover, an increased durability of the battery would be expected by this alternative energy storage system.

Key words: Electrochemical Supercapacitor, EDLC, Ultracapacitor, Hybrid Electric Vehicle, Energy Storage.

## Sammanfattning

I detta examensarbete har ett alternativt energilagret för den elektriska drivlinan i elhybridfordon undersökts. Projektet fokuserar på möjligheten att reducera slitaget på batteriet m.h.a. elektrokemiska kondensatorer, även kallade superkondensatorer. Som ett första steg beskrivs komponenterna i energilagret och en förenklad drivlina simuleras i simuleringsprogramvaran *MATLAB*<sup>®</sup>/*SIMULINK*<sup>®</sup>. Olika kontrollstrategier för energilagret utvecklas och systemprestandan utvärderas. Med utgångspunkt från simuleringsresultaten byggs och testas därefter ett nedskalat system bestående av NiMH-batterier, elektrokemiska kondensatorer, en DC/DC-omvandlare och en extern last.

En jämförelse mellan simulerade och experimentella resultat görs med avseende på batterislitage och verkningsgrad. Resultaten visar en markant minskning av batterislitaget och en god överensstämmelse mellan simuleringar och testresultat.

För att ytterligare undersöka möjligheterna med detta alternativa energilagret dimensioneras och simuleras ett förenklat fullskalesystem för en stadsbuss. Denna simulering visar att den totala vikten för energilagret kan reduceras betydligt när batterier kombineras med elektrokemiska kondensatorer. Dessutom torde livslängden på batteriet förlängas avsevärt i detta alternativa energilagarsystem.

*Nyckelord: Elektrokemisk superkondensator, EDLC, ultrakondensator, elhybridfordon, energilagret.*

## **Acknowledgements**

We would like to thank our supervisors Dr. Helena Berg and Lic. Eng. Joachim Lindström for their valuable support during our work. We would also thank the rest of the personal in group 6120 at Volvo Technology Corporation for their support and for taking the time to answer our questions.

At Chalmers University of Technology, we would like to thank our supervisor Assoc. Prof. Torbjörn Thiringer for continuous support during our work.

Volvo Technology Corporation is gratefully acknowledged for the financial support.

## List of Symbols

$\rho$	Air density	[kg m <sup>-3</sup> ]
$\tau$	Filter constant	[s]
$\varepsilon$	Permittivity	[A s V <sup>-1</sup> m <sup>-1</sup> ]
$A$	Area	[m <sup>2</sup> ]
$A_f$	Vehicle frontal area	[m <sup>2</sup> ]
$C$	Capacitance	[F]
$C_{Bat}$	Capacity of battery	[Ah]
$C_d$	Coefficient of aerodynamic drag	-
$C_r$	Coefficient of rolling resistance	-
$D$	Distance	[m]
$E$	Energy	[Wh]
$E_{Battery}$	Battery energy	[Wh]
$E_{EC}$	EC energy	[Wh]
$E_{EC\ reduction}$	EC reduction energy	[Wh]
$E_{Load}$	Load energy	[Wh]
$G$	Acceleration of gravity	[m s <sup>-2</sup> ]
$H_{LP}$	Filter function	-
$I$	Current	[A]
$I_{Battery, final}$	Final battery current	[A]
$I_{Battery, mac}$	Maximum battery current	[A]
$I_{EC}$	Current from EC	[A]
$M$	Vehicle mass	[kg]
$P$	Power	[W]
$P_\tau$	Peak power during acceleration	[W]
$P_a$	Acceleration power	[W]
$P_{Battery}$	Battery power	[W]
$P_{EC\_input}$	Input power in EC	[W]
$P_{EC\_output}$	Output power in EC	[W]
$P_{Input}$	Input power	[W]
$P_{Load}$	Load power	[W]
$P_{Loss}$	Loss power	[W]
$P_{Output}$	Output power	[W]
$R$	Resistance	[ $\Omega$ ]
$R_{Battery}$	Battery internal series resistance	[ $\Omega$ ]
$R_{Loss}$	Loss resistance	[ $\Omega$ ]
$T$	Time	[s]
$T_{Battery\ cycle}$	Cycle time of battery	[s]
$t_m$	Time to reach maximum speed	[s]
$U$	Voltage	[V]
$U_{Battery}$	Battery voltage	[V]
$V$	Vehicle speed	[km h <sup>-1</sup> ]
$V_{Drop}$	Voltage drop in the IGBT's	[V]
$v_m$	Maximum speed	[km h <sup>-1</sup> ]
$V_{OC}$	Battery open circuit voltage	[V]

## Abbreviations

DC	Direct Current
EC	Electrochemical Capacitor
EDLC	Electrochemical Double Layer Capacitor
EV	Electric Vehicle
FC	Fuel Cell
HEV	Hybrid Electric Vehicle
ICE	Internal Combustion Engine
IGBT	Insulated Gate Bipolar Transistor
NiMH	Nickel Metal Hydride
PI	Proportional-Integral
PWM	Pulse Width Modulation
RMS	Root Mean Square
RWV	Rated Working Voltage
SOC	State of Charge
VOC	Open Circuit Voltage



# Table of Contents

<b>1. INTRODUCTION .....</b>	<b>1</b>
1.1 PURPOSE AND METHOD.....	1
1.2 LIMITATIONS.....	2
<b>2. DRIVE TRAIN OF A HYBRID ELECTRIC VEHICLE .....</b>	<b>3</b>
2.1 GENERAL DESIGN OF A SERIES HYBRID ELECTRIC VEHICLE.....	3
2.2 ENERGY STORAGE: BATTERY–EC SYSTEM .....	4
<b>3. SYSTEM DIMENSIONING.....</b>	<b>7</b>
3.1 GENERAL DIMENSIONING STRATEGY.....	7
3.2 DIMENSIONING EXAMPLE: A CITY BUS .....	7
<b>4. MODELLING OF THE SYSTEM.....</b>	<b>13</b>
4.1 ELECTROCHEMICAL CAPACITORS .....	13
4.2 BATTERY .....	13
4.3 DC/DC CONVERTER.....	14
4.4 LOAD .....	14
<b>5. SIMULATIONS.....</b>	<b>15</b>
5.1 SYSTEM PERFORMANCE .....	15
5.2 CONTROL STRATEGIES AND METHODS .....	16
5.3 SIMULATION RESULTS .....	21
5.4 SIMULATION SUMMARY .....	27
<b>6. EXPERIMENTAL LABORATORY SET-UP .....</b>	<b>29</b>
6.1 CONTROL AND MEASUREMENT SYSTEM .....	29
6.2 CALIBRATION.....	30
6.3 CONTROL OF THE DC/DC CONVERTER.....	30
<b>7. EXPERIMENTAL RESULTS.....</b>	<b>31</b>
7.1 VERIFICATION OF MODELS .....	31
7.2 SIZE I SYSTEM .....	31
7.3 SIZE II SYSTEM .....	32
7.4 DISCUSSION .....	34
<b>8. CONCLUSIONS AND SUGGESTIONS TO FUTURE WORK.....</b>	<b>37</b>
<b>9. REFERENCES.....</b>	<b>39</b>
<b>APPENDIX A MATLAB®/SIMULINK® MODELS AND MATLAB® FILES</b>	
<b>APPENDIX B RESULTS FROM SIMULATIONS AND EXPERIMENTS</b>	
<b>APPENDIX C ECE15-L POWER PROFILE AND BUS TEST CYCLE</b>	
<b>APPENDIX D OPTOCOUPLING CARD, LEM MODULES AND CALIBRATION</b>	
<b>APPENDIX E SPECIFICATIONS</b>	
<b>APPENDIX F PERFORMANCE PARAMETERS</b>	



## 1. Introduction

The motorised vehicle is more than a hundred years old and has been continuously developed. Today, consumers are more considering the environmental effects of vehicular traffic, but also demands economic and user-friendly solutions. Due to this, the technological development in the area is aiming towards environmental friendly alternatives to the present technology, with preserved or enhanced performance.

One interesting approach is to exchange the conventional mechanical drive train with an electrical one. The benefit above all of this system is that the overall losses from the on board energy source to traction are reduced. Furthermore, there is a wide range of options to produce the electrical power needed, and the braking energy can be converted back into electrical energy (regenerative braking).

Today, any vehicle with an electric drive train is either an all-electric vehicle (EV), or a hybrid electric vehicle (HEV). An EV has no internal combustion engine (ICE), but instead a large battery, charged from an external source when the vehicle is at rest. The HEV has a smaller battery, charged from either a generator driven by an on board ICE, or a fuel cell (FC).

Both the EV and the HEV need an energy source that can supply both the required energy and power for sufficient radius of action and acceleration. The two types of energy sources most likely to be used in an EV or HEV are conventional electrochemical batteries, like lead-acid or NiMH, or electrochemical capacitors (EC).

Unfortunately, energy density [Wh/kg] and power density [W/kg] of conventional batteries are often dependent on each other. Batteries with high energy density have poor power density and vice versa. In addition, large charge and discharge currents cause losses and heating of the battery, which significantly decreases the battery lifetime. For these reasons, batteries must be oversized in terms of energy capacity to meet the power requirements of an HEV.

EC's, also called *supercapacitors* or *ultracapacitors*, have extremely high capacitance compared to conventional capacitors (kF compared to  $\mu$ F). In contrast to batteries, EC's have high power density and poor energy density. Furthermore, they have almost negligible losses and a comparably long lifetime. Consequently, a combination of these two types of energy storage will in theory yield an equivalent energy storage system with both high energy density and power density, where energy is stored in the battery and peak power is supplied by the EC's.

However, since the charge and discharge profiles of the batteries and EC's are fundamentally different, they cannot be combined without a DC/DC converter. Adding this component also implicate the possibility to separately control the power flow between load, battery and EC's. With this ability, the high currents needed during acceleration and braking can be supplied / absorbed by the EC's, potentially increasing the battery lifetime. Moreover, with the EC's supplying peak power, batteries with lower power density and higher energy density can be used, thus reducing the total weight.

This battery-EC system has been proposed already in the early nineties [1], but has not been put into production due to the complexity and, onto now, expensive design. Development has, however, accelerated during the past decade, yielding better performance and lower prices [2].

### 1.1 Purpose and Method

The aim of this master thesis is to investigate the battery-EC system in an HEV drive train. In particular, it concentrates on the potential reduction of the stresses of the battery. As a first step, the system is described and a simplified drive train is simulated in the simulation software MATLAB<sup>®</sup>/SIMULINK<sup>®</sup>. Different control strategies are tested and an estimation of the performance is given. With the simulation results at hand, a downscaled HEV drive train consisting of NiMH batteries, EC's, DC/DC-converter and an external load are built and tested. Finally, a comparison between simulated and experimental results is made, in terms of estimated battery stresses and efficiency.

## **1.2 Limitations**

Charging of the battery can be made from different sources, such as an ICE or an FC. None of these sources can, however, absorb energy and are therefore not used during regenerative braking. In comparison with the electric drive train, they are slow systems and not able to adjust to the fast changing characteristics of the load (the electric traction motor). Therefore, the utilisation and control of these slow energy sources cannot reduce stresses in the battery significantly. Consequently, this project does not include the ICE or FC in simulations, calculations or experimental set-up.

Impacts of different environmental conditions like temperature, humidity, mechanical stresses are not included in this work. Moreover, the results are obtained from the use of equipment (battery, EC's and DC/DC-converter) at hand in the laboratory, not primarily used in this project. Consequently, large differences and / or improvements are likely if the system is evaluated with another, more optimised set of test equipment.

## 2. Drive Train of a Hybrid Electric Vehicle

As a first step in the investigation of the battery-EC system, the drive train of an HEV is simplified in order to find appropriate models of each component. In general, there are two main design topologies of an HEV, the *series design* and *parallel design*.

The *parallel hybrid vehicle* has an ICE and an electric motor arranged in parallel. The vehicle can be directly driven from the ICE or the electric motor, or both at the same time. When not used as a traction motor, the ICE can charge the battery via a generator. Acceleration performance is advantageous with both the ICE and electric motor driving the vehicle, however the design with to separate drive trains is complicated and expensive.

In the *series hybrid vehicle*, the traction motor is electric, with its electrical energy supplied from both a battery and an ICE driven generator or an FC. Using the series hybrid design, the ICE or FC can be kept at their optimum driving conditions and only operating when the battery needs to be charged. Moreover, when an ICE is used it can be made much smaller than a conventional traction ICE, since the battery supplies the peak power needed during acceleration. On the other hand, containing several energy conversions, the overall efficiency of the series HEV might be low compared to that of a parallel design HEV.

### 2.1 General Design of a Series Hybrid Electric Vehicle

In this project, the drive train of a series HEV presented in Figure 2.1 is simplified and modelled at several levels in MATLAB<sup>®</sup>/SIMULINK<sup>®</sup>. With the focus set on the energy storage configuration and its performance, large simplifications are made. This section briefly describes each component and their operation from a general point of view.

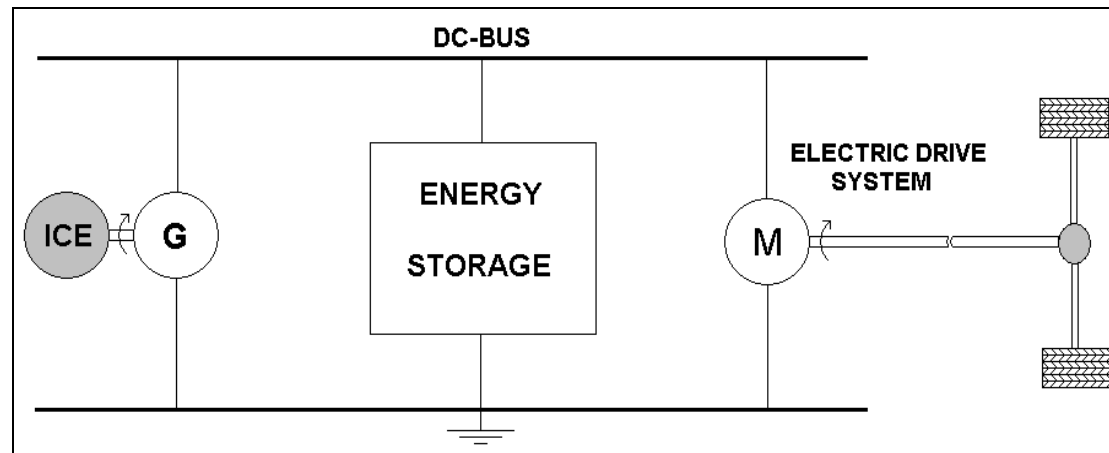


Figure 2.1 Model of a series HEV drive train.

#### ICE and Generator

The ICE supplies the steady-state energy when the HEV is driven at high constant speed and charges the energy storage when needed. This component is designed to run at its optimum speed only, thus increasing the total efficiency and reducing fuel consumption. Since it is dimensioned for constant speed and charge of the energy storage, its maximum power rating is significantly lower than that of the traction motor. Lower maximum power rating decreases the physical size and weight of the ICE. In addition, the ICE can be placed virtually anywhere within the vehicle since there is no mechanical connection between the ICE and the traction wheels. Naturally, the ICE could also be substituted by an FC.

### Energy Storage

In contrast to the ICE, the energy storage supplies the power needed during relatively short periods, for example accelerations and when driven in urban traffic. The total time of each charge / discharge cycle is typically in the order of minutes. The size and type of energy storage is determined by the specific requirements on peak power, energy capacity, maximum weight etc. This particular dimensioning is described in chapter 3. In a vast majority of applications, the energy storage consists of battery, or a battery and a DC/DC converter to boost and / or stabilise the voltage.

### Electric Drive System

This component consists of a DC/AC converter and a traction motor. Dependent directly of the demanded power during acceleration, hill climbing, constant speed, braking etc., this system absorbs from or delivers energy to the DC-bus. Thus, it can be modelled as a time dependent power source, as will be described in detail in section 4.4.

## 2.2 Energy Storage: Battery-EC System

In this project, a system consisting of a battery and EC's is investigated, see Figure 2.2. Naturally, each of these components must be carefully dimensioned and controlled in order to obtain the desired system. The dimensioning is a delicate task, determined from several vehicle specification and drive-cycle data. The general dimensioning strategy and a simplified example is presented in chapter 3.

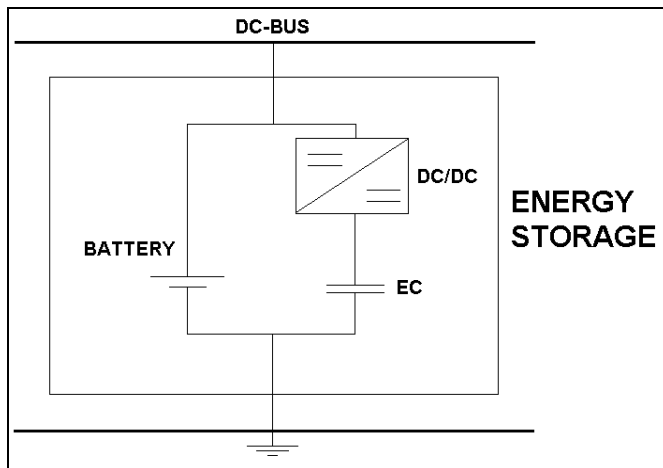


Figure 2.2 Battery-EC energy storage system.

### Battery

The battery is the main energy storage for electrical energy and is directly connected to the DC-bus. Consequently, charge and discharge is directly dependent on the DC-bus voltage and the *open circuit voltage* (VOC) of the battery. The VOC depends on several conditions, including battery type, number of cells, temperature and *state of charge* (SOC). During normal operating conditions, the variation in VOC is rather small. The SOC is a parameter describing the relative amount of stored energy in the battery. In other words, a SOC equal to one corresponds to a fully charged battery and a SOC equal to zero a fully discharged battery. Battery capacity is often measured in  $C_{Bat}$  [Ah].

### DC/DC Converter

As mentioned earlier, a DC/DC converter is necessary to connect the EC's to the DC-bus and to control the power flow between the battery and the EC's. Ideally, the DC/DC converter transfers electric power between two sources having different voltages. Unfortunately, it possesses losses and restrictions on voltages and currents. These losses affect the overall efficiency of the system, and require a proper cooling system.

### Electrochemical Capacitor

The peak power needed for acceleration and produced during regenerative braking is delivered / absorbed by the EC's, connected via the DC/DC converter to the DC-bus. In other words, the EC is used as temporary energy storage for short intervals of large power. The EC's consist of a large number of series connected elements, since the voltage of each unit is rather low, but can in most aspects be treated as one equivalent, called "EC bank". The capacitance of each unit is in the order of kF.

Like a conventional capacitor, the capacitance of an electrochemical capacitor is described by Equation 2.1. In electrochemical capacitors, the distance between the two electrodes is made very small, which means that the area per volume becomes very high. In addition, the effective area of the electrodes is made very large using porous materials. In theory, the maximum capacitance of this type of capacitors is between 10 to 100 F/g of active material [3].

**Equation 2.1** 
$$C = \frac{\epsilon A}{d}$$

One way to achieve this is to use activated porous carbon between the electrodes. In this way, the distance between the electrode and the carbon is approximately 5Å [3]. Having a carbon layer between the electrodes results in an extra layer, acting as a pseudo electrode. Therefore, this particular type of electrochemical capacitor is called electrochemical double layer capacitor (EDLC). In this project however, a general type of electrochemical capacitor is treated (EC).

At laboratory conditions, the EC can be cycled up to 10<sup>6</sup> times, which compared to batteries is an extremely high value.

As a direct consequence of the small distance between the electrodes, the maximum working voltage of an EC is typically in the range of 2-2.7 Volt. However, the drive train of an HEV is designed to work at much higher voltages (several hundred volts) to avoid high currents and the associated resistive losses. In addition, the efficiency of a DC/DC converter is poor when the voltage is far below its rated value. Owing to these facts, any real HEV drive train designed to use EC's, utilises a bank of capacitors connected in series.

On the other hand, energy and charge transferred to such systems will not be evenly distributed to the capacitors due to small differences in component parameters. When working with high power applications, this phenomenon might cause severe damage to elements exposed to overvoltages. There are several solutions to the problem [4]. The simplest one, passive balancing, is used in this project: a resistance in the order of 1/10 –1/100 of the parallel resistance is connected in parallel with each capacitor, forming a voltage divider to distribute the charge evenly to the capacitors. This method suffers from losses and fast self-discharge, but these can be neglected in this particular case. Other methods, such as different types of active balancing, are not included or presented in this work.



### 3. System Dimensioning

In order to optimise the overall performance of the energy storage system, each component should be optimised. Therefore, the battery-EC system should be optimised to meet the specifications of energy capacity and power rating with minimal weight, volume and cost.

#### 3.1 General Dimensioning Strategy

Generally, to dimension an energy storage system, a power profile for a typical driving cycle is required (see Appendix C). With such a profile at hand, the maximum power and energy that the system should be able to deliver can be calculated.

The ICE must be able to deliver enough energy to satisfy the maximum continuous demand of the vehicle, depending on speed and transport capacity etc. The ICE must also be able to efficiently charge the battery whenever needed.

During urban driving, it is desirable to drive short distances on battery only. In such cases, the battery should deliver the maximum steady-state power required, assuming that the EC's supply the energy and power needed during acceleration. This maximum specific power that is required for urban driving, is obtained from the typical driving cycle used (see Appendix C).

Moreover, if the ICE is assumed to have a relatively short start-up time, it might be possible to exclude the conventional battery from the energy storage system. In that case, the EC's are dimensioned to deliver the maximum energy and power required during acceleration from zero to maximum speed. This implies that the all-electric driving time becomes very short compared to a energy storage system containing batteries.

The energy and power demands of the EC's depend on the control strategy. This particular issue is treated in section 5.2. One general design rule and first assumption might however be that the EC's should be able to deliver the peak power and energy required during the highest acceleration.

The voltage levels of the battery and the EC's depend on the maximum rated current of the components in the system and the peak power needed specified by Equation 3.1. Generally, the voltage of each component should be as high as possible to reduce currents and the ohmic losses associated to them, see Equation 3.2.

**Equation 3.1**  $P = U \cdot I$

**Equation 3.2**  $P_{Loss} = R_{Loss} \cdot I^2$

The DC/DC converter should be designed to minimise losses, weight and volume. Current ripple can on the other hand be allowed to be rather high due to the capacitive nature of the system.

#### 3.2 Dimensioning Example: a City Bus

Since the battery stresses are difficult to evaluate, the dimensioning strategy in this example focuses on the weight and cost of a battery-EC system compared to that of a pure battery system. The performance of each system is analysed during the same conditions.

The instantaneous power,  $P_a$ , required for a general vehicle can be calculated using Equation 3.3 [5].

**Equation 3.3**  $P_a = Mv \frac{dv}{dt} + \frac{1}{2} \rho A_f C_d v^3 + MgvC_r$

By integrating this expression during a typical acceleration, and then dividing by specified acceleration time, the average power needed during acceleration is obtained (Equation 3.4). In this calculation, the acceleration is assumed to be constant.

$$\text{Equation 3.4} \quad P_{\tau} = \frac{M}{t_m} \left[ \frac{1}{2} v_m^2 + C_r g \int_0^{t_m} v dt \right] + \frac{\rho A_f C_d}{2 t_m} \int_0^{t_m} v^3 dt$$

Since the acceleration is assumed to be constant, the velocity as a function of time, can be calculated according to Equation 3.5, where  $x$  is approximately equal to 0.5 [5].

$$\text{Equation 3.5} \quad v = v_m \left( \frac{t}{t_m} \right)^x$$

The required energy  $E$  during acceleration is calculated (Equation 3.6), and the total capacitance of the EC's is given by Equation 3.7.

$$\text{Equation 3.6} \quad E = \int P dt$$

$$\text{Equation 3.7} \quad E_{EC} = \frac{1}{2} C \cdot U^2$$

The vehicle parameters used in the calculations above are presented in Appendix E.

These equations and the assumption that the total efficiency of the electric machine is 90 %, results in a peak power demand during acceleration of approximately 220 kW and an acceleration energy of 1.8 kWh. Auxiliary devices like fans, AC and headlights, are not included in these figures. According to Medin [7], auxiliary devices should be added as a constant load of approximately 13 kW.

### 3.2.1 Battery Dimensioning

Battery dimensioning is a delicate task since the maximum discharge current the batteries could deliver without being damaged is not well defined. According to the manufacturer of the batteries used in experiments, the maximum discharge current should be  $5C_{Bat}$ , where  $C_{Bat}$  is the battery capacity in Ah. Since this rather high discharge current generates significant losses, a calculation with maximum discharge current equal to  $2C_{Bat}$  is performed as well.

According to Equation 3.3 and the vehicle parameters in Appendix E, the constant power needed for a city bus at the speed of 90 km/h is 44 kW. Assuming an electrical machine efficiency of 90 %, and an auxiliary power of 13 kW, the constant load power to be delivered by the battery is approximately 60 kW.

The corresponding number of battery cells is calculated from Equation 3.8, where the battery is modelled as a *Thevenin equivalent* (see section 4.2). Using the battery parameters of the NiMH battery type used in the laboratory tests, the battery VOC is approximately 260 V, which corresponds to 210 series connected cells (Maximum discharge current equal to  $2C_{Bat}$  yields  $V_{OC} = 550$  V and 440 cells). In comparison, an energy storage system consisting of a battery alone should according to the same calculation method consist of approximately 770 battery cells (Maximum discharge current equal to  $2C_{Bat}$  yields 1620 cells).

$$\text{Equation 3.8} \quad P_{Battery, \max} = V_{Battery} \cdot I_{Battery, \max} = (V_{oc} - R_{Battery} \cdot I_{Battery, \max}) \cdot I_{Battery}$$

Since the DC/DC converter requires that the DC bus voltage must be higher than the EC voltage, either a DC/DC converter between the battery and the DC bus is needed, or the battery voltage has to be higher than the EC maximum voltage. In this case, it is necessary to have a DC/DC converter between the battery and the DC bus. This DC/DC converter could however be rated lower than the one between the EC and the DC-bus, since it only delivers continuous power.

One way to further reduce the stresses of the battery is to limit the variation of SOC during each driving cycle. If it is assumed that the SOC varies  $\pm 10\%$ , there is enough energy in the battery for the vehicle to drive at maximum speed for approximately 3 minutes according to Equation 3.9.

**Equation 3.9** 
$$T_{Battery\ cycle} = \frac{E_{Battery} \cdot \Delta SOC}{P_{Battery}}$$

### 3.2.2 EC Dimensioning

In order to dimension the EC-bank, the limits of the DC/DC converter must be considered. The current limit of the DC/DC converter yields, according to Equation 3.1, the minimum voltage for the EC's to deliver the required power. In this example, the DC/DC converter is assumed to have the limit of 850 A, which means that the minimum voltage over the EC's,  $U_{cap,min}$ , should not be below 260 V (assuming rated power output).

To calculate the possible energy supplied from the EC's having minimum voltage,  $U_{cap,min}$ , left in the EC bank, Equation 3.10 is used. The parameter  $x$  is the number of series connected EC's in the bank and  $C$  is the capacitance per EC.

**Equation 3.10** 
$$E_{EC} = \frac{1}{2} \frac{C}{x} (U_{cap,max}^2 - U_{cap,min}^2)$$

Solving Equation 3.10,  $x$  is approximately equal to 387 elements. From this calculation, the maximum voltage over the EC's,  $U_{cap,max}$ , becomes 1043 V. However, this equations does not consider the control strategy for controlling the power flow in the system. Using a low pass filter control strategy (see section 5.2), the number of elements could be reduced.

Using the low pass filter control strategy, the required power from the EC's is decreasing with time, which also decreases the minimum allowed EC voltage. Equation 3.11 gives the battery power at  $t$  seconds during a step in load power. The magnitude of the filter function  $H_{LP}$  is equal to the relative, possible reduction of EC power (see section 5.2).

**Equation 3.11** 
$$P_{Battery} = P_{Load} \cdot H_{LP} = P_{Load} \left( 1 - e^{-\frac{t}{\tau}} \right)$$

The ideal filter constant can be obtained from Equation 3.12, where the final battery current,  $I_{Battery, final}$  is equal to  $I_{Battery, max}$ . Using the values of load power and battery parameters calculated above, a filter constant  $\tau$  of approximately 80 s is obtained. This calculation is merely a rough approximation and does not include losses etc.

**Equation 3.12**

$$I_{Battery, final} = I_{Load} \cdot \left( 1 - e^{-\frac{30}{\tau}} \right) \approx \frac{P_{Load}}{U_{Battery}} \cdot \left( 1 - e^{-\frac{30}{\tau}} \right) \approx \frac{P_{Load}}{V_{OC} - \frac{I_{Battery, final}}{2} \cdot R_{Battery}} \cdot \left( 1 - e^{-\frac{30}{\tau}} \right)$$

Integrating the battery power function in Equation 3.11 from zero to  $T$ , where  $T$  is the time required to accelerate the vehicle and  $\tau$  is the filter constant, and dividing the result with the total load energy (Equation 3.13 and Equation 3.14), the relative reduction in total EC energy is given.

$$\text{Equation 3.13} \quad E_{\text{Battery}} = P_{\text{Load}} \int_0^T 1 - e^{-\frac{t}{\tau}} dt = P_{\text{Load}} \left( T + \tau e^{-\frac{T}{\tau}} - \tau \right)$$

$$\text{Equation 3.14} \quad E_{\text{EC Reduction}} = 1 - \frac{E_{\text{Battery}}}{E_{\text{Total}}} = 1 - \frac{T + \tau e^{-\frac{T}{\tau}} - \tau}{T}$$

When applying a filter constant,  $\tau$ , of 80 s and  $T=30$  s, the number of EC's required decrease from 380 to 320. Since all system losses, for example in the DC/DC converter, is neglected in this calculation, the simulation results are expected to differ from this values. If an EC system without batteries is dimensioned, this reduction is not relevant.

### 3.2.3 Weight Estimation of Energy Storage Systems

When dimensioning a system it is not only important to fulfil the specifications, but it is also important to keep the weight and cost as low as possible. To calculate the weight, the data above together with Appendix E are used. Based on specifications of the converter used in the experiments, the DC/DC converters in this example are assumed to weight 45 kg each. These numbers are shown for different battery types in Table 3.1 to Table 3.3 (see Appendix E for details).

**Table 3.1 Weight of the energy storage systems with NiMH batteries,  $I_{\text{battery, max}} = 5 C_{\text{Bat}}$**

DC/DC converter, 220 kW	45	kg
Battery, 220 kW	1150	kg
<b>Total weight for battery system</b>	<b>1195</b>	<b>kg</b>
EC bank, 320 elements	280	kg
DC/DC converters, 60+220 kW	90	kg
Battery, 60 kW	310	kg
<b>Total weight of the battery-EC system</b>	<b>680</b>	<b>kg</b>
Weight compared to battery system	57	%

**Table 3.2 Weight of the energy storage systems with NiMH batteries,  $I_{\text{battery, max}} = 2 C_{\text{Bat}}$**

DC/DC converter, 220 kW	45	kg
Battery, 220 kW	2400	kg
<b>Total weight for battery system</b>	<b>2445</b>	<b>kg</b>
EC bank, 320 elements	280	kg
DC/DC converters, 60+220 kW	90	kg
Battery, 60 kW	650	kg
<b>Total weight of the battery-EC system</b>	<b>1020</b>	<b>kg</b>
Weight compared to battery system	42	%

**Table 3.3 Weight of the energy storage systems with Li-ion batteries,  $I_{\text{battery, max}} = 2.2 C_{\text{Bat}}$**

DC/DC converter, 220 kW	45	kg
Battery, 220 kW	650	kg
<b>Total weight for battery system</b>	<b>695</b>	<b>kg</b>
EC bank, 320 elements	280	kg
DC/DC converters, 60+220 kW	90	kg
Battery, 60 kW	180	kg
<b>Total weight of the battery-EC system</b>	<b>550</b>	<b>kg</b>
Weight compared to battery system	79	%

**Table 3.4 Weight of the energy storage system with EC's only.**

EC bank, 380 elements	331	kg
DC/DC converter, 220 kW	45	kg
<b>Total weight of the EC system</b>	<b>376</b>	<b>kg</b>
Weight compared to battery system	33	%

From these figures, it can be concluded that the total weight of the energy storage system is significantly decreased using a battery-EC system compared to a conventional battery system. However, the weight reduction is strongly dependent on the battery type. The largest weight reduction is obtained if only EC's are used as an energy storage, assumed that the start-up time of the ICE-generator is less than the maximum acceleration time 30s.

The performance of the system in terms of specific energy and power is summarised in Table 3.5. The specific energy of the system increases compared to the EC's alone, and the specific power increases compared the battery alone. In other words, both energy and power performance is enhanced using a battery-EC energy storage system.

**Table 3.5 Specific energy and specific power.**

	Wh / kg	W / kg
NiMH battery, $I_{\text{battery, max}} = 5 C_{\text{Bat}}$	50	253
NiMH battery, $I_{\text{battery, max}} = 2 C_{\text{Bat}}$	50	101
LiION battery, $I_{\text{battery, max}} = 2.2 C_{\text{Bat}}$	150	419
EC	5.8	3000
Combined system, NiMH battery, $I_{\text{battery, max}} = 5 C_{\text{Bat}}$	23	412
Combined system, NiMH battery, $I_{\text{battery, max}} = 2 C_{\text{Bat}}$	32	275
Combined system, Li-ion battery, $I_{\text{battery, max}} = 2.2 C_{\text{Bat}}$	49	509
EC system (without battery)	5.1	585



## 4. Modelling of the System

Consisting of two or more energy sources, the drive train in an HEV is a complex system. In order to control the power flow between the traction motor and energy storage, the dynamic behaviour of each component of the simplified system, presented in Figure 4.1 must be investigated. In this section, the origin and implementation of models are presented from a general point of view, with the resulting MATLAB®/SIMULINK® models presented in detail in Appendix A.

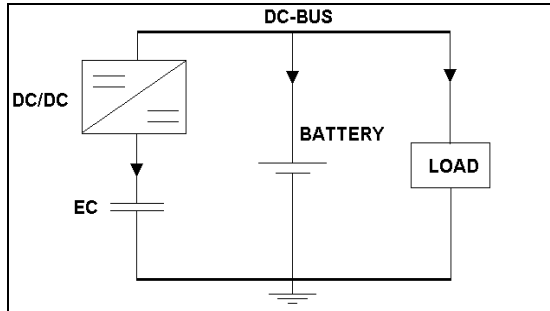


Figure 4.1 Simplified drive train of an HEV.

### 4.1 Electrochemical Capacitors

One of the simplest, but still quite accurate way of modelling the EC, is to model it as a generic capacitor, having one resistance in parallel and one in series with the capacitor (Figure 4.2) [3], [8].

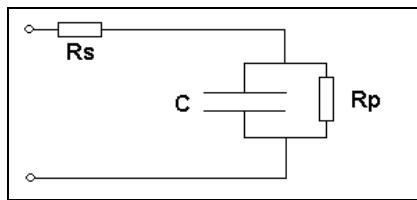


Figure 4.2 Simplified equivalent circuit of the EC.

The EC parameters are presented in Appendix E and are verified in the experiments.

### 4.2 Battery

Compared to the EC, a battery is much more complicated to model. Internal temperature and SOC are two examples of important parameters difficult or practically impossible to measure. Therefore, a model developed by Advisor [6] is used in combination with Volvo internal experimental data in the simulations. Basically, this model is a *Thevenin equivalent* with parameters dependent on current, temperature and SOC etc. (see Figure 4.3). In addition, the model calculates the total power losses, which is a valuable parameter for the evaluation of the system.

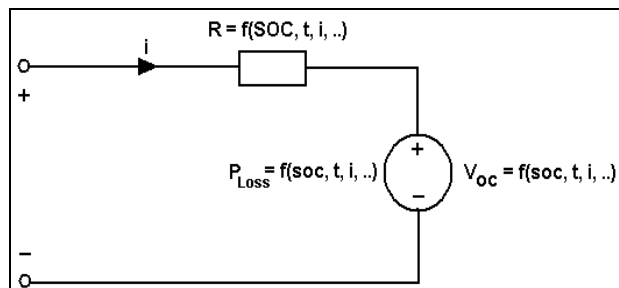


Figure 4.3 Battery model used in simulations.

### 4.3 DC/DC Converter

The DC/DC converter used in this project is a two-quadrant type designed for an input voltage of 10 to 500 V and an output voltage of 10 to 650V. The converter has also the operation limit that the output voltage must be greater than the input voltage.

The basic operation principle of the converter is not complicated to model or simulate. Nevertheless, including its own internal controllers and operation modes, the modelling becomes difficult from an application point of view. Therefore, the model used in the project is an ideal mathematical model adjusted to available data on resistive and switching losses. Its behaviour can be summarised in Equation 4.1 to Equation 4.3 and in Figure 4.4. The losses are modelled as a sum of constant voltage drop and ohmic losses at the low voltage side. These loss parameters are obtained from product specifications and real system measurements, see chapter 7.

EC input power

**Equation 4.1** 
$$P_{EC\ input} = P_{Input} - P_{Loss}$$

Output power

**Equation 4.2** 
$$P_{Output} = P_{EC\ output} - P_{Loss}$$

Losses in the DC/DC converter

**Equation 4.3** 
$$P_{Loss} = V_{Drop} \cdot I_{EC} + R_{Loss} \cdot I_{EC}^2$$

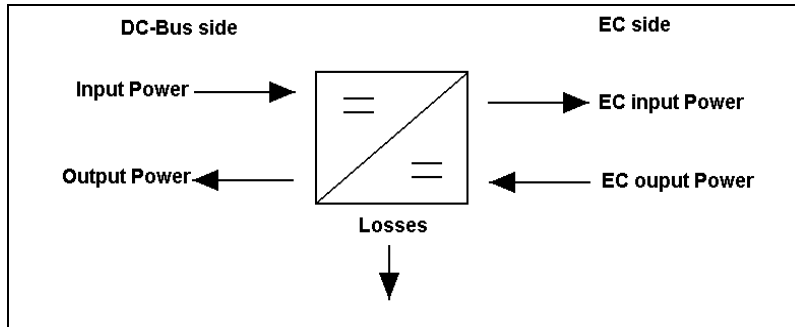


**Figure 4.4** Generic model of the DC/DC converter.

### 4.4 Load

The load can be modelled as a time dependent power source, using values according to the specific driving cycle and vehicle. In simulations and experiments, the required power is scaled by the system voltage, resulting in a component equivalent to an ideal current source. In this project, the required power is calculated using ECE15-L power profile (Appendix C). This profile is developed by EUCAR [10] and is widely used in life cycle tests for battery systems. In the experimental set-up, a Digatron® thyristor based two-quadrant converter was used as the load.

## 5. Simulations

By dimensioning and modelling each component of the drive train, the complete drive train can be simulated and evaluated. This is made in order to find appropriate control strategies and to investigate if the battery-EC combination strategy is likely to improve the performance. In the first part, possible system performance parameters are discussed. In the second part, different control strategies are described and evaluated. In the last part, simulations of systems having different dimensions and driving cycles are described, evaluated and discussed.

### 5.1 System Performance

There are numerous ways to characterise the performance of a battery-EC system. In addition, the choice of evaluation method and performance parameters are probably of vital importance for the final conclusion on the overall performance. In this project, four different parameters are calculated after each test cycle (section 5.1.1). The results from these tests have been used in the optimisation of controllers and control strategies. Even though significant improvements of certain terms are achieved, full-scale tests must be performed in order to determine if the systems performance is sufficient. Nevertheless, simulation and experimental results can undoubtedly give valuable information on the basic concepts of a battery-EC system.

#### 5.1.1 Performance Parameters

- **RMS Battery Current**

If the chemical processes in the battery are neglected, and the battery is modelled as a *Thevenin-equivalent*, the RMS-current gives a rough measure of the relative ohmic loss of the internal resistance. This parameter is only used as a first step in the evaluation, where the actual battery current is compared to the load current. The reduction ratio is presented in percent.

- **Power Loss in Battery**

As mentioned earlier, a reduction of battery stresses is one of the most important aims of this project. Even so, this is perhaps the most difficult parameter to measure. The total loss of energy in the battery is obtained from the Advisor model [6], after simulating the battery using measured (or simulated) battery current and voltage. The result is then compared with the case when the measured (or simulated) load current is fed to the battery only, yielding a reduction ratio.

- **Total Energy Efficiency**

All components of the system suffer from losses, for example ohmic losses in battery, EC's, balancing circuitry, DC/DC converter, cables and switching losses. Even though the focus is set on reducing the battery losses, the overall efficiency is an important parameter since all losses in the system generate heat and, consequently, demand proper cooling.

The total energy is calculated as the ratio between the energy absorbed / supplied by the load and the energy drawn from the battery. Absorbed / supplied energy from the EC's and the estimated losses in the battery are included in the calculations, but not the internal chemical losses in the battery.

- **Charge Control**

In order to operate during steady-state conditions and longer cycles, the EC's must be sufficiently charged during low-power load and pauses. This charging should ensure that the final EC voltage becomes equal or close to the initial EC voltage after running each test cycle. In other words, it is obvious that battery losses can be greatly reduced by using energy from the EC's, leaving the EC bank fully discharged after the cycle. This performance parameter is defined as the relation between the average EC voltage during each cycle and the initial EC voltage. This value is calculated after each cycle, to ensure that a steady-state value is reached.

These parameters are described in detail in Appendix F.

## **5.2 Control Strategies and Methods**

In any vehicle, driven in urban or suburban regions, the power required from the traction motor is characterised by several acceleration and braking events with relatively short intervals of constant speed. In a series HEV, accelerations demand large discharge currents from the DC bus, and regenerative braking large charge currents. As commonly known in the field, high currents, especially during charging, significantly reduce the battery lifetime and performance. Therefore, the aim of the control of the EC current is to reduce large battery currents, using the EC's as temporary energy storage during short intervals. From the following basic control strategy, a complete controller is designed and simulated in four steps. Summarised simulation results are presented to point out the differences between the control strategies. Details and full documentation of the control system is presented in Appendix A.

The main control strategy can be summarised in the following specification:

- Large currents during acceleration and regenerative braking should be diverted from the battery to the EC using the DC/DC converter.
- Slow variations and/or constant current to the load, for instance when driving at constant speed for several minutes, should be delivered from the battery only.
- During periods with low or no load currents, the EC's should be charged from the battery to a set point determined by vehicle speed, needed acceleration capability and braking energy uptake etc. This particular calculation is briefly discussed in section 5.2.4.

### 5.2.1 Step 1 – Low Pass Filtering of Load Current

One approach to meet the specification of the main control strategy is to control the battery current to follow a low-pass filtered load current, diverting fast-changing currents to the EC. In other words, a large load current during a short acceleration should result in a slow increase in battery current and immediate step in EC current. An example of this first control strategy is shown in Figure 5.1, where the load is in accordance to the first part of the *ECE15-L Urban Cycle* [10]. Negative values correspond to discharge currents during acceleration and positive values correspond to charge currents during regenerative braking.

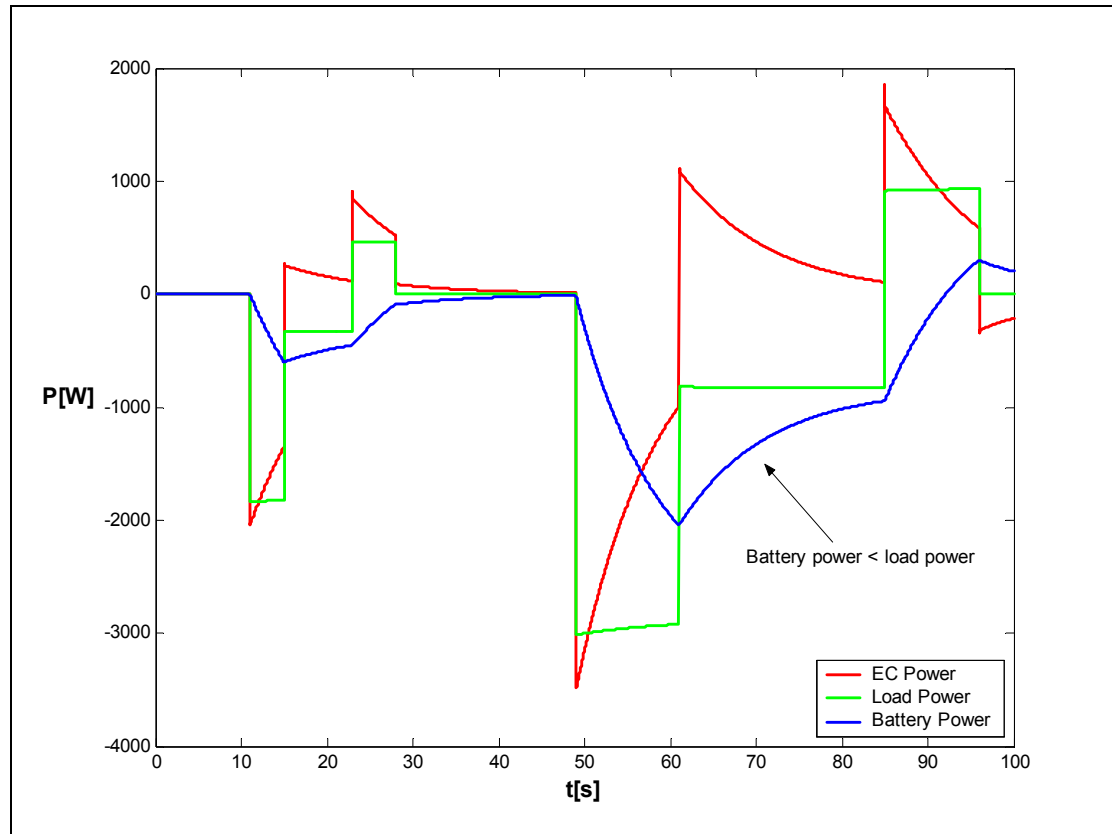


**Figure 5.1 Step 1 – Low pass filtering of load current.**

Adjusting the filter constant, this control method can be used to fit different load cycles. In this example, the filter constant is set to 10 s., a value chosen to point out the characteristic behaviour of this control strategy.

First of all, the benefit of this strategy is the simplicity and easy implementation. Secondly, the peak power delivered from the battery is significantly reduced, and thus the charge current from short periods of regenerative braking is fed to the EC.

### 5.2.2 Step 2 – Modified Low Pass Filtering

A consequence of the filtering method is that the rise time of the battery current is large in both directions, charge and discharge, resulting in long periods when the battery discharge current is larger than the load current (see arrow in Figure 5.1). Even though the energy drawn from the battery is fed to the EC's during such periods, large battery currents still increase the stresses in the battery. One way to avoid this behaviour is to limit the EC charge current to zero whenever the load current is less than the actual battery discharge current.

In Figure 5.2, the EC's are active during rapid *increases* of load current, resulting in a large reduction of battery current (see section 5.3 and chapter 7 for simulations and calculations from experimental data).

However, two problems must still be solved: power delivered from the load during regenerative braking should not be fed to the battery, and a separate charge control for the EC's is needed.

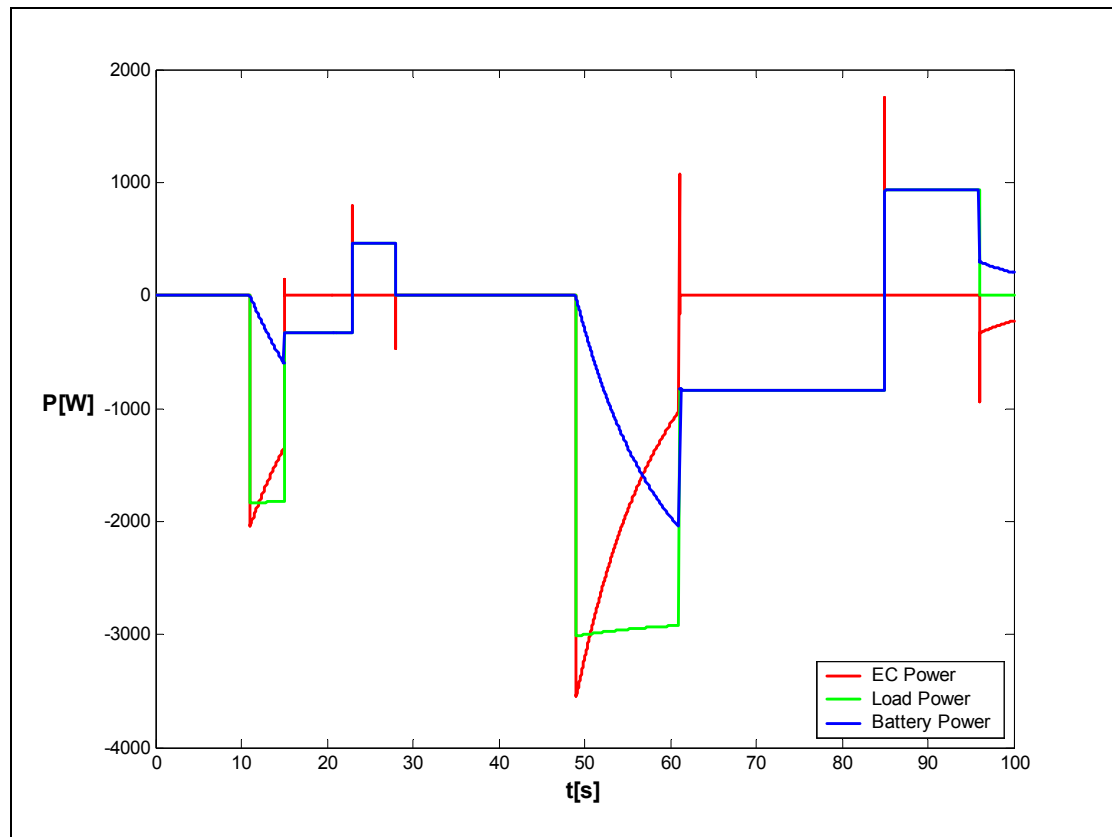


Figure 5.2 Step 2 - Modified low pass filtering of load current.

### 5.2.3 Step 3 – Modified Low Pass Filtering with Zero-Limited Battery Current

The first disadvantage pointed out in the previous strategy (section 5.2.2), battery charge during regenerative braking, can be eliminated by small modifications. Since the brake energy is relatively small compared to the rest of the cycle, it can be diverted directly to the EC's, limiting the battery charge current to zero. Of course, this method must be carefully monitored in order to avoid over-charging of the EC's.

The result of a simulation using this strategy is shown in Figure 5.3. The stresses in the battery are significantly reduced since only the EC's are charged during braking (battery current is zero around  $t=23$  to  $28$ s and  $t=85$  to  $96$ s). Constant power levels are handled by the battery alone, for example during constant speed operation after acceleration.

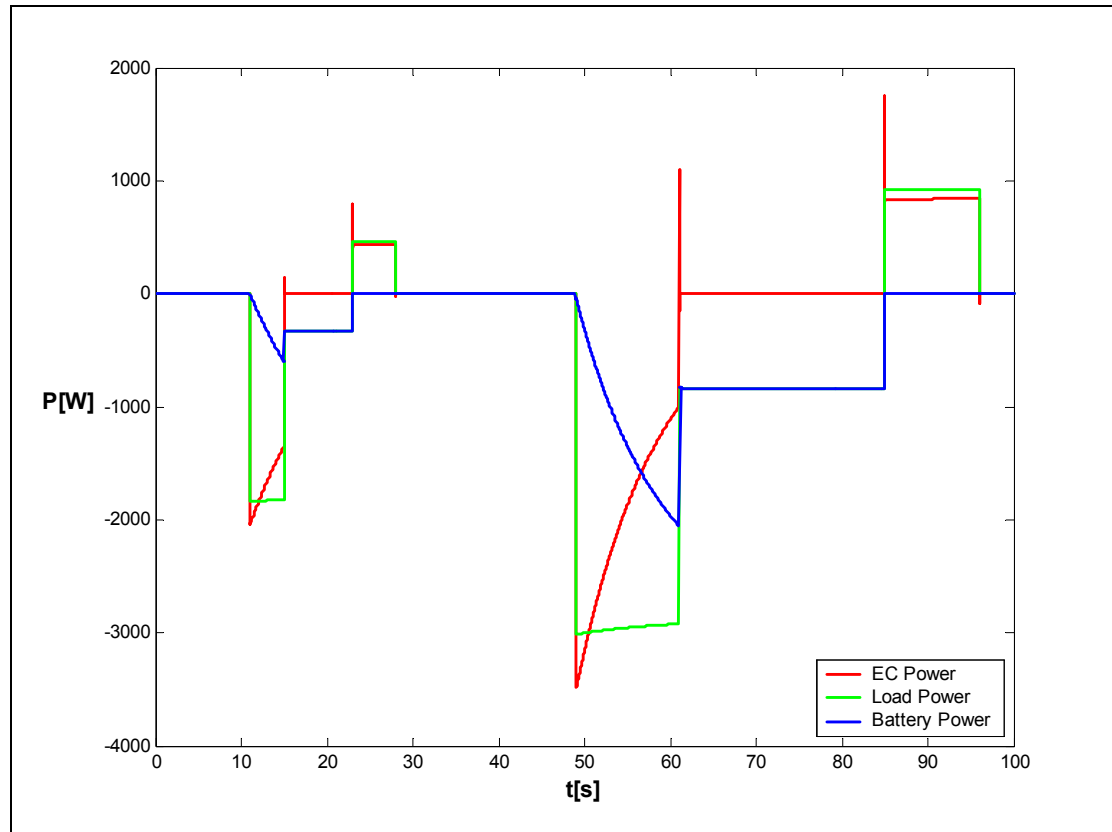


Figure 5.3 Step 3 - Modified low pass filtering with zero-limited battery current.

#### 5.2.4 Step 4 - Modified Low Pass Filtering with Zero-Limited Battery Current and Charge Control

Using *Step 3* (section 5.2.3), the two first aims of the EC control are achieved: battery current is reduced and braking energy is fed to the EC's. Finally, a charge controller for the EC's is needed. In this project, no dynamic controller, handling for example vehicle speed, is designed. This can, on the other hand, easily be added in the future.

The charge control strategy can be summarised as:

- When the required load current is less than a certain specified value, the EC's are charged from the battery, using a standard proportional controller having a fixed reference voltage.
- The total discharge current from the battery (sum of load current and charge current) is limited to a value determined by battery data, for example  $C_{Bat}/3$ .
- Overcharge or undercharge is avoided using an external safety system.
- All energy from regenerative braking is fed to the EC's.

Further details and implementation in MATLAB®/SIMULINK® can be found in Appendix A. Simulation results using the final control strategy are presented in Figure 5.4.

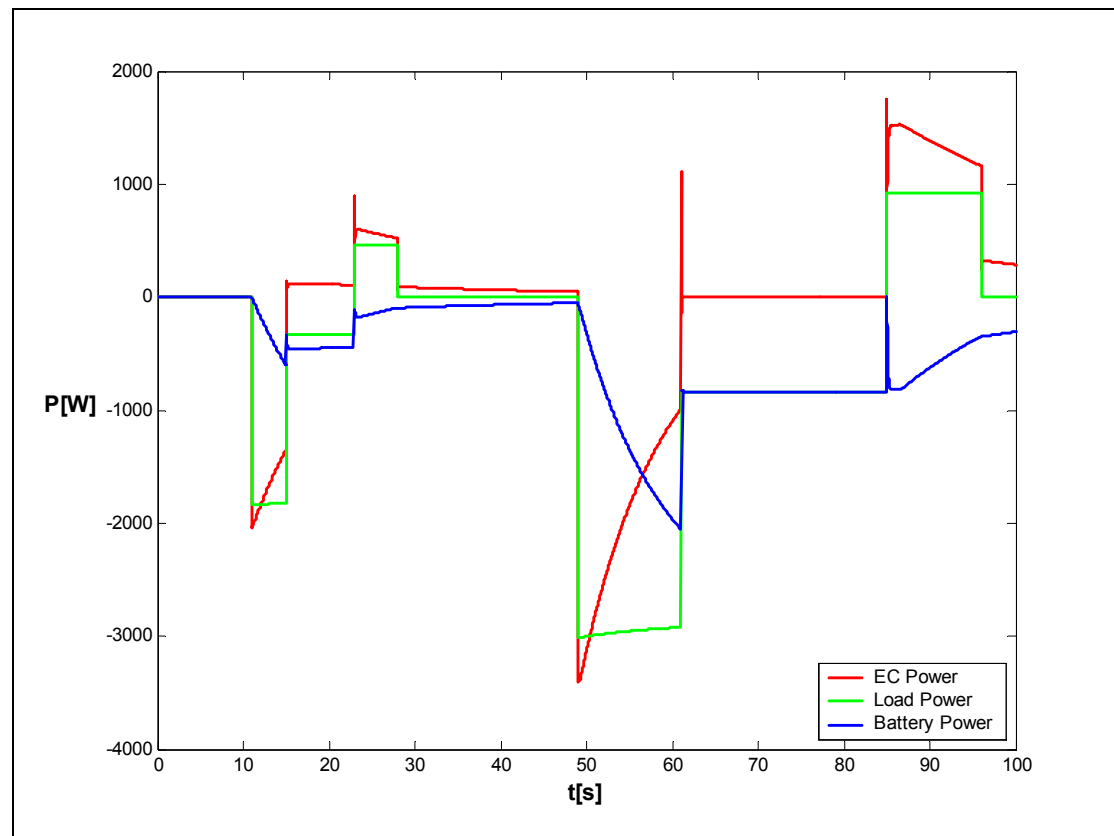


Figure 5.4 Step 4 – Modified low pass filtering of load current with zero-limited battery current and charge control.

### 5.3 Simulation Results

The control strategies and performance parameters described in the previous section define the simulation set-up: different control strategies are to be tested on a complete system and evaluated with respect to performance. Moreover, the relation between capacity and voltage levels of batteries and EC's are varied in three sizes, where the two first sizes correspond directly to experiments and the equipment presented in chapter 6. The third size is a simplified model of the city bus dimensioned in section 3.2. The simulation results from each of the three sizes investigated are summarised and viewed in figures showing load power, battery power and EC power. Complete results together with all settings and controller parameters are presented in Appendix B.

#### 5.3.1 Simulation Set-Up

The laboratory is equipped with two sets of EC's and batteries. These two sets are therefore built and simulated separately, and referred to as "Size I" and "Size II" (see specifications in each subsection). In section 3.2, a full-scale battery-EC system is simplified and dimensioned for the use in a city bus. This set-up cannot be built within the scope of this project. However, it can be simulated using assumptions of component specifications. This is done as a final simulation, to give a rough estimation of real application performance and referred to as "Size III".

In simulations of the *Size I* and *Size II* systems, the urban part of the ECE15-L driving cycle is used. The *Size III* system is simulated using the *Bus Test Cycle* (see Appendix C).

#### 5.3.2 Size I System – First Laboratory Set-up

The main system properties are presented in Table 5.1, and complete information can be found in Appendix E. In Figure 5.5, the EC's simulated in this section is shown.

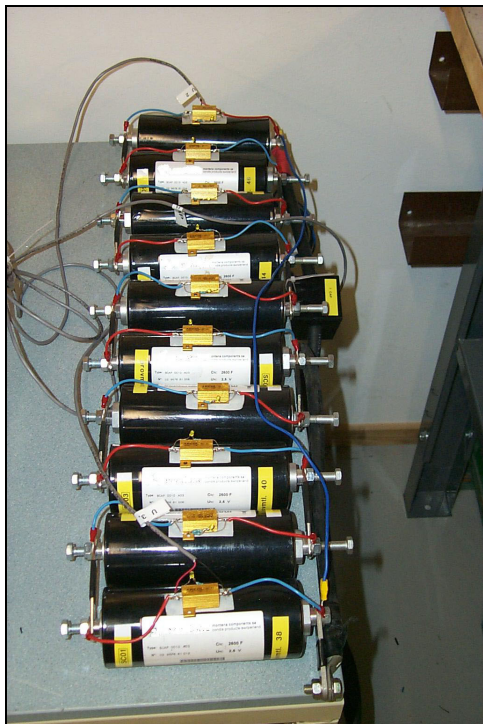


**Figure 5.5 EC bank with passive balancing simulated in the *Size I* system.**

**Table 5.1 *Size I* system: properties.**

<b>EC bank</b>		
Rated working voltage (RWV)	25	V
Total capacitance (10 elements)	260	F
Initial and reference voltage	100	% of RWV
Balancing*	Passive, 10Ω	
<b>Battery</b>		
Nominal voltage	50	V
<b>Simulated Vehicle**</b>		
Weight	125	kg

\* In the first simulation (section 5.3.2), it is assumed that an ideal balancing method is used. In the second simulation of the *Size I* system (section 5.3.3), the system is assumed to use passive balancing with 10Ω.

\*\* The simulated vehicle is scaled down to correspond to the available battery and EC bank.

The urban part of the driving cycle consists of four identical cycles, each 195 s long. The last cycle from the simulation is presented in Figure 5.6. Using the control method according to *Step 4* (see

section 5.2.4), the system is simulated with different values of filter constant and charge current, until optimum values of the system performance parameters are found. These values are presented together with the filter constant, initial EC voltage and set point for steady-state charge current in Table 5.2.

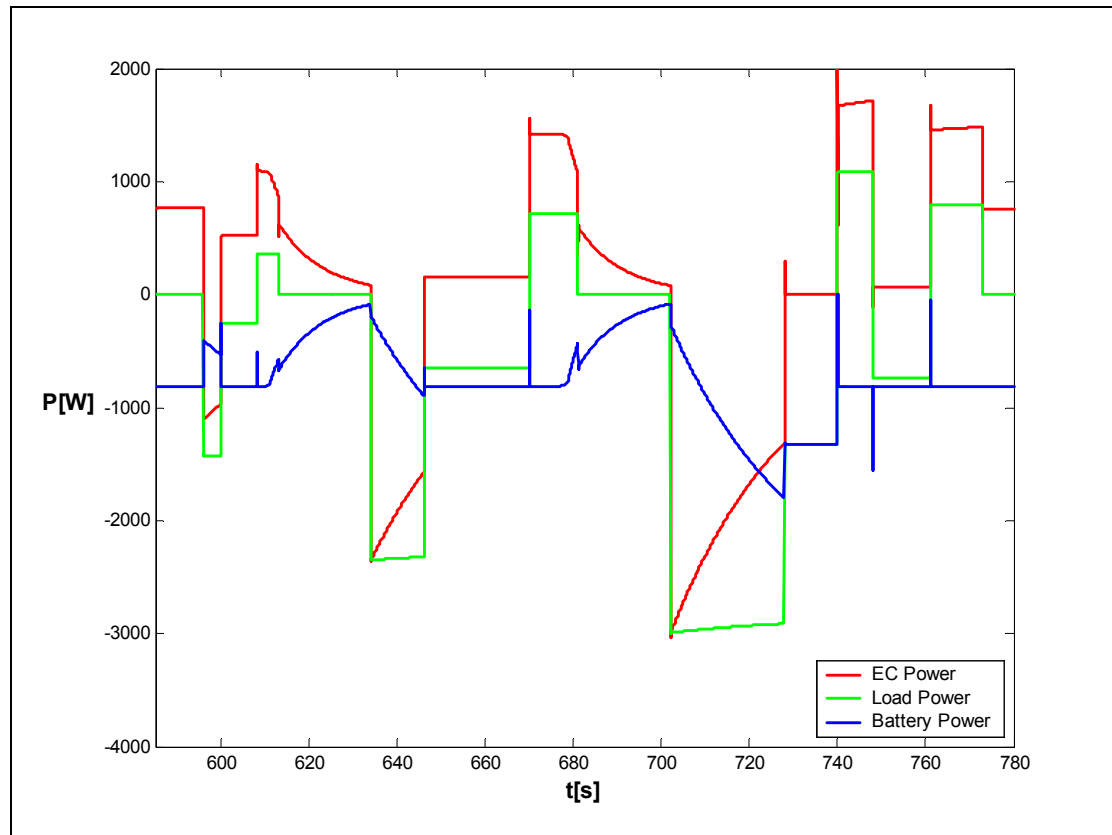


**Figure 5.6 Simulation results of the *Size I* system.**

As seen in Figure 5.6, it is obvious that the peak power from the battery is significantly reduced if EC's are added. In addition, the power generated during braking is efficiently diverted from the battery. Subsequently, the performance parameters presented in Table 5.2 were calculated.

**Table 5.2 *Size I* system: simulation results.**

<b>Performance parameter</b>		
RMS battery current	61	Reduction ratio in %
Power loss in battery	33	Reduction ratio in %
Total energy efficiency	84	%
Charge control (average value)	84	% of reference voltage
<b>Control parameters</b>		
Initial EC voltage	100	% of RWV
Filter constant	30	s
EC Charge current	0.27	$C_{Bat}$

The “EC Charge current” in Table 5.2, is the maximum discharge current drawn from the battery during steady-state charge of the EC's. Higher value decreases the charge time for the EC's, but increases the RMS battery current and the associated losses. The optimum relation between charge current and losses is given by the choice of driving cycle.

### 5.3.3 Size I System with Passive Balancing

As mentioned earlier, differences between the EC's may cause unbalance between the cells. Since the maximum capacitor voltage must not be exceeded, a simulation of the system with lower initial EC voltage was performed. With 88% of maximum initial voltage, the energy in the EC's is decreased to 77%, yielding less decrease in battery loss. According to Magnusson [4], the balancing problem is likely to be solved if an active balancing circuit is used.

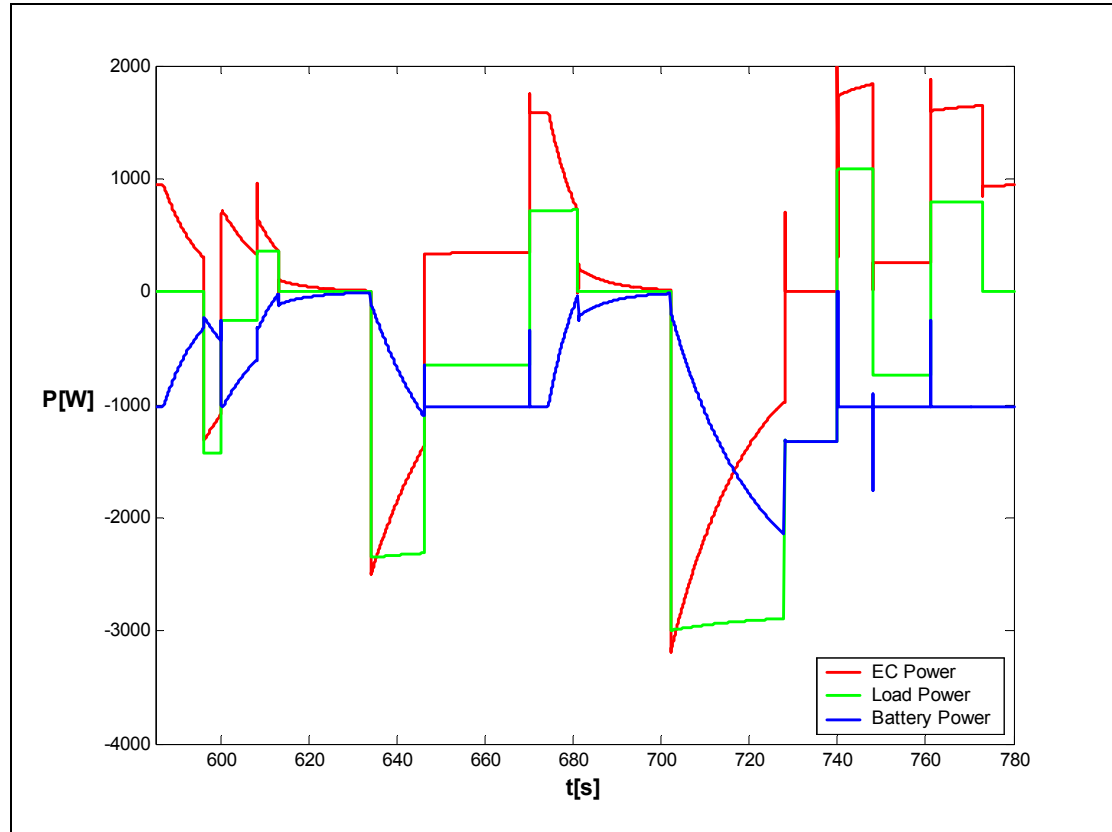


**Figure 5.7 Simulation results of the *Size I* system with passive balancing.**

Compared to the case with 100% RWV in Figure 5.6, the maximum battery power in Figure 5.7 has increased to relatively high level. This is due to the lower filter constant of 20 s needed with the lower available energy in the EC's. With merely 88% of rated working voltage available, the EC's are underdimensioned for the current driving cycle. This is also seen in Table 5.3, where the battery power loss and RMS current has increased compared to the value in Table 5.2.

**Table 5.3 *Size I* system: simulation results with passive balancing.**

Performance parameter		
RMS battery current	69	Reduction ratio in %
Power loss in battery	43	Reduction ratio in %
Total energy efficiency	81	%
Charge control (average value)	82	% of reference voltage
Control parameters		
Initial EC voltage	88	% of RWV
Filter constant	20	s
EC Charge current	0.33	$C_{Bat}$

### 5.3.4 Size II – Second Laboratory Set-up

This set-up is dimensioned with higher voltages at both the battery and the EC bank, but the same DC/DC converter as in *Size I*. The EC bank (Figure 5.8) in *Size II* uses an active balancing circuit, other system properties is presented in Table 5.4. The overall efficiency is expected to increase due to decreased relative power losses in the DC/DC converter and the battery. The simulations of *Size II* are performed in the same way as in previous section.

The main system properties are presented in Table 5.4, and complete information can be found in Appendix E.



**Figure 5.8** EC bank with active balancing simulated in the *Size II* system.

**Table 5.4** *Size II* system: properties.

<b>EC bank</b>		
Rated working voltage (RWV)	56	V
Capacitance	96	F
Initial and reference voltage	100	% of RWV
Balancing	Active	
<b>Battery</b>		
Nominal voltage	100	V
<b>Simulated Vehicle*</b>		
Weight	250	Kg

\* The simulated vehicle is scaled down to correspond to the available battery and EC bank.

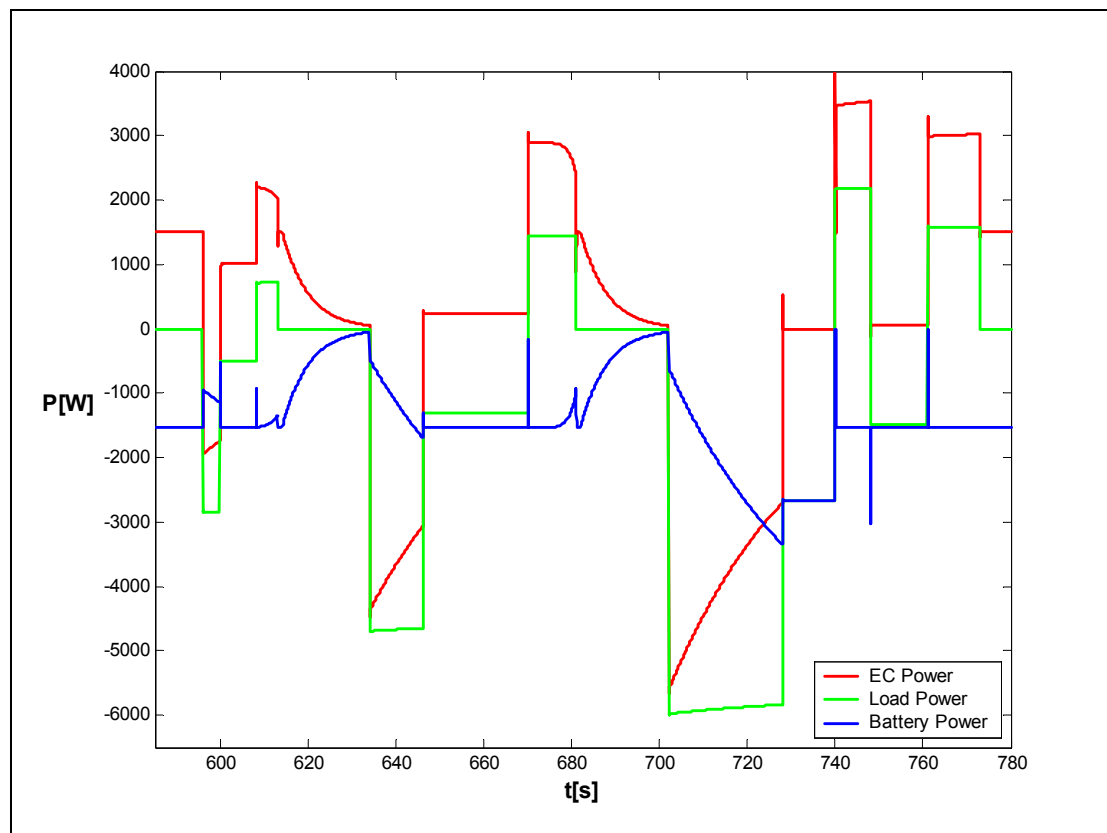


**Figure 5.9** Simulation results of the *Size II* system.

As seen in Table 5.5, the total efficiency is increased, and at the same time, battery losses are decreased. The battery power is set at a constant discharge level as long as the EC's are charged. In Figure 5.9, the battery power is presented together with load power and EC power.

**Table 5.5 Size II system: simulation results.**

<b>Performance parameter</b>		
RMS battery current	57	Reduction ratio in %
Power loss in battery	30	Reduction ratio in %
Total energy efficiency	90	%
Charge control (average value)	84	% of reference voltage
<b>Control parameters</b>		
Initial EC voltage	100	% of RWV
Filter constant	35	S
EC Charge current	0.25	$C_{Bat}$

### 5.3.5 Size III: City Bus Example

The simulated system in this subsection is dimensioned from a simplified model discussed in section 3.2. The ECE15-L driving cycle is not used in this simulation, since it is dimensioned for passenger cars. Instead, a short test cycle is obtained from the calculated parameters of a typical acceleration, constant speed and regenerative braking sequence for a bus. This cycle is referred to as the *Bus Test Cycle* and presented in Appendix C.

From the expected EC current and the measured losses in the DC/DC converter, assumptions are made regarding the converter loss function. The main system parameters are presented in Table 5.6. A complete specification of the bus system is presented in Appendix E.

In this simulation, no performance parameters are calculated. The aim of the simulation is merely to confirm that the dimensioned energy storage system is likely to work even when losses are included. In Table 5.6 and Table 5.7, a comparison between the estimated and simulated system properties is made. The required battery size for an energy storage system without an EC bank is also included. In Figure 5.10, battery power is presented together with EC power and load power during a *Bus Test Cycle*.

**Table 5.6 Size III system: properties and simulation results, NiMH batteries  $I_{Battery, max.} = 5C_{Bat}$ .**

<b>EC bank</b>	<b>Simulation</b>	<b>Estimated</b>	
Number of series connected units	380	320	-
Rated working voltage (RWV)	1026	864	V
Total capacitance	13.2	15.6	F
Initial and reference voltage	100	100	% of RWV
Balancing	Active	Active	
<b>Battery</b>			
Number of series connected cells	200	210	-
Nominal voltage	250	263	V
<b>Required batteries without EC bank</b>			
Number of series connected cells	740	770	-
Number of parallel connected cells	1	1	
Nominal voltage	925	965	V
<b>Simulated Vehicle</b>			
Weight		18 900	kg
<b>Performance parameters</b>			

<b>(battery-EC system)</b>			
Total energy efficiency	75	-	%
<b>Control parameters</b>			
Initial EC voltage	100	100	% of RWV
Filter constant	100	80	S
EC Charge current	5	5	C <sub>Bat</sub>

**Table 5.7 Size III system: properties and simulation results, NiMH batteries  $I_{\text{Battery, max.}} = 2C_{\text{Bat}}$ .**

<b>EC bank</b>	<b>Simulation</b>	<b>Estimated</b>	
Number of series connected units	380	320	-
Rated working voltage (RWV)	1026	864	V
Total capacitance	13.2	15.6	F
Initial and reference voltage	100	100	% of RWV
Balancing	Active	Active	
<b>Battery</b>			
Number of series connected cells	400	440	-
Nominal voltage	500	550	V
<b>Required batteries without EC bank</b>			
Number of series connected cells	760	810	-
Number of paralell connected cells	2	2	
Nominal voltage	950	1015	V
<b>Simulated Vehicle</b>			
Weight		18 900	kg
<b>Performance parameters (battery-EC system)</b>			
Total energy efficiency	81	-	%
<b>Control parameters</b>			
Initial EC voltage	100	100	% of RWV
Filter constant	100	80	S
EC Charge current	5	5	C <sub>Bat</sub>

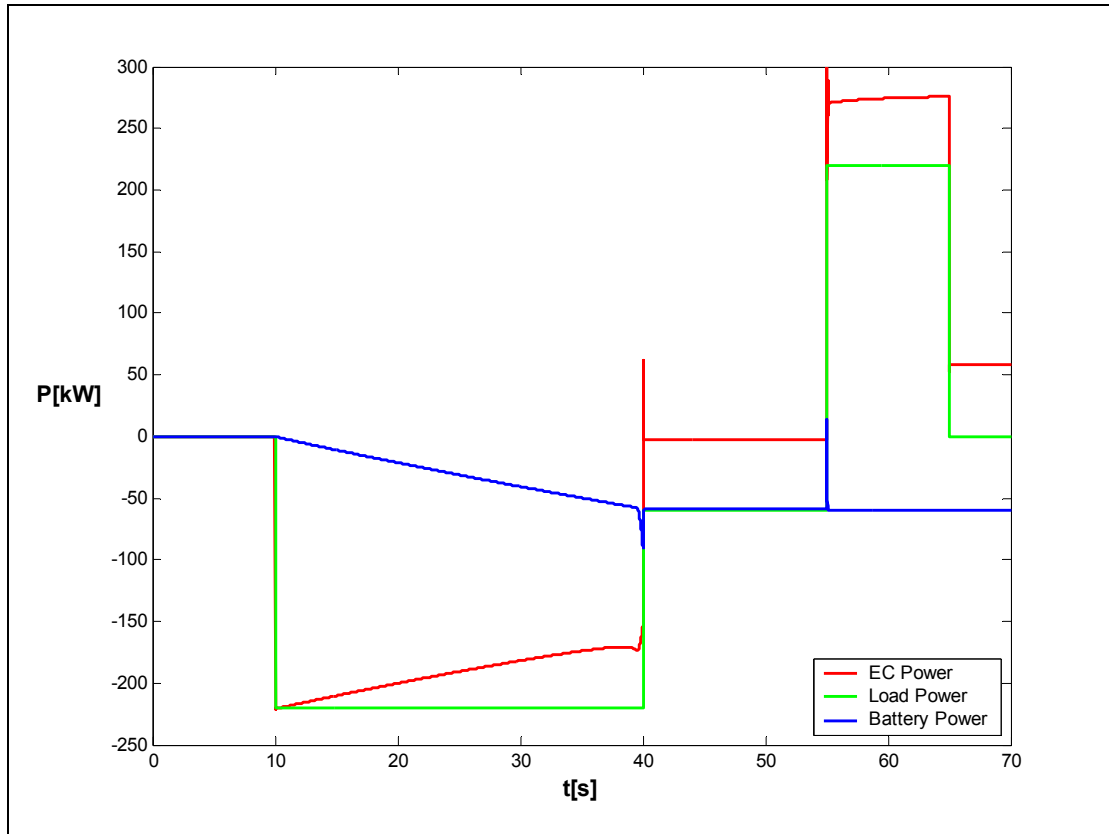


**Figure 5.10** Simulation results of the *Size III* system (city bus).

In this system, the battery power is slowly increasing during a maximum acceleration sequence, and constant when the load power is constant. The EC's are efficiently charged during steady-state and regenerative braking, and discharged during accelerations. In the acceleration part, the EC's are fully discharged. As presented in Table 5.6, the simulated size of the EC bank differs from the size calculated in section 3.2. This difference is due to the fact that all system losses are neglected in the calculations. In this case, instead of comparing performance parameters the total weight and/or cost of the system should be compared to a conventional system (see section 3.2.3). The system efficiency is increased if the maximum battery discharge current is decreased from  $5 C_{Bat}$  to  $2 C_{Bat}$ .

#### 5.4 Simulation Summary

From the simulations of *Size I*, the system performance is found to be promising in terms of reduced battery losses and RMS current. Nevertheless, if the passive method is used, the reduced EC voltage causes significant reduction of system performance. The overall system efficiency is rather low, due to the low system voltage and the associated losses in the DC/DC converter.

When the voltage levels are increased and active balancing method is used, as in the *Size II* system, both system performance and efficiency are increased. The losses in the battery are estimated to be less than 30% of the losses of a conventional battery energy storage system.

In the city bus example, size III, where component parameters of batteries, EC's and DC/DC converter is assumed to be that of the laboratory components, the alternative battery-EC system is found to work with merely 200 battery cells compared to 740 battery cells for a conventional battery system. As presented in section 3.2.3, the total weight is reduced with maintained acceleration performance. At a maximum battery discharge current of  $5 C_{Bat}$ , the overall efficiency is rather low, owing to the low efficiency of the batteries at high discharge currents. This value is increased to 94 % if  $I_{Battery\ max} = 2 C_{Bat}$ .



## 6. Experimental Laboratory Set-Up

A downscaled test system was built using existing components (NiMH battery, EC's, DC/DC converter) and a dSPACE® system. In this section, the system (Figure 6.1) is described including controllers, measurement system and computer interface.

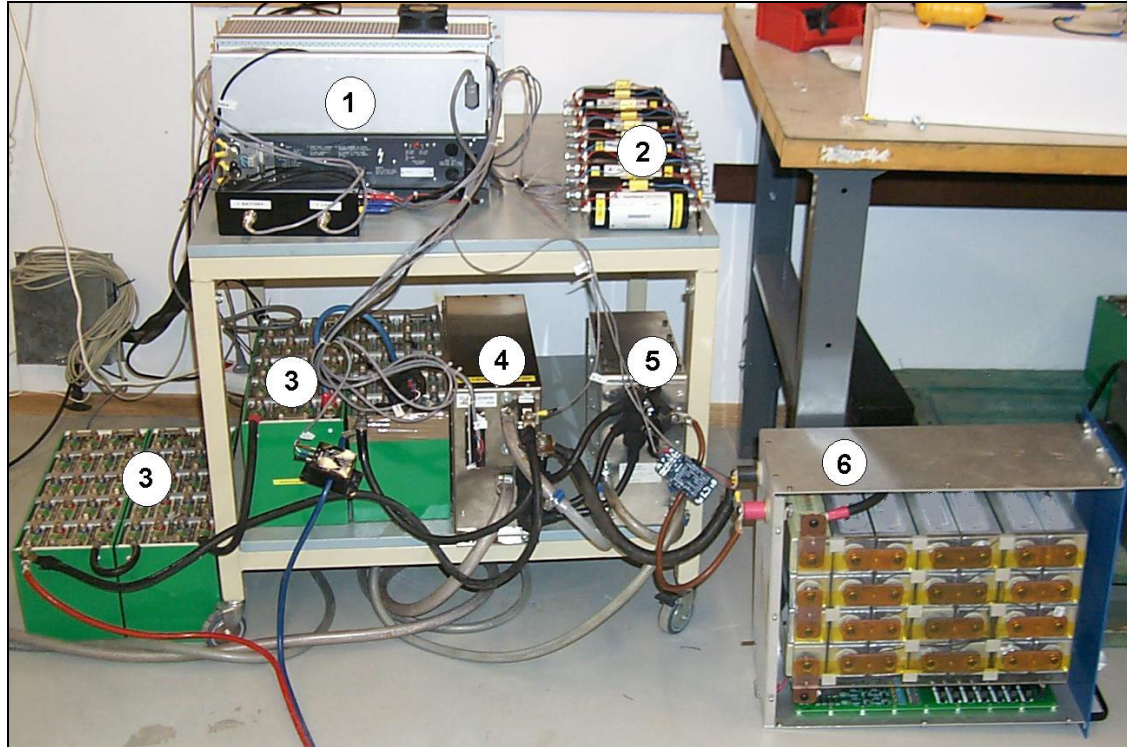


Figure 6.1 The laboratory system used in tests of the *Size I* and *Size II* systems:

1. Power supply, opto-coupling card, dSPACE interface.
2. EC Bank with passive balancing, used in the *Size I* system.
3. NiMH Batteries
4. DC/DC Converter
5. Inductance for the DC/DC Converter
6. EC Bank with active balancing, used in the *Size II* system.

The test system was limited to the existing components and equipment in the laboratory at Volvo Technology. The available batteries were NiMH batteries of 20-cell each, and the EC's were available in either ten separate elements or one package of 28-cells (referred to as *Size I* and *Size II* in section 5.3.1). In practice, this means that the maximum voltage of the EC's was 25 V or 56 V, thus limiting the system performance together with the current limit of the DC/DC converter (see Appendix E for specifications). Since the battery voltage, due to the design of the DC/DC converter, must be higher than the EC bank voltage, two (*Size I*) or four (*Size II*) NiMH batteries were connected in series.

### 6.1 Control and Measurement System

To control the system, a dSPACE® system was used. The benefits of this system are the utilisation of MATLAB®/SIMULINK® models, greatly simplifying the step from simulation to experimental tests. In this way, models, parameters and controllers can easily be developed and evaluated in MATLAB®/SIMULINK® before the tests. Moreover, parameters such as controller constants can be changed in real time to find their optimum values.

On the other hand, the dSPACE® system is very sensitive to over-voltages. To limit the maximum signal amplitudes, and thereby protect the dSPACE® system, an analogue galvanic separated

optocoupling card was built (see Appendix D). This 8-channel component includes filtering, amplification (or attenuation) and galvanic protection of the computer – dSPACE® interface.

Voltage measurements were performed by adding a simple voltage division circuit at the input of the optocoupling card. Current measurements were performed using LEM-modules (Appendix D). A simple schematic layout of the measurement system is presented in Figure 6.2.

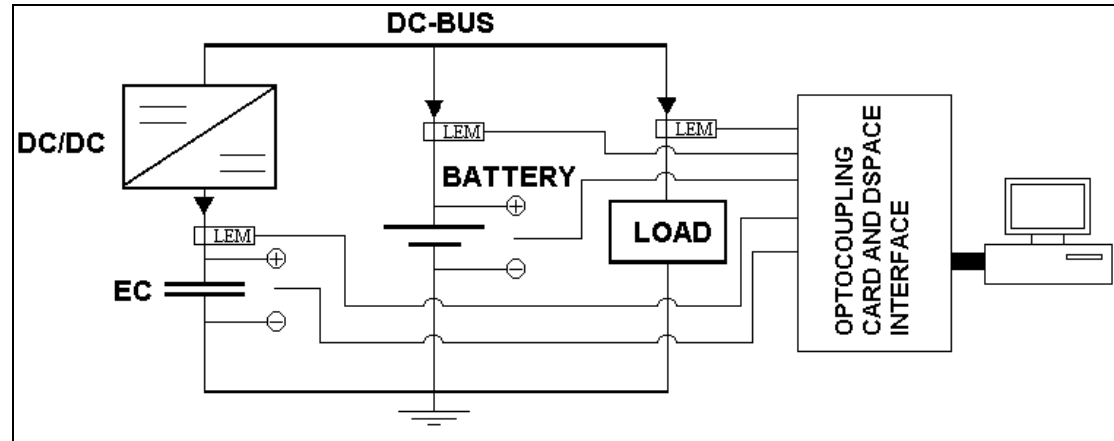


**Figure 6.2 Schematic layout of the measurement system.**

To reduce the noise level, a filter having a cut-off frequency of 450 Hz was added directly on the optocoupling card's output terminals. The current measurements showed to be especially sensitive to interference. To further reduce this noise, another filter having a cut-off frequency of 1 kHz was added on the outputs of the LEM-modules.

## 6.2 Calibration

The complete measurement / control system was calibrated using “chain calibration”: several reference voltages / currents were applied at the inputs and their values presented in dSPACE®/ ControlDesk® were recorded. After these test series, the measured values were fitted to the reference values, yielding a conversion function for each channel. The reference voltage was obtained from a variable power supply and measured using a calibrated multimeter, and reference currents were obtained directly from the Digatron® converter (see Appendix D for details).

## 6.3 Control of the DC/DC Converter

The only difference between the simulated and experimental control systems is the control of the DC/DC converter. In simulations, the converter is assumed to be ideal. Therefore, the needed battery current is assumed to be the actual as long as the converter is operating within its limits.

In the experimental set-up, the DC/DC converter is controlled by setting a reference voltage for the high voltage side. An internal circuit in the converter controls the switching of the IGBT:s. The input signal to this controller is a PWM signal with the duty cycle proportional to the output voltage. Another internal controller limits the current at the low voltage side.

In the experimental set-up, a current controller for battery current was added. This controller receives the reference battery current, and controls the DC/DC *via* the PWM input and a standard PI-controller. The optimum values of the controller parameters were determined after several tests. Full documentation and specifications of the controllers are presented in Appendix A.

## 7. Experimental Results

Subsequent system simulations, numerous experiments were performed. Firstly, the models were verified and some parameters, like total series resistance in the EC bank, were determined. The control system developed (section 5.2) was implemented and adopted to the MATLAB®/SIMULINK®/dSPACE®-environment.

### 7.1 Verification of Models

Even if the model parameters used in simulations are obtained from previous experiments, brief system verifying tests were performed.

#### Electrochemical Capacitors

The total series resistance,  $R_s$ , of the EC bank was measured by applying a current step and observe the immediate associated voltage. The second component parameter, the leakage resistance  $R_p$ , is in the order of a hundred times higher than the resistance used in the passive balancing circuitry. Therefore, it was not verified. An internal Volvo report provided information on the measured capacitance of the EC's.

#### Battery

Using the same method as for verifying the EC's, the internal series resistance of the battery was measured. The open circuit voltage (VOC) was also determined for use in the MATLAB®/SIMULINK® model.

#### DC/DC Converter

As mentioned earlier, the DC/DC converter is controlled by a PWM signal. The relation between the pulse width and the actual output voltage was obtained from several early experiments. The losses in the converter are dependent on several parameters such as current at high and low voltage side and the voltage conversion ratio. The loss function is, however, modelled to only depend on the current at the low voltage side. This function is determined from experimental data (see section 4.3 and Appendix A).

### 7.2 Size I System

As a first step, the *Size I* system was tested. Several tests were performed to find the highest possible EC voltage (using passive balancing). Two capacitor voltages are monitored individually to avoid overvoltages. After each test, performance parameters is calculated and compared with simulated values.

In Table 7.1, the performance parameters of the experimental system (see section 5.1.1) are presented together with results from the corresponding simulations. Three important control parameters are also included in the same table.

**Table 7.1 The *Size I* system performance.**

Performance parameter	Experiment	Simulation	Unit
RMS battery Current	70	67	Reduction ratio in %
Power Loss in Battery	41	41	Reduction ratio in %
Total Energy Efficiency	81	81	%
Charge Control (average value)	84	83	% of reference voltage
<b>Control parameters</b>			
Initial EC voltage	88	88	% of RWV
Filter constant	20	20	s
EC Charge current	0.33	0.33	$C_{Bat}$

In Figure 7.1, the battery power from both simulation and experiment is shown. The experimental values show a slight time shift and differences in the load power magnitude. However, the main characteristics are very similar. This experiment is performed in order to verify the models and to point out the discovered drawbacks of the passive balancing method rather than to give a realistic estimation of the performance of a real system. In the next experimental set-up, the *Size II* system, the measurement system is re-calibrated to obtain better accuracy of the load power.

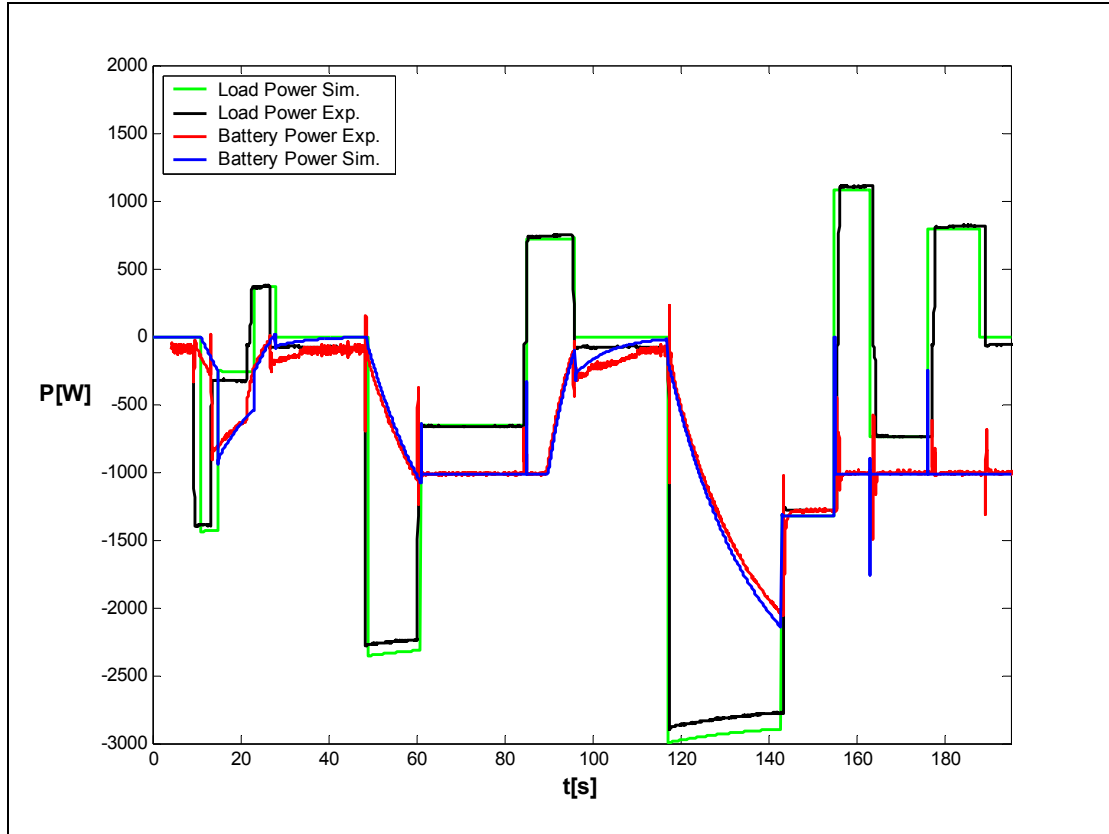


**Figure 7.1 Battery and load power from experiment and simulation with the *Size I* system.**

### 7.3 *Size II* System

Subsequent the *Size I* test series, the experimental laboratory system was re-built according to the *Size II* specification described in section 5.3.4 and Appendix E. Since this EC bank has active balancing, no upper voltage level other than the RWV is present. Consequently, the initial EC voltage can be set at the RWV. The results are discussed in section 7.4.

In Table 7.2, the performance parameters of the experimental system (see section 5.1.1) are presented together with results from the corresponding simulations.

**Table 7.2 The *Size II* system performance.**

Performance parameter	Experiment	Simulations	Unit
RMS battery Current	56	55	Reduction ratio in %
Power Loss in battery	26	27	Reduction ratio in %
Total Energy Efficiency	93	90	%
Charge Control (average value)	85	84	% of reference voltage
<b>Control parameters</b>			
Initial EC voltage	100	100	% of RWV
Filter constant	35	35	s

EC Charge current	0.25	0.25	$C_{Bat}$
-------------------	------	------	-----------

When the results from simulations and experiments are compared (see Figure 7.2), they are found to be in good accordance expect the time shift of the load power curve. However, even after re-calibration of the current measurements, there is a difference in magnitude of load power. This difference is due to the difference in battery voltage between simulations and experiment, as seen in Figure 7.3.

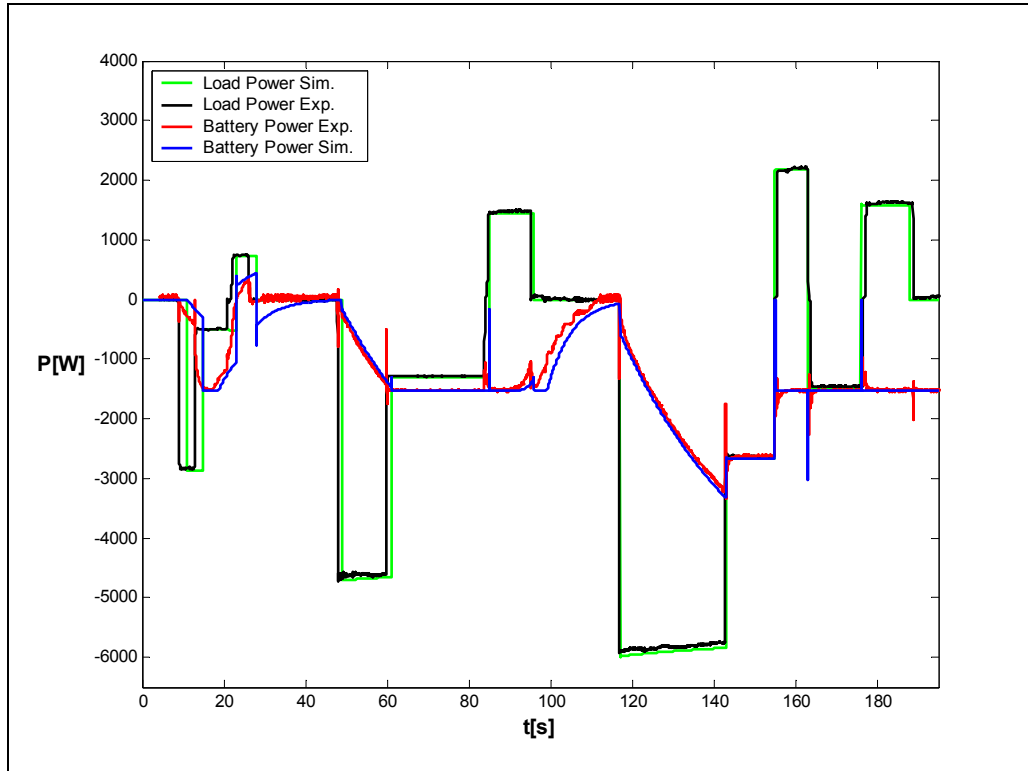


Figure 7.2 Battery and load power from experiment and simulation with the *Size II* system.

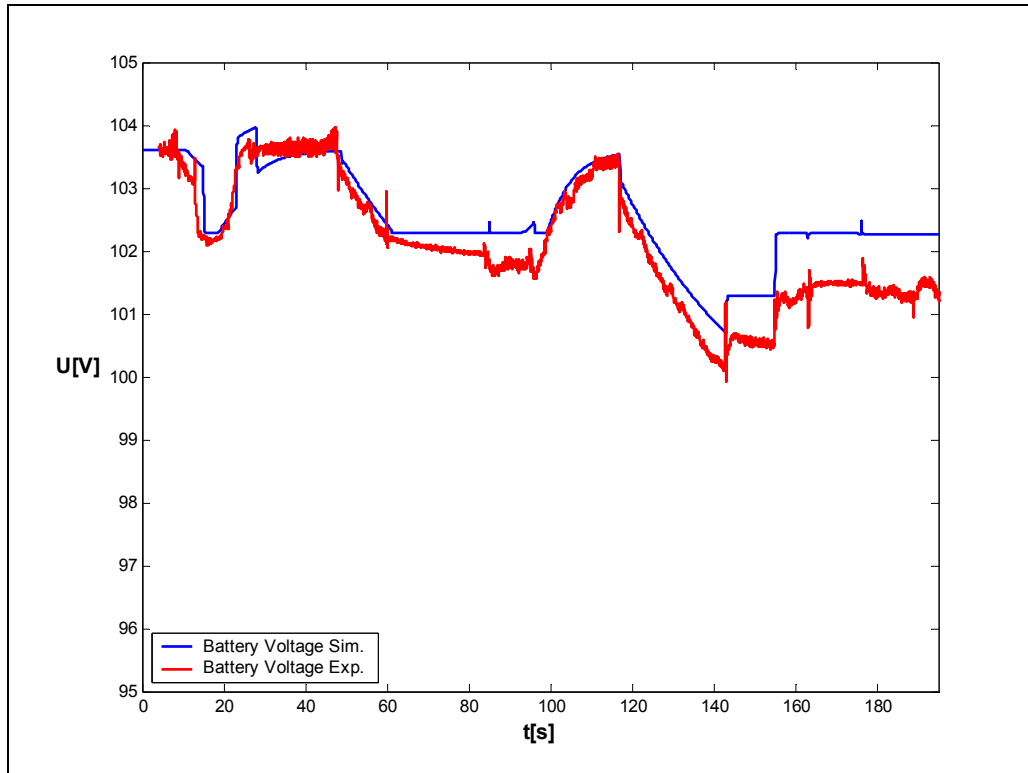


Figure 7.3 Battery voltage from experiment and simulation with the *Size II* system.

#### 7.4 Discussion

From the performance values (Table 7.1 and Table 7.2) and the power profiles presented in Figure 7.1 and Figure 7.2, it can be concluded that the models and assumptions used in the simulations are in good agreement with the real system. In other words, the simulated system offers a good estimate of how a real battery-EC system will perform. Three particular differences can be pointed out though:

- The time shift between the load power profiles is a consequence of the limited rise time for the current drawn / supplied by the Digatron<sup>®</sup> converter. Moreover, the current direction cannot be altered instantaneously, resulting in a short period of zero current during each transition from acceleration to regenerative braking.
- The difference in magnitude of the load power during high currents, for example during the period  $t=120$  to  $140$  s, can be explained by two reasons. Firstly, the calibration of the current measurements in the *Size I* system is made using relatively low currents and having the Digatron<sup>®</sup> converter as reference. This might cause inaccuracies in the current measurements, together with possible interference from strong electric fields during the test. The current measurement system is re-calibrated before the *Size II* system is built. Secondly, the battery model used in the simulations does not include the temporary decrease of VOC associated to high battery currents. This behaviour is shown in Figure 7.3. The difference is not significant in the tests performed within this project, but since it increases by time, it could possibly become too large during longer tests.
- The loss function used for the DC/DC converter is merely an estimation of the actual losses in the real system, causing additional inaccuracies in the simulations.

Compared to the results from the experiments of *Size I*, the over all efficiency of the *Size II* system is, as expected, increased due to the higher voltage levels, which decrease the relative system losses. In addition, the battery losses is further reduced in the *Size II* system, since the relation between the battery and the EC capacity is more in accordance with the reasoning in chapter 3.

It is possible that the performance of a real battery-EC system is further enhanced, since the necessary cooling of the batteries is decreased when the maximum battery power is decreased. Moreover, the total efficiency of the energy storage system could possibly be improved, compared to a conventional battery system, when the internal losses associated with large battery power are reduced. This could compensate for the added losses in the DC/DC converter and the EC bank.



## **8. Conclusions and Suggestions to Future Work**

According to the results, the lifetime of the battery could be increased if a battery-EC system is used instead of a pure battery system. If the lifetime is satisfying without an EC system, the objective of using EC's could instead be that the total weight of the energy storage system can be decreased when adding EC's to the energy storage system.

It should be pointed out that EC's for vehicle application are relatively new, not properly tested in production yet. Consequently, this leads most likely to a high initial total cost for the system, until production volumes have increased.

The battery-EC system is, in a basic sense, easy to implement and control. Nevertheless, other aspects not covered in this project, like electromagnetic interference and safety issues of a real vehicle, might complicate the final application.

When using a bank of series connected EC's, the balancing circuit is important. The passive balancing method is not likely to work in a real battery-EC system, because it is unable to work fast enough and leads to self discharge of the EC's. Therefore, a more complex and expensive active balancing method is necessary. The use of an active balancing method will probably be worth its price, since it makes it possible to use the full rated capacity of the EC's and reduces the EC's self-discharge to negligible levels.

The drawbacks of the battery-EC system are that the estimated system cost is higher, at least initially, and that the acceleration capability is limited to the state of charge in the EC's. In other words, the maximum acceleration capability is limited for a certain time after an acceleration.

If an ICE or fuel cell is used as a primary power source, and assumed to have a start-up time in the order of seconds, the battery may possibly be excluded from the drive train. In this case, the ICE or fuel cell handles slow and steady state power and the EC's peak power during acceleration and braking. This idea has not been investigated in this project, but its possibilities are promising so far.

The performance and lifetime of batteries are known to be strongly dependent on temperature. Consequently, it would be of interest to test the battery-EC system at different temperature conditions. Such a test will probably promote the battery-EC system, because the battery performance is strongly dependent on temperature. For many batteries, optimum performance is obtained at temperatures around 20 °C. On the other hand, EC's are known to be less temperature dependent, which probably leads to significant performance improvements at low temperatures compared to a conventional battery system. This also implies that the EC's could also be used as a start battery for an ICE during subzero conditions, when conventional batteries could have difficulties to deliver enough power.

Moreover, a full-scale test in a laboratory or a vehicle, including an ICE or a fuel cell, would be necessary to perform to evaluate the total system performance. Furthermore, more extensive tests are vital to investigate if the battery lifetime is increased in real applications. Such a test would also provide more valuable information on how battery lifetime is dependent on parameters like temperature, magnitude and duration of charge and discharge currents, cooling and delivered peak power. This knowledge is extremely important when control strategies are developed and the battery-EC system is dimensioned.

Another investigation of importance is the optimisation of the system dimensioning, concerning total costs, lifetime, maintenance demands etc.



## 9. References

- [1] Lai J-S, Levy S, Rose M F, *High Energy Density Double-Layer Capacitors for Energy Storage Applications*, IEEE AES magazine, p14-19, 1992
- [2] Hansson J, Volvo Technology, personal discussions
- [3] Conway B E, *Electrochemical Supercapacitors: Seientific fundametalns and Technological Applications*, New York, Kluwer Academic / Plenum Publishers, ISBN 0-306-45736-9, 1999
- [4] Magnusson R, *Active and Passive Equalization of Supercapacitor Voltages*, University College of Borås, Department of Electrical Engineering, 2003
- [5] Ng H K, Vyas A D, Santini D J, *The Prospects for Hybrid Electric Vehicles, 2005-2020: Results of a Delphi Study*, Argonne National Laboratory, ANL/ES/CP-99612, 1999
- [6] Advisor, <http://www.ctts.nrel.gov/analysis/advisor.html>, 2003-08-21
- [7] Medin C, *Modelling of a Planetary Gear Train for Simulation of a Power Split Hybrid Vehicle*, Chalmers University of Technology, Dept. of Signals and Systems, 2003
- [8] Bodén A, *Numerisk modellering av superkondensator*, Royal Institute of Technology, Dept. of Numerical Analysis and Computer Science, 2003
- [9] Torstensson P, Persson R, *Development of a Battery Simulator*, Master thesis, Lund Institute of Technology, Dept. of Industrial Electric Engineering and Automation, 2002
- [10] EUCAR Traction Battery Working Group, *Specification of Test Procedures for Electrical Vehicle Traction Batteries*, 1998
- [11] Axelsson F, *Investigation of Supercapacitors in a Series Hybrid Vehicle*, Chalmers University of Technology, Dept. of Signals and Systems, 1998
- [12] NessCap Co., Ltd., <http://www.nesscap.com>, 2003-10-16
- [13] Saft, <http://www.saftbatteries.com>, 2003-10-16

# Appendix A: MATLAB<sup>®</sup>/SIMULINK<sup>®</sup> Models and MATLAB<sup>®</sup> files

This document contains all MATLAB<sup>®</sup>/SIMULINK<sup>®</sup> models and MATLAB<sup>®</sup> files used in simulations, calculations in MATLAB<sup>®</sup> and laboratory tests in MATLAB<sup>®</sup>/SIMULINK<sup>®</sup>/dSPACE<sup>®</sup>. There are small differences between models used in different simulations. To obtain the exact implementation of each simulated system, see CD-ROM.

## Section 1: Simulations

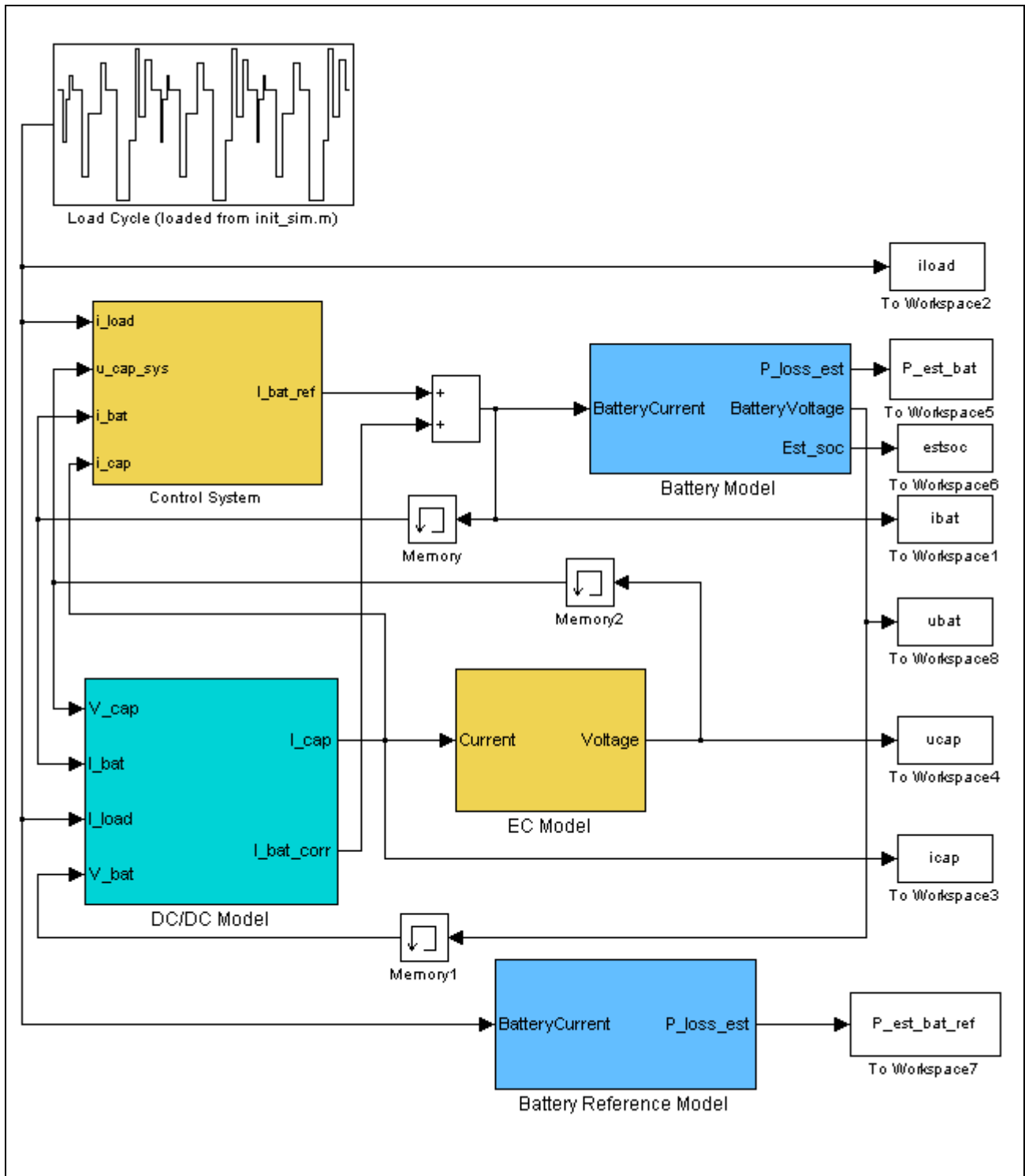


Figure 1 system\_sim02.mdl

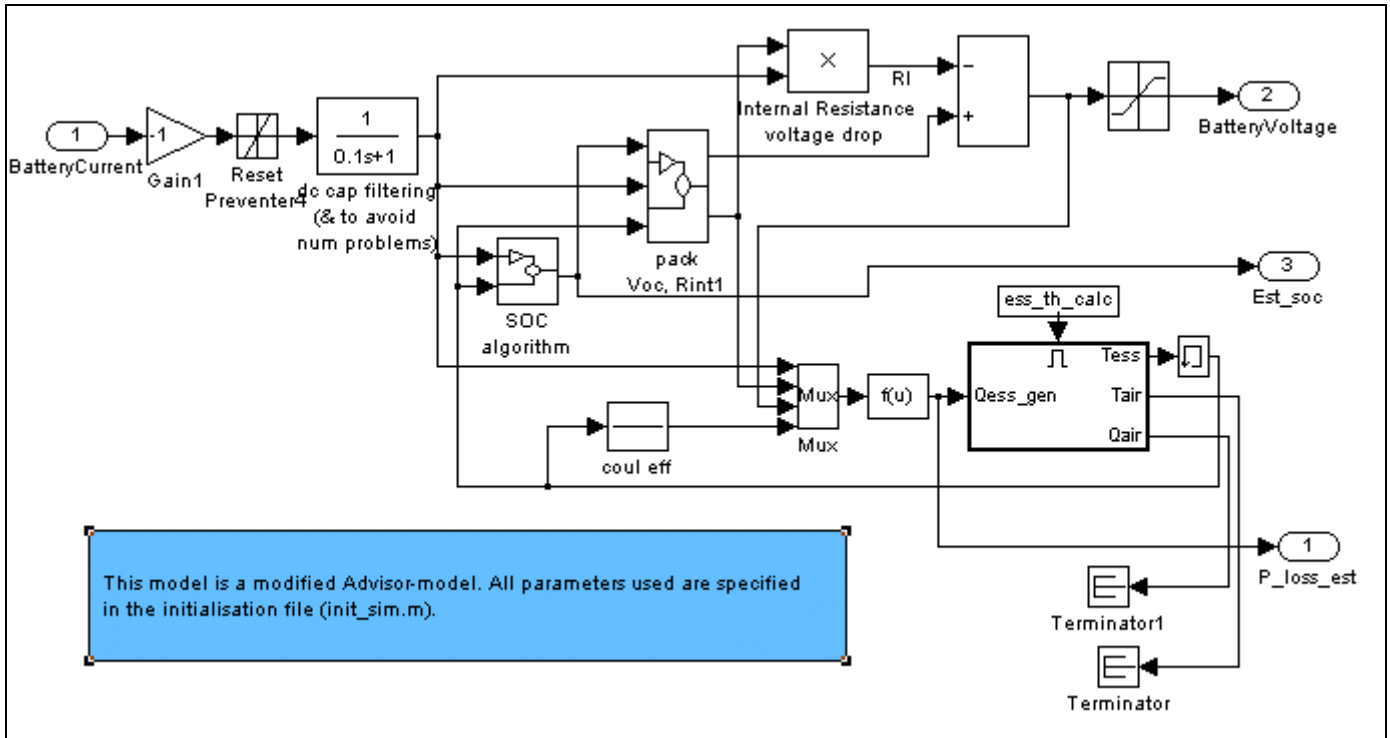


Figure 2 system\_sim02.mdl/Battery Model

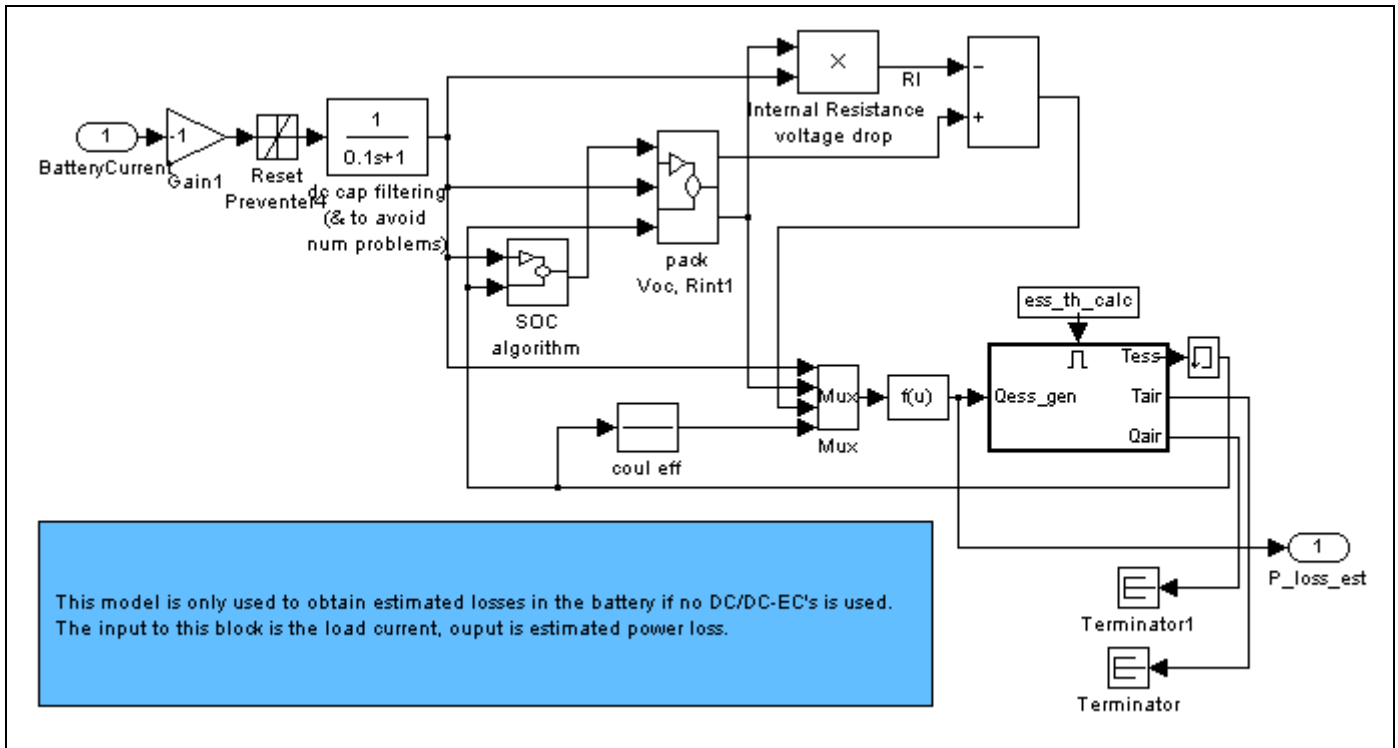


Figure 3 system\_sim02.mdl/Battery Reference Model

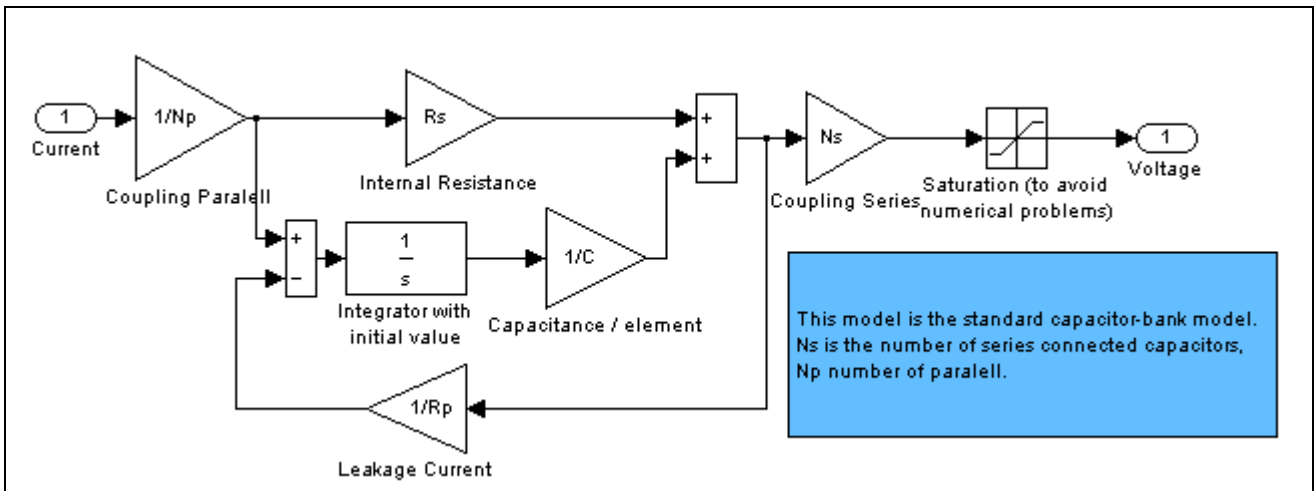


Figure 4 system\_sim02.mdl/EC Model

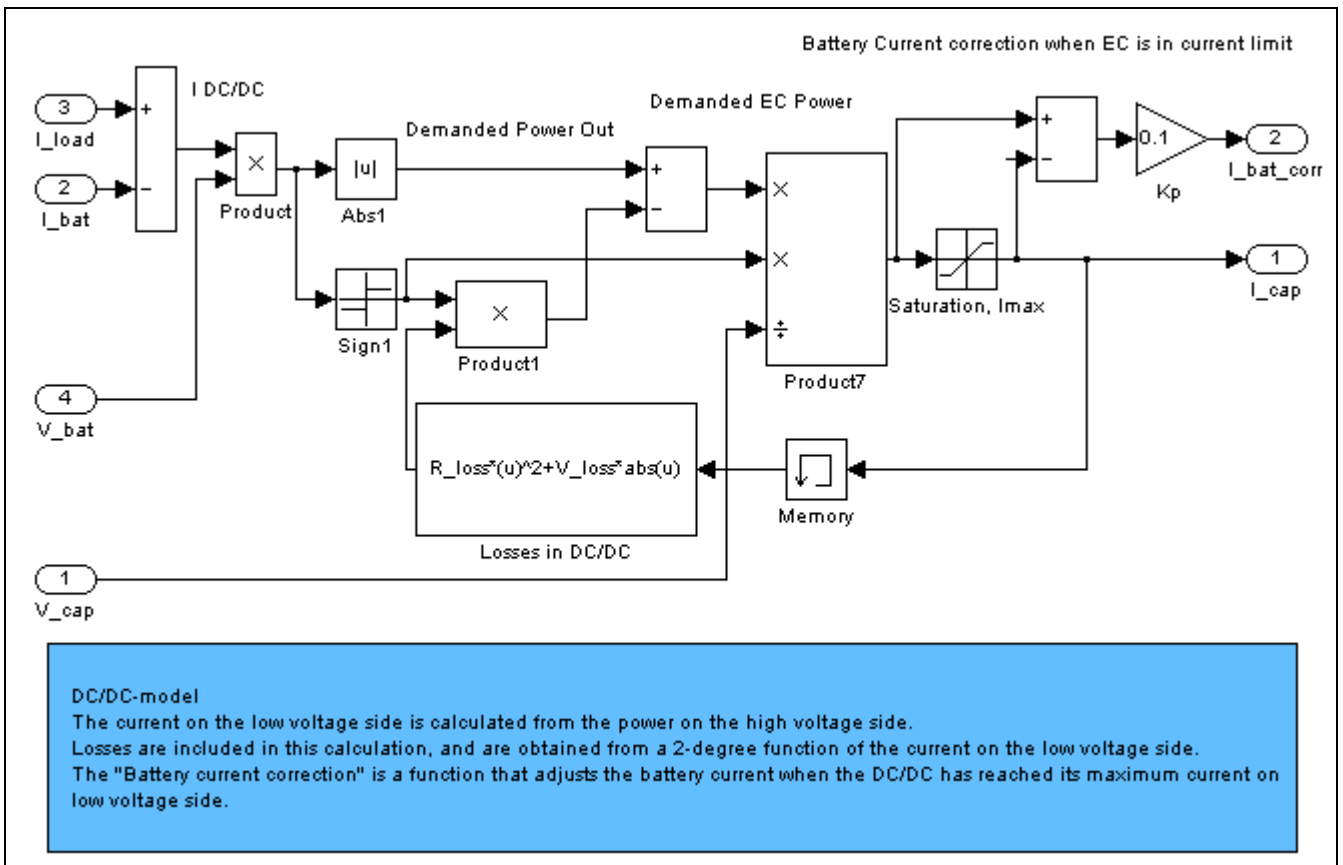


Figure 5 system\_sim02.mdl/DC/DC Model

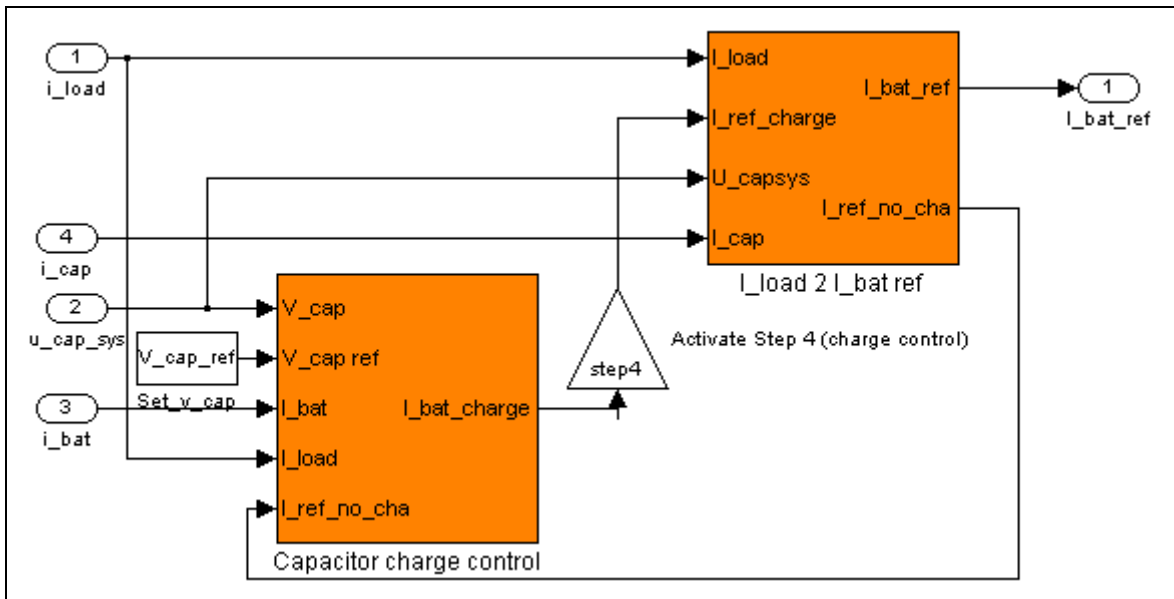


Figure 6 system\_sim02.mdl/Control System

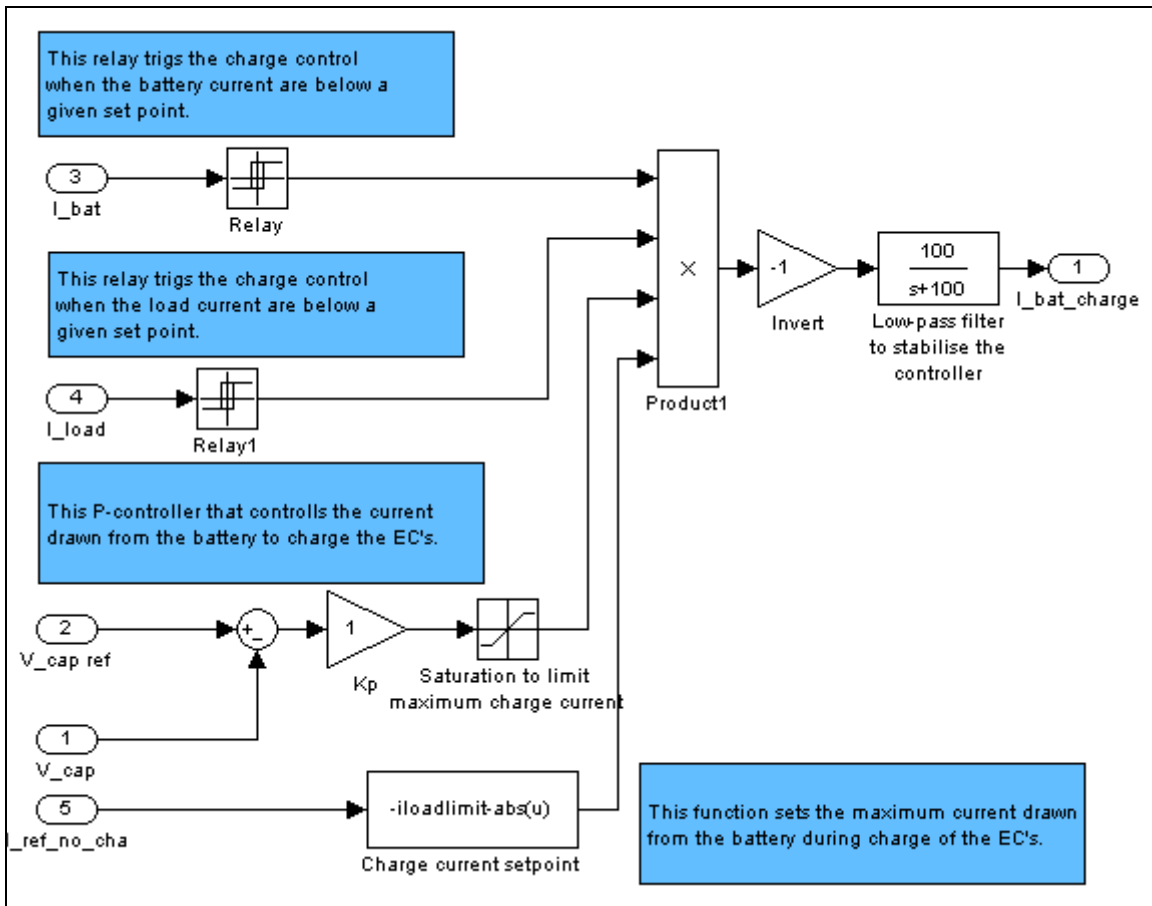


Figure 7 system\_sim02.mdl/Control System/Capacitor charge control

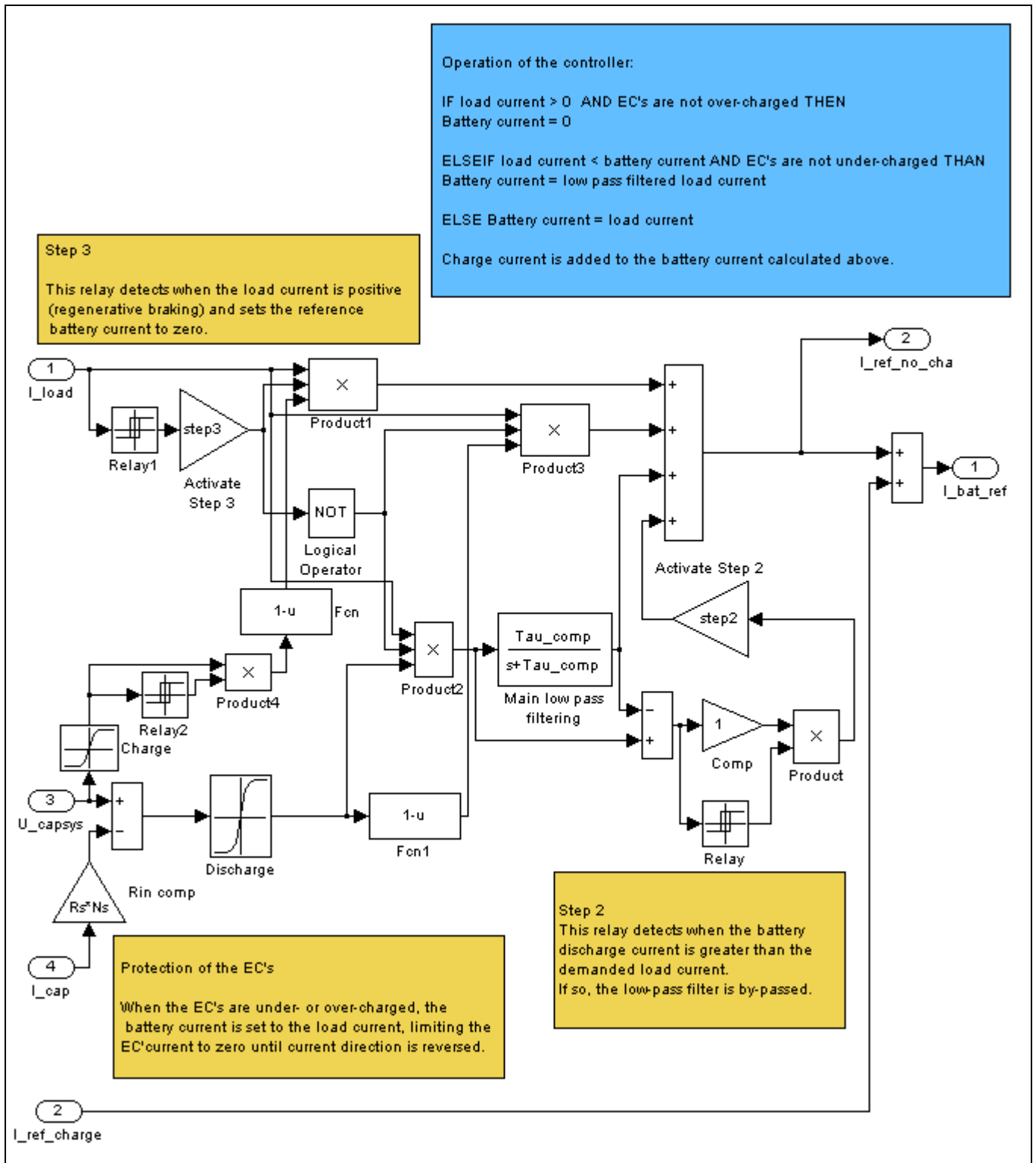


Figure 8 system\_sim02.mdl/ Control System/I\_load\_2\_I\_bat\_ref

The two files shown below is used in the *Size II* simulations.

```
%init_sim.m
%-----
% Initiation file for simulations of battery-EC system
%
% Tobias Andersson and Jens Groot 2003
% Last modification date 2003-10-16
%-----

%-----
% Initiation of Load
%-----

t_load=[0 11 11 15 15 23 23 28 28 49 49 61 61 85 85 96 96 117 117 143 143 155 155 163 163 176 176 188 188
195];
p_load=[0 0 11.1 11.1 2 2 -2.8 -2.8 0 0 18.2 18.2 5.1 5.1 -5.6 -5.6 0 0 23.2 23.2 10.5 10.5 -8.5 -8.5 5.8
5.8 -6.2 -6.2 0 0];
weight_constant=-2.5;
i_cycle=p_load.*weight_constant;

%-----
% Initiation of Controllers
%-----

Risetime_load_comp=35;           % Rise time of low pass filter
Tau_comp=1/Risetime_load_comp; % Timeconstant of low pass filter

step1=1;
step2=1;           %Set to 1 to activate step 2
step3=1;           %Set to 1 to activate step 3
step4=1;           %Set to 1 to activate step 4
label2='';
label3='';
label4='';

if step4==1
    label4=' ,4';
end

if step3==1
    label3=' ,3';
end

if step2==1
    label2=' ,2';
end

label=['Control using Step 1' label2 label3 label4];

%-----
% Initiation of Charge Control
%-----

ibatlimit=-25;           %Battery limit when charging is possible
iloadlimit=-15;         %Load limit when charging is possible. Also sets the maximum battery discharge
current                 %under steady-state charge

%-----
% Initiation of supercap
%-----

Ns=28;                   % Number of capacitors in series
Np=1;                   % Number of capacitors in parallel

V_max_per_cap=2;        % (V) The maximum capacitor voltage per capacitor
V_min_per_cap=0.5;      % (V) The minimum capacitor voltage per capacitor

Rs=0.89e-3;             % (Ohm) The series resistanse per capacitor
Rp=1e3;                 % (Ohm) The parallel resistanse per capacitor
```



```

#####Limit
settings#####
max_current=400*num_para_lines;           % A Maximum current for this battery
ess_min_volts=0.87*10;                    % V Minimum voltage times 10 cells (per module)
ess_max_volts=1.65*10;                    % V Maximum voltage times 10 cells (per module)
min_SOC=0.1;                              % Minimum SOC
max_SOC=0.9;                              % Maximum SOC
max_temp=(50 + 273);                      % K Maximum temperature in battery

#####End limit
settings#####

#####Temperature in Battery#####

ess_th_calc=1;                            % -- 0=no ess thermal calculations, 1=do calc's
ess_mod_cp=830;                            % J/kgK ave heat capacity of module (estimated for NiMH)
ess_set_tmp=35;                            % C thermostat temp of module when cooling fan comes on
ess_area_scale=1.6*(ess_module_mass/11)^0.7; % -- if module dimensions are unknown, assume rectang
shape and scale vs PB25
%tm:3/24/00 ess_mod_sarea=0.2*ess_area_scale; % m^2 total module surface area exposed to
cooling air (typ rectang module)
ess_mod_sarea=2*(0.385*0.119+0.102*0.119); % m^2 total module surface area exposed to cooling
air (typ rectang module)
ess_mod_airflow=0.01*4;                    % kg/s cooling air mass flow rate across module (20 cfm=0.01
kg/s at 20 C)
%tm:3/24/00 ess_mod_flow_area=0.005*ess_area_scale; % m^2 cross-sec flow area for cooling air per
module (assumes 10-mm gap btwn mods)
ess_mod_flow_area=0.005*2*(0.385+0.102); % m^2 cross-sec flow area for cooling air per module
(assumes 10-mm gap btwn mods)
ess_mod_case_thk=2/1000;                  % m thickness of module case (typ from Optima)
ess_mod_case_th_cond=0.20;               % W/mK thermal conductivity of module case material (typ
polyprop plastic - Optima)
ess_air_vel=ess_mod_airflow/(1.16*ess_mod_flow_area); % m/s ave velocity of cooling air
ess_air_htcoef=30*(ess_air_vel/5)^0.8; % W/m^2K cooling air heat transfer coef.
ess_th_res_on=((1/ess_air_htcoef)/ess_mod_sarea+(ess_mod_case_thk/ess_mod_case_th_cond)); % K/W tot
thermal res key on
ess_th_res_off=((1/4)/ess_mod_sarea + (ess_mod_case_thk/ess_mod_case_th_cond)); % K/W tot thermal res key
off (cold soak)
% set bounds on flow rate and thermal resistance
ess_mod_airflow=max(ess_mod_airflow,0.001);

Rth=ess_th_res_on;
ess_mod_cp=830;                            % J/kgK Ave heat capacity of module (estimated for NiMH)
air_cp= 1010;                              % J/kgK Heat capacity of air under 50 C and at low
humidity

clear ess_mod_sarea ess_mod_flow_area ess_mod_case_thk ess_mod_case_th_cond ess_air_vel ess_air_htcoef
ess_area_scale
%END#####Temperature in Battery#####

#####
% SOC RANGE over which data is defined
#####
ess_soc=[0:.1:1]; % (--)

#####
% Temperature range over which data is defined
#####
ess_tmp=[0 22 40]; % (C)

#####
% LOSS AND EFFICIENCY parameters
#####
% Parameters vary by SOC horizontally, and temperature vertically

ess_max_ah_cap=[
60
60

```

```

60
]; % (A*h), max. capacity at C/5 rate, indexed by ess_tmp

% average coulombic (a.k.a. amp-hour) efficiency below, indexed by ess_tmp
ess_coulombic_eff=[
    1
    1
    1
]*0.975; % (--); unknown

ess_r_dis=[2.1 1.5 1.2 1.16 1.13 1.1 1.1 1.1 1.05 0.95 0.8
    2.1 1.5 1.2 1.16 1.13 1.1 1.1 1.1 1.05 0.95 0.8
    2.1 1.5 1.2 1.16 1.13 1.1 1.1 1.1 1.05 0.95 0.8
    ]*10/1000; % (ohm)

% module's resistance to being charged, indexed by ess_soc and ess_tmp
ess_r_chg=ess_r_dis;% (ohm), no other data available
ess_voc=[12.8 13.2 13.5 13.7 13.8 13.8 13.9 14 14.1 14.3 14.6;
    12.8 13.2 13.5 13.7 13.8 13.8 13.9 14 14.1 14.3 14.6;
    12.8 13.2 13.5 13.7 13.8 13.8 13.9 14 14.1 14.3 14.6]; % (V), Source: Ovonic Charge-increasing

corr_voc=ess_voc(1,round(SOC/0.1))/voc_real;
ess_voc=ess_voc./corr_voc;

```



```

%p_proc.m
%-----
% Simulation file for battery-EC system
%
% Tobias Andersson and Jens Groot 2003
% Last modification date 2003-10-16
%-----

%clear all
%close all
%Simulation time
disp('Settings: ')
disp(' ')
Num_cycle=1; %Number of urban cycles
T=Num_cycle*195; %Length of each cycle

init_sim %Initialisation of system

sim('system_sim02r121',[0 T])

%Mapping - simulation output to variables
I_bat=ibat;
I_load=iload;
I_cap=icap;
U_cap=uacap;
U_bat=ubat;

%Display settings

disp_all
disp(' ')
disp('Results: ')

%Time steps in simulation and reality. Necessary if 'Variable Step' is used
%in Simulink

L=length(P_est_bat)-1;
t=[0:T/L:T];
t_s=t;

time_step_sim=t_s(2)-t_s(1);
time_step_real=time_step_sim;

%Reduction of RMS-current
n_I=length(I_bat);

```

```

RMS_I_bat=norm(I_bat)/sqrt(n_I);
RMS_I_load=norm(I_load)/sqrt(n_I);
RMS_I_cap=norm(I_cap)/sqrt(n_I);
RMS_Ratio=RMS_I_bat/RMS_I_load*100;
disp(['Battery RMS Current Ratio = ' num2str(round(RMS_Ratio)) ' %'])

%Reduction of losses in battery. Losses is calculated from directly in the
%Advisor battery model
W_loss_bat=-sum(P_est_bat.*time_step_sim);
W_loss_bat_ref=-sum(P_est_bat_ref.*time_step_sim);
W_loss_ratio=W_loss_bat/W_loss_bat_ref*100;
disp(['Battery Loss Ratio = ' num2str(round(W_loss_ratio)) ' %'])

%Total Energy efficiency. Calculated as the ratio between total energy
%absorbed by the load and the total energy delivered from the battery and
%the EC's
Total_load=sum(U_bat.*I_load).*time_step_real;
Total_bat=sum((U_bat-I_bat.*R_per_cell*ess_module_num*10).*I_bat).*time_step_real;
%Total_bat=sum(U_bat.*I_bat).*time_step_real+W_loss_bat;

W_initcap=(C/Ns)*0.5*mean(U_cap(1:10)).^2;
U_capfinal=mean(U_cap(length(U_cap)-10:length(U_cap)))-mean(I_cap(length(U_cap)-10:length(U_cap)))*Rs*Ns;
W_finalcap=(C/Ns)*0.5*U_capfinal.^2;
Total_cap=W_finalcap-W_initcap;
Total_sys=Total_bat+Total_cap;
Energy_efficiency=Total_load/Total_sys*100;
disp(['Total Efficiency = ' num2str(round(Energy_efficiency)) ' %'])

% %DC/DC Energy Efficiency
% s1=find(I_load-I_bat>0);
% s2=find(I_load-I_bat<0);
%
% %Charge Efficiency
% delta_cap_W=sum(U_cap(s1).*I_cap(s1))*time_step_real;
% In_W=sum(U_bat(s1).*(I_load(s1)-I_bat(s1)))*time_step_real;
% cha_eff=delta_cap_W/In_W*100;
% disp(['DC/DC Charge Efficiency = ' num2str(round(cha_eff)) ' %'])
%
% %Discharge Efficiency
% delta_cap_W=sum(U_cap(s2).*I_cap(s2))*time_step_real;
% Out_W=sum(U_bat(s2).*(I_load(s2)-I_bat(s2)))*time_step_real;
% dca_eff=Out_W/delta_cap_W*100;
% disp(['DC/DC Discharge Efficiency = ' num2str(round(dca_eff)) ' %'])

% Charge capacity. This parameter is the mean value of the EC-voltage
% compared to the reference voltage.
for k=1:Num_cycle
v(k)=mean(U_cap((k-1)*195+1:k*195/time_step_real));
ch(k)=v(k)/V_init_cap.*100;
end

disp(['Charge performance = ' num2str(round(ch)) ' %'])

plot_all

```

**Section 2: Laboratory test set-up in MATLAB®/SIMULINK®/dSPACE®**

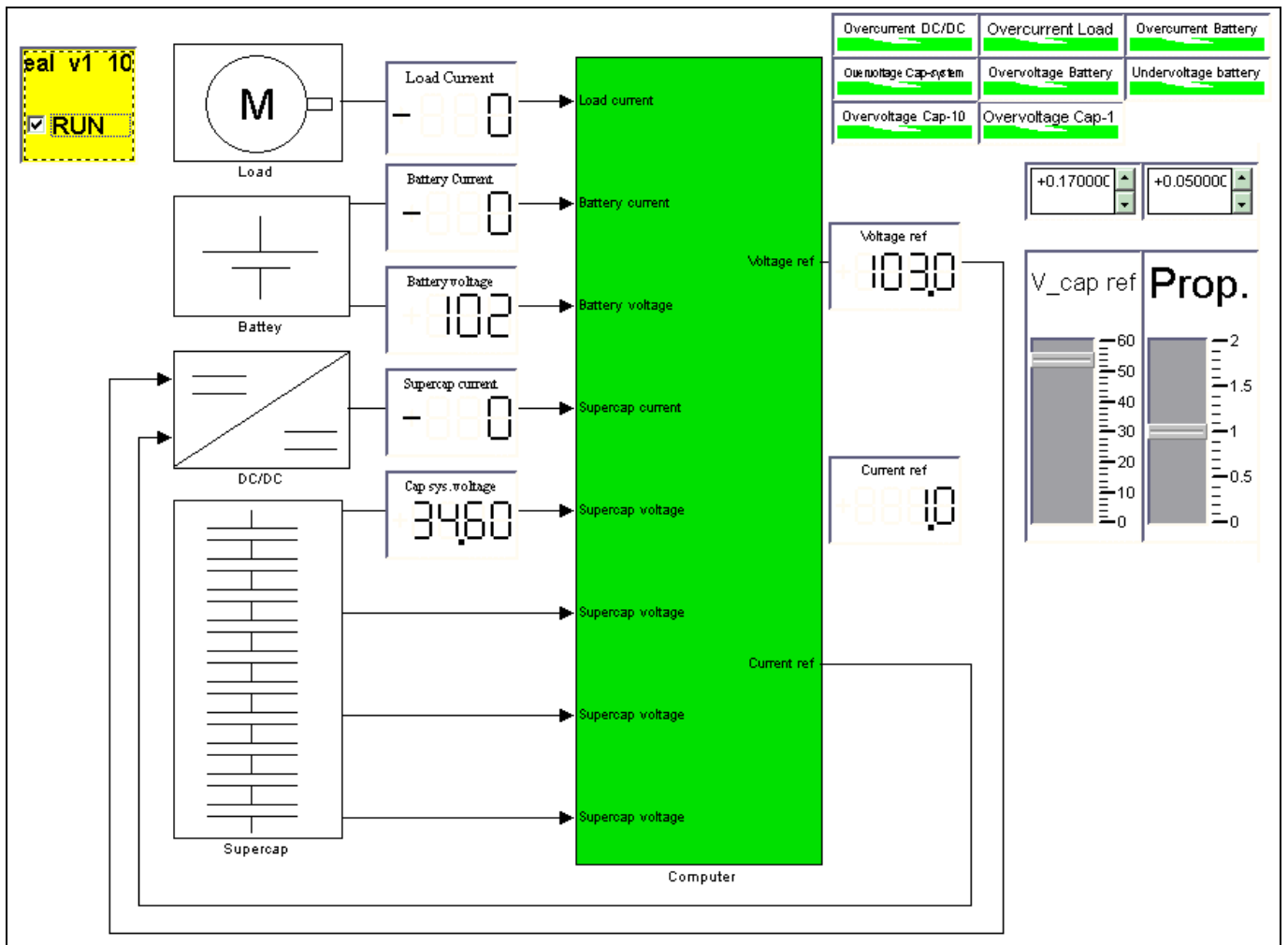


**Figure 9 View from dSPACE®/ControlDesk®**

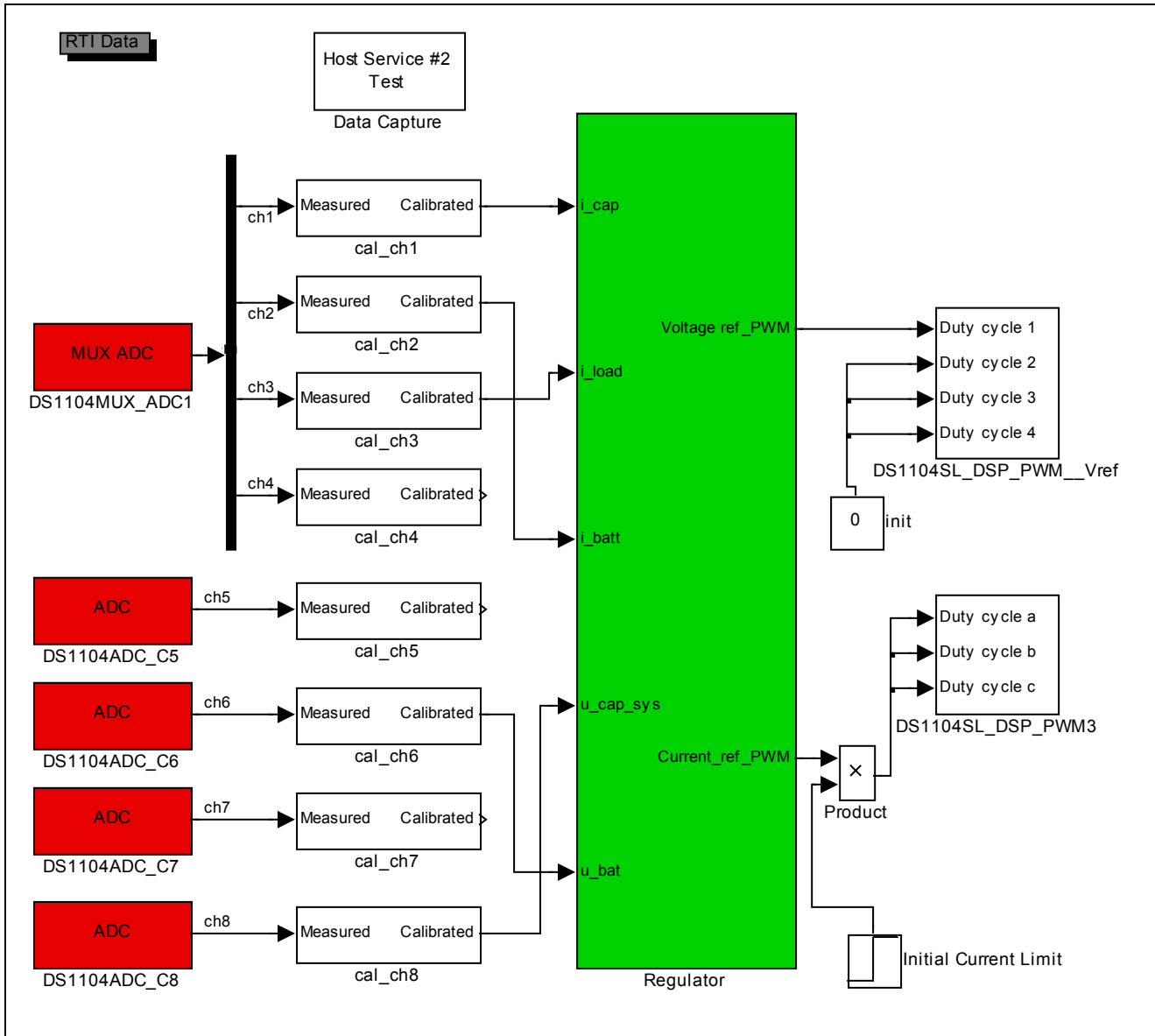


Figure 10 system\_real\_v1\_10.mdl

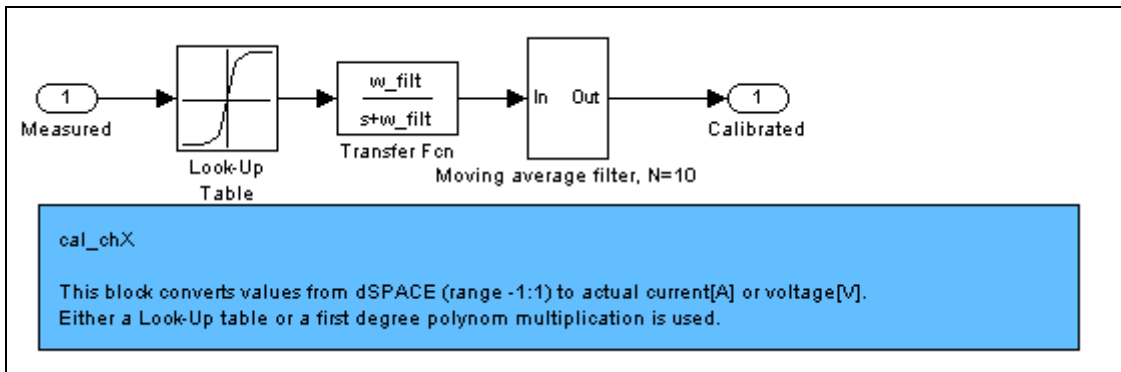


Figure 11 system\_real\_v1\_10.mdl/cal\_chX

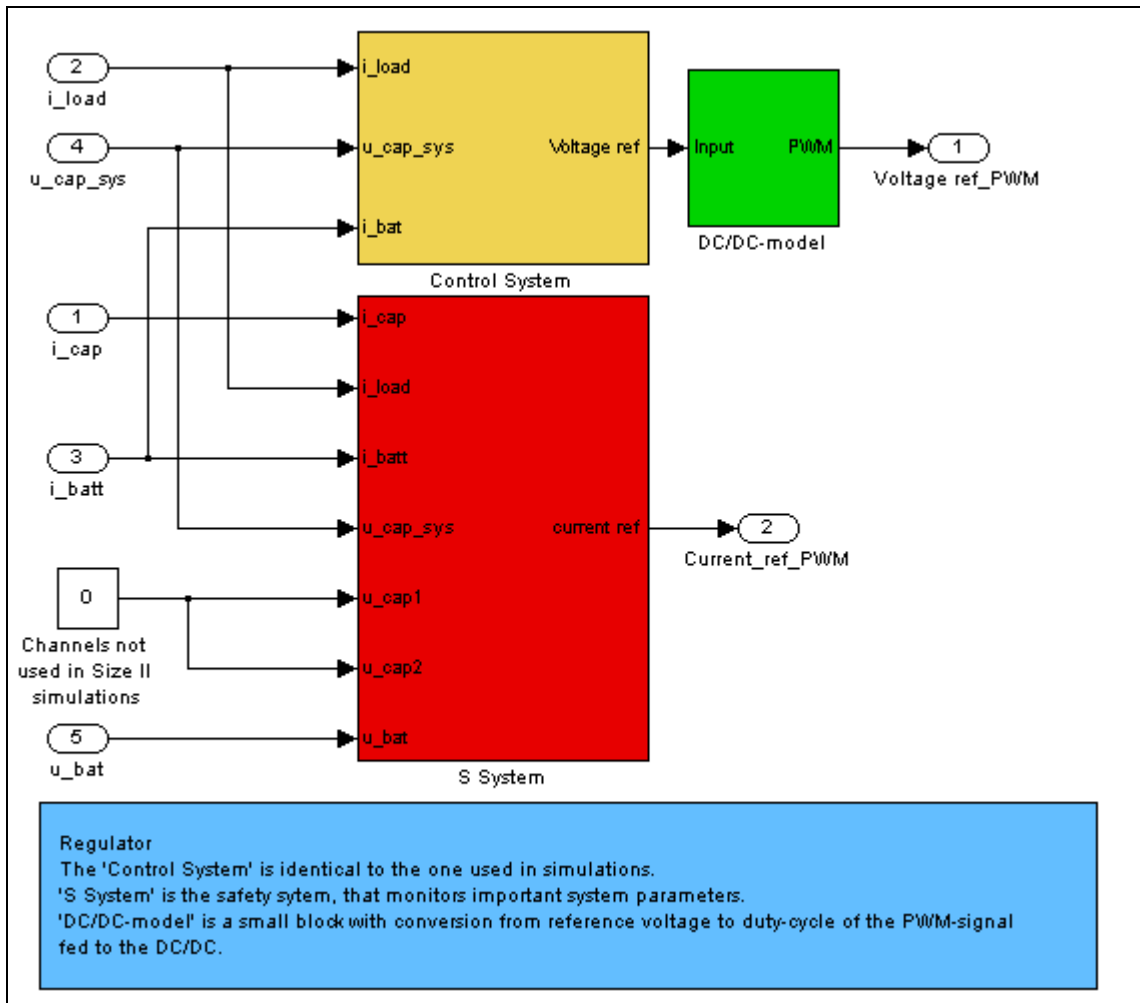


Figure 12 system\_real\_v1\_10.mdl/Regulator

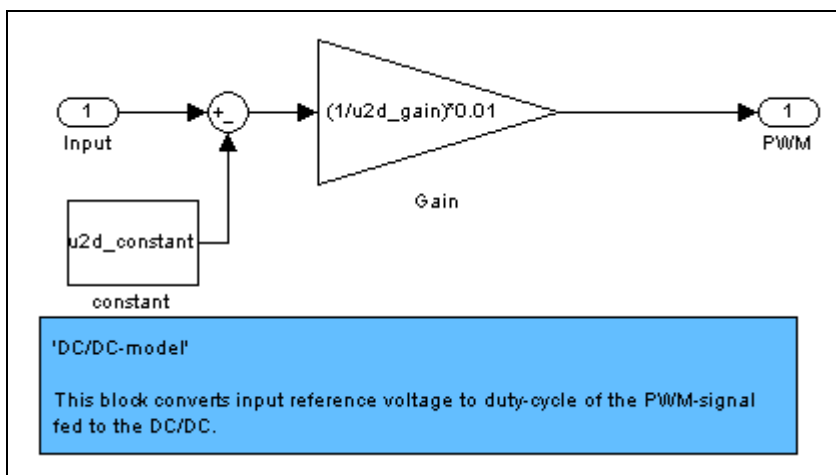


Figure 13 system\_real\_v1\_10.mdl/Regulator/DC/DC-model

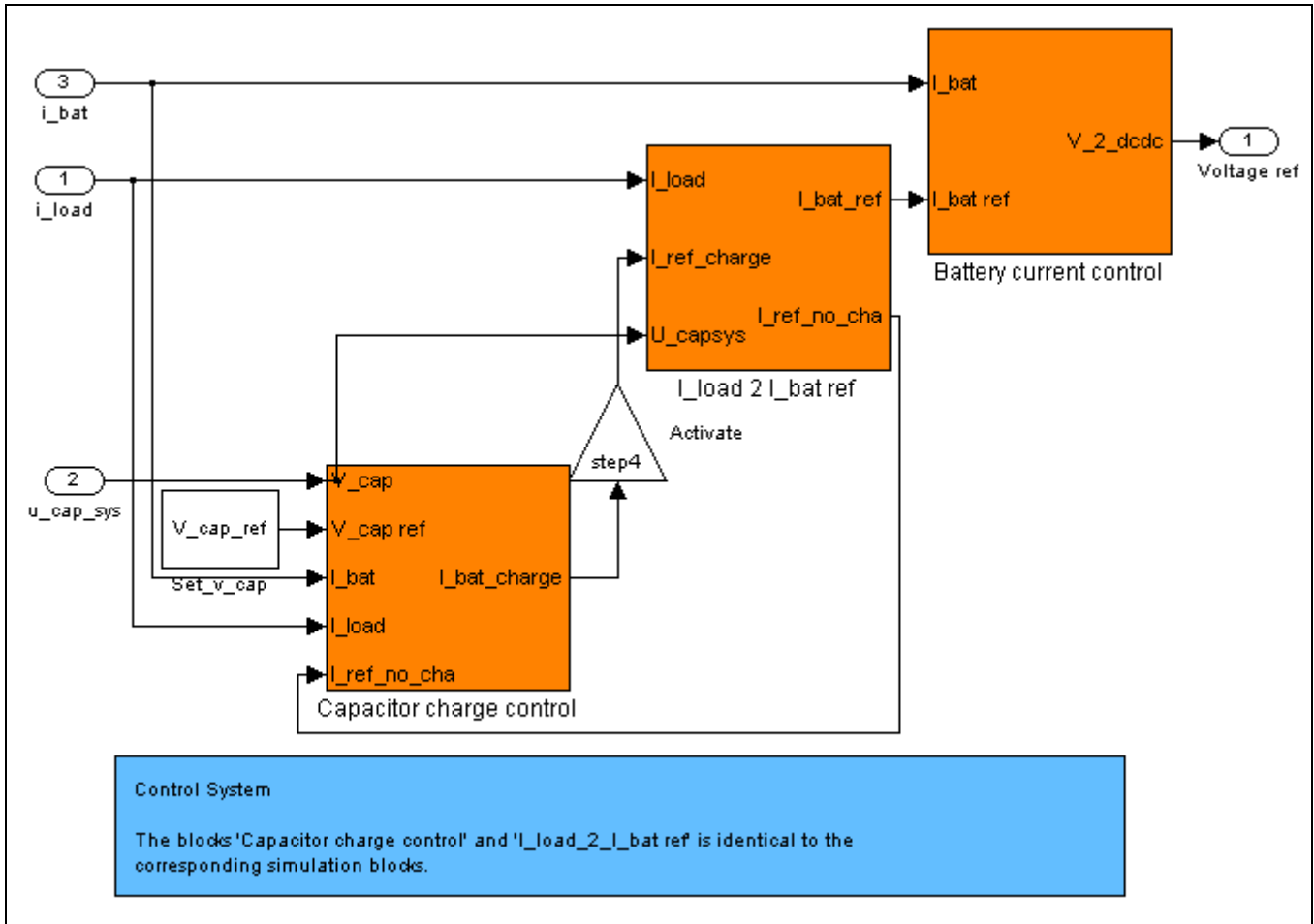


Figure 14 system\_real\_v1\_10.mdl/Regulator/Control System

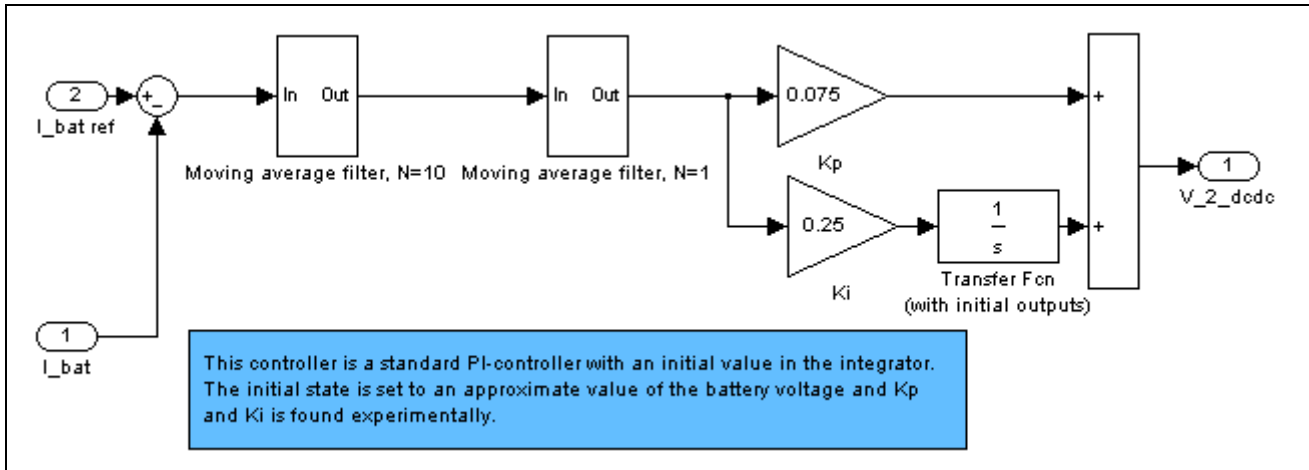


Figure 15 system\_real\_v1\_10.mdl/Regulator/Control System/Battery current control

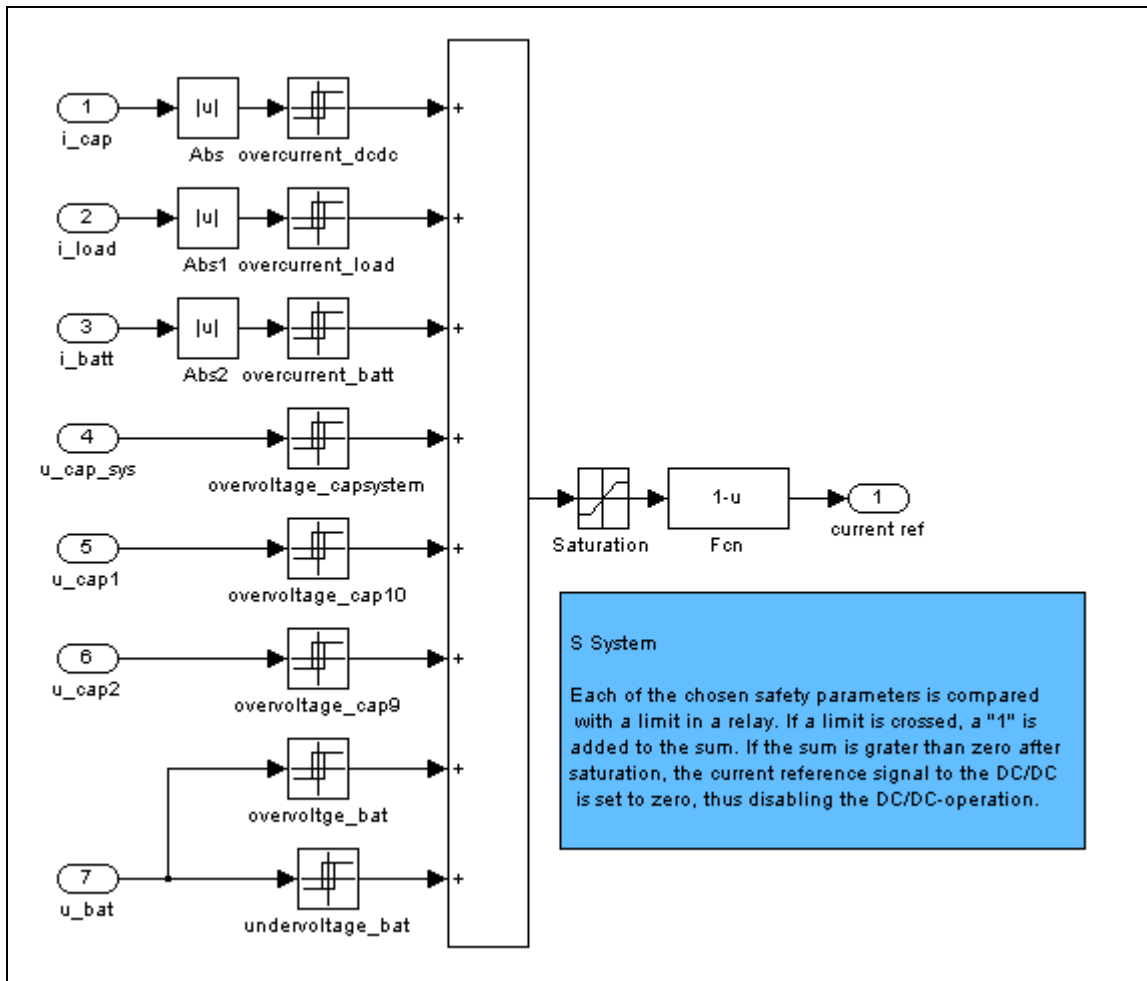


Figure 16 system\_real\_v1\_10.mdl/Regulator/S System

The SIMULINK<sup>®</sup> models are initialised via an init-file, similar to init\_sim.m.

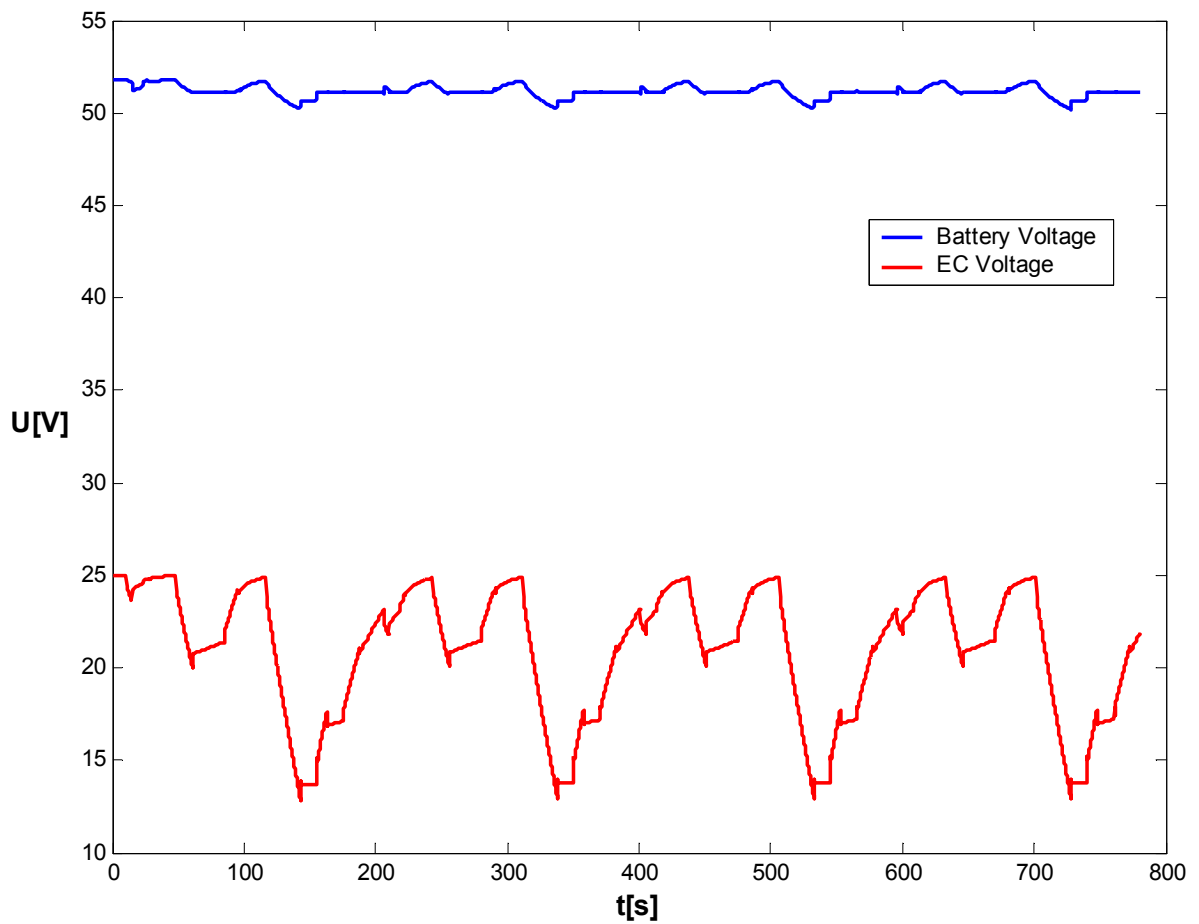
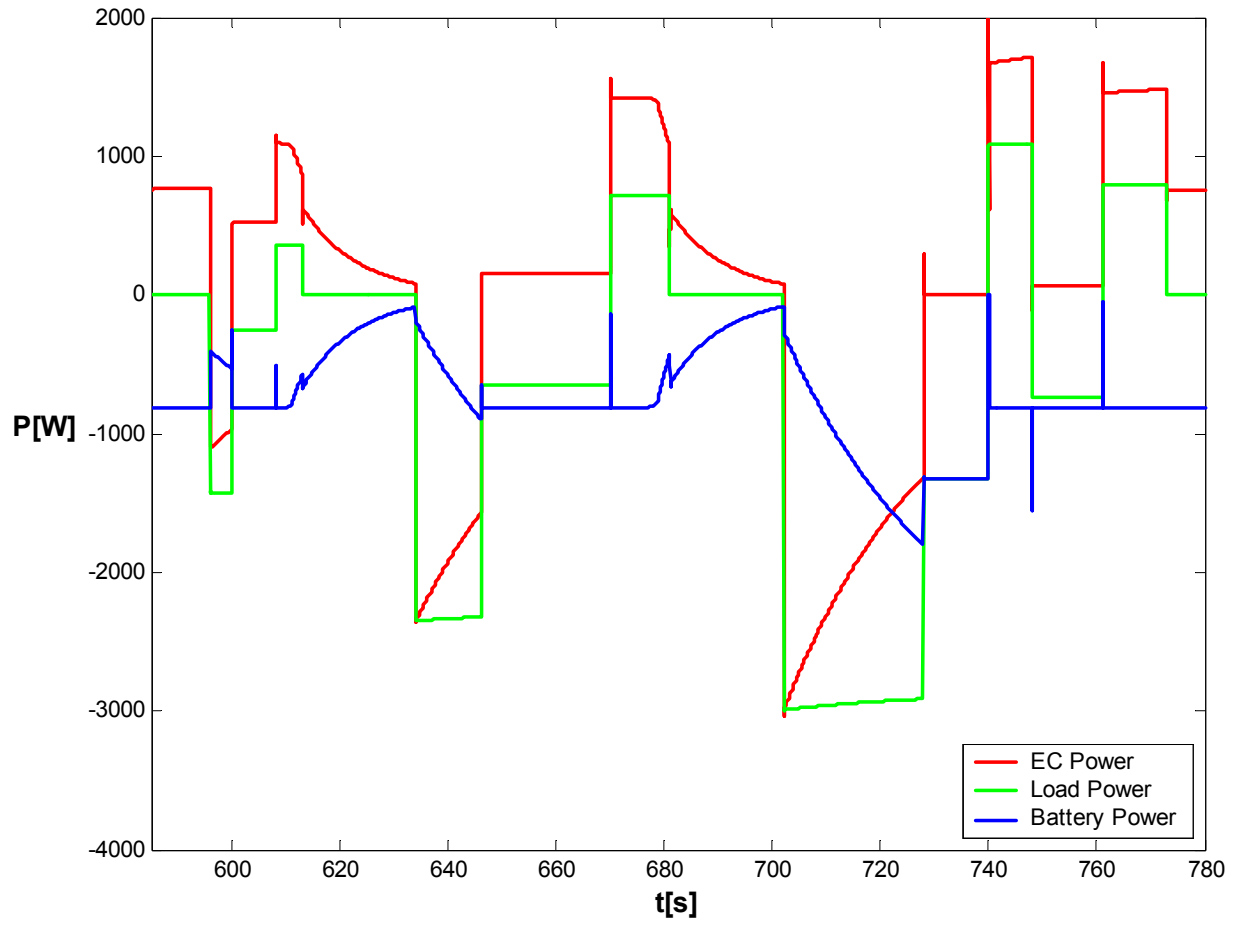
**Appendix B Results from Simulations and Experiments**

### Simulation of *Size I* system, 4 urban cycles.

Parameter	Matlab-variable	Value	Unit
Load cycle	p_load	ECE15-L	-
Number of cycles	Num_cycle	4	-
Weight constant to scale load	weight_constant	-2.5	-
Rise-time of low pass filter	Risetime_load_comp	30	s
Control strategy (see init_sim.m)	step1	1	-
	step2	1	-
	step3	1	-
	step4	1	-
Battery current limit (controls EC charge)	ibatlimit	-25	A
Load current limit (controls EC charge)	iloadlimit	-16	A
Number of series connected EC's	Ns	10	-
Number of parallel connected EC's	Np	1	-
Maximum unit voltage	V_max_per_cap	2.5	V
Minimum unit voltage	V_min_per_cap	0.5	V
Series Resistance	Rs	0.0008	$\Omega$
Leakage Resistance	Rp	1000	$\Omega$
Charge protection constant	c_cha	-100	-
Discharge protection constant	c_dch	-15	-
Unit capacitance	C	2605.522	F
EC-bank reference voltage	V_cap_ref	25	V
EC-bank initial voltage	V_init_cap	25	V
Battery SOC	SOC	0.5	-
DC/DC current limit	Imax	300	A
DC/DC loss function, resistive losses	R_loss	0.0028	$\Omega$
DC/DC loss function, voltage drop losses	V_loss	1.8921	V
Measured battery VOC (10cells)	voc_real	12.95	V
Measured battery internal resistance per cell	R_per_cell	0.0011326	$\Omega$
Number of 10cell-battery units	ess_module_num	4	-

Performance parameter	Matlab-variable	Value	Unit
RMS Battery Current	RMS_Ratio	61	%
Power loss in main battery	W_loss_ratio	33	%
Total energy efficiency	Energy_efficiency	84	%
Charge Control	ch	85 84 84 84	%

Simulation of *Size I* system, 4 cycles.

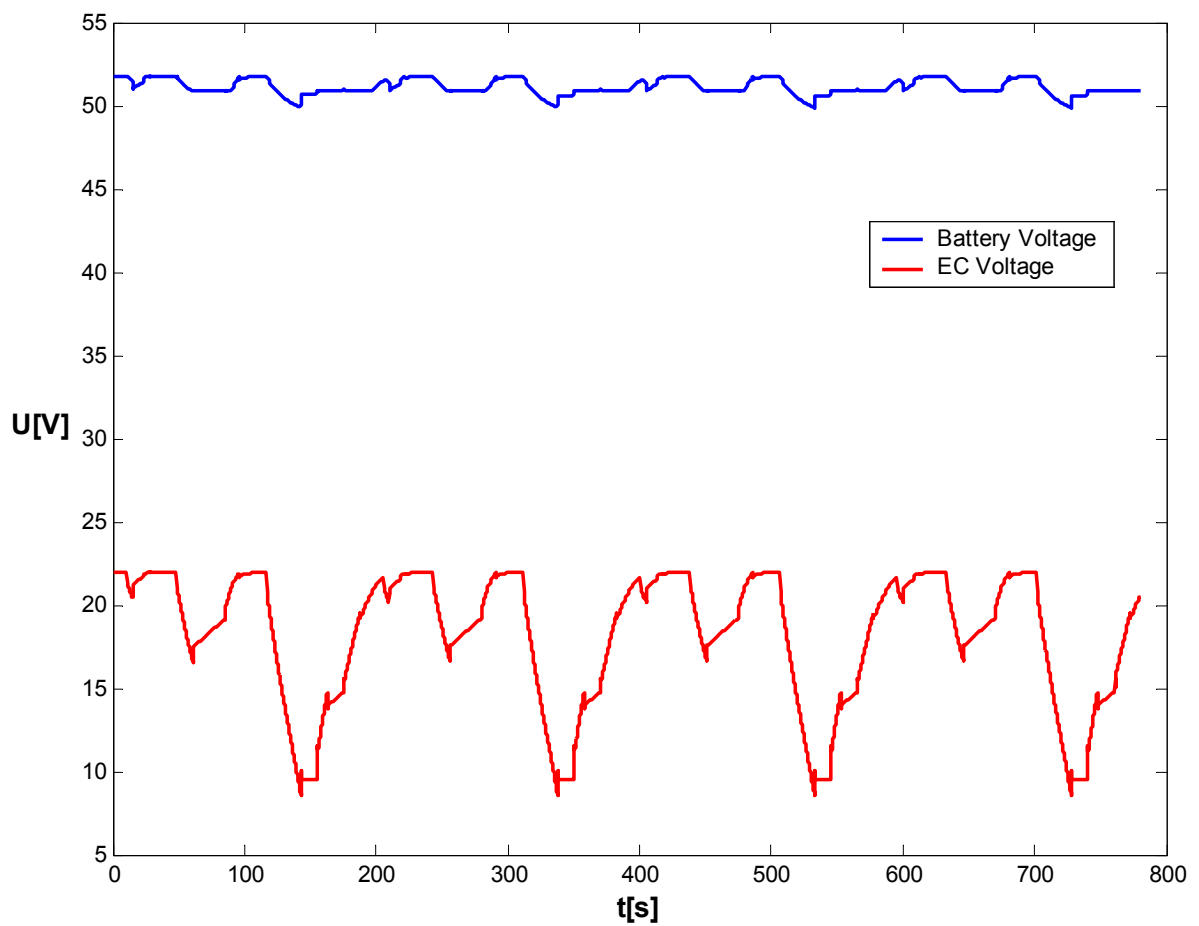
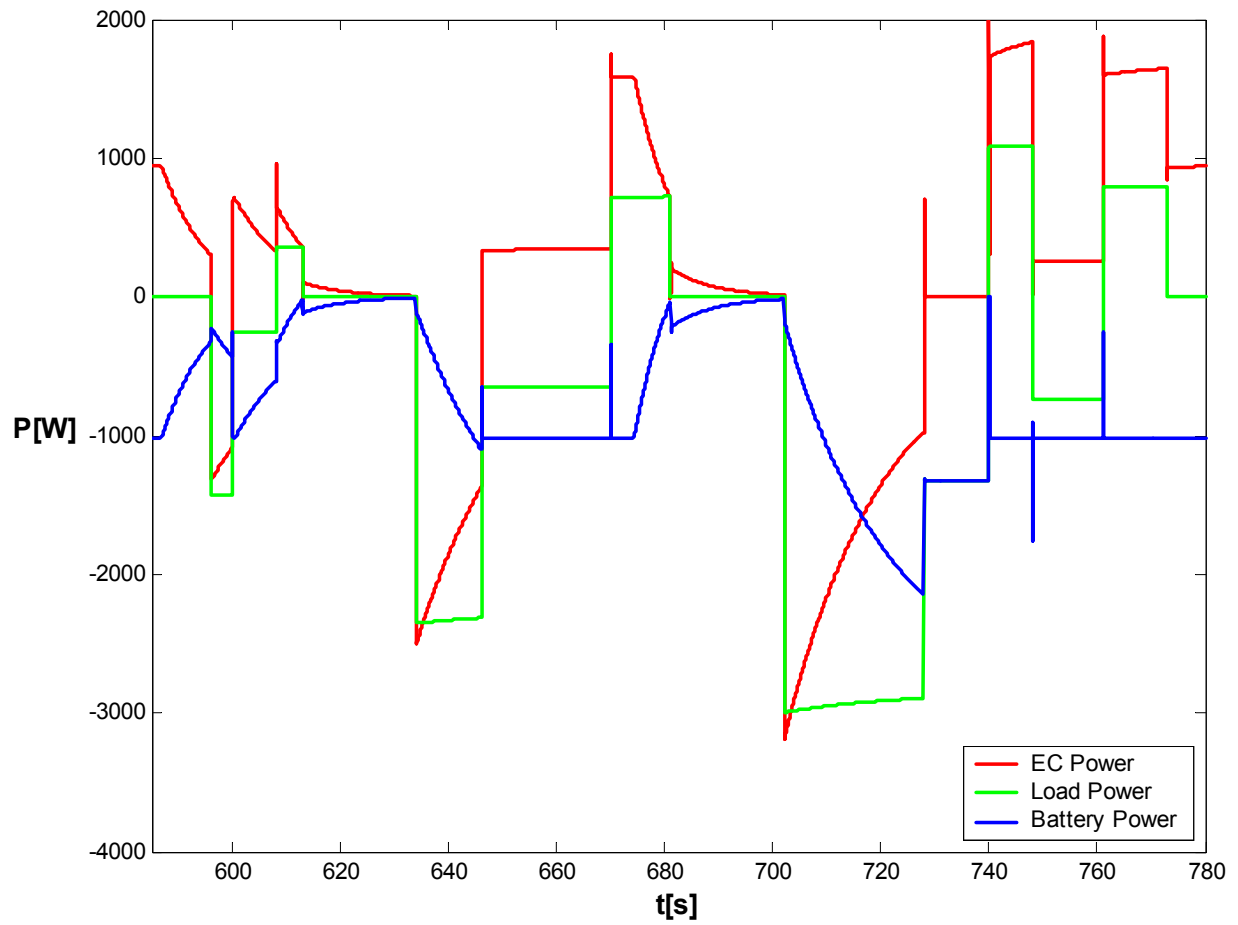


### Simulation of *Size I* system with passive balancing, 4 urban cycles.

Parameter	Matlab-variable	Value	Unit
Load cycle	p_load	ECE15-L	-
Number of cycles	Num_cycle	4	-
Weight constant to scale load	weight_constant	-2.5	-
Rise-time of low pass filter	Risetime_load_comp	20	s
Control strategy (see init_sim.m)	step1	1	-
	step2	1	-
	step3	1	-
	step4	1	-
Battery current limit (controls EC charge)	ibatlimit	-25	A
Load current limit (controls EC charge)	iloadlimit	-20	A
Number of series connected EC's	Ns	10	-
Number of parallel connected EC's	Np	1	-
Maximum unit voltage	V_max_per_cap	2.5	V
Minimum unit voltage	V_min_per_cap	0.5	V
Series Resistance	Rs	0.0008	$\Omega$
Leakage Resistance	Rp	1000	$\Omega$
Charge protection constant	c_cha	-100	-
Discharge protection constant	c_dch	-15	-
Unit capacitance	C	2605.522	F
EC-bank reference voltage	V_cap_ref	22	V
EC-bank initial voltage	V_init_cap	22	V
Battery SOC	SOC	0.5	-
DC/DC current limit	I <sub>max</sub>	300	A
DC/DC loss function, resistive losses	R_loss	0.0028	$\Omega$
DC/DC loss function, voltage drop losses	V_loss	1.8921	V
Measured battery VOC (10cells)	voc_real	12.95	V
Measured battery internal resistance per cell	R_per_cell	0.0011326	$\Omega$
Number of 10cell-battery units	ess_module_num	4	-

Performance parameter	Matlab-variable	Value	Unit
RMS Battery Current	RMS_Ratio	69	%
Power loss in main battery	W_loss_ratio	43	%
Total energy efficiency	Energy_efficiency	81	%
Charge Control	ch	83 83 82 82	%

Simulation of *Size I* system with passive balancing, 4 cycles.

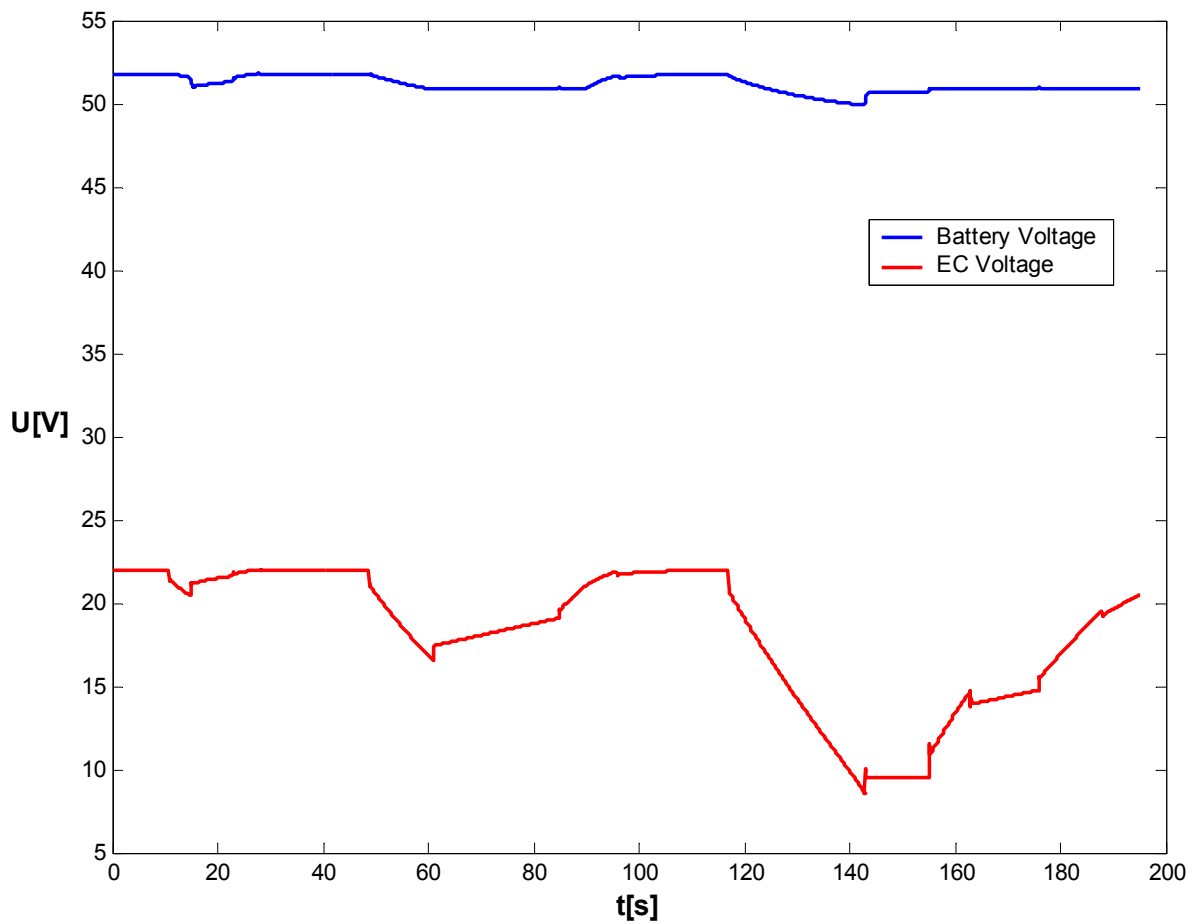
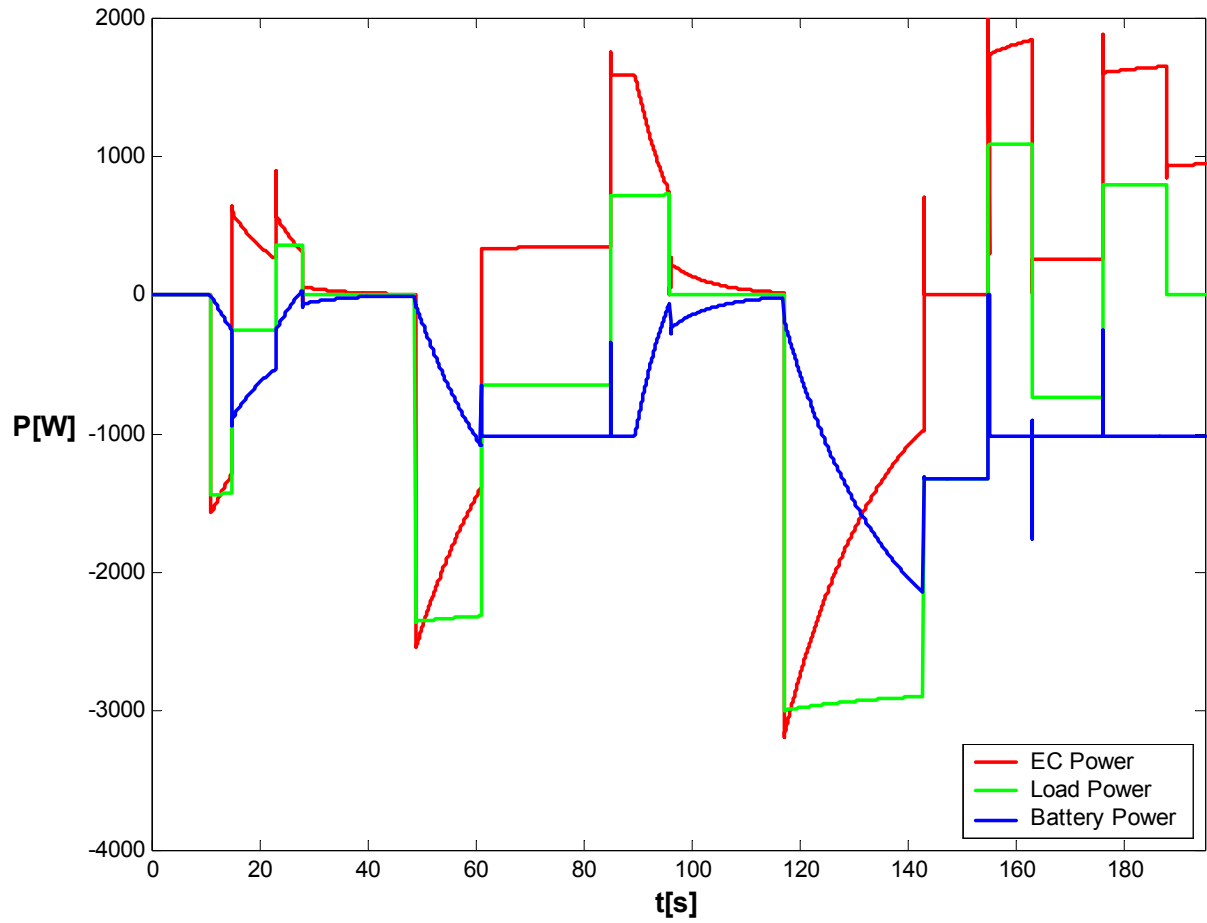


### Simulation of *Size I* system with passive balancing, 1 urban cycle.

Parameter	Matlab-variable	Value	Unit
Load cycle	p_load	ECE15-L	-
Number of cycles	Num_cycle	1	-
Weight constant to scale load	weight_constant	-2.5	-
Rise-time of low pass filter	Risetime_load_comp	20	s
Control strategy (see init_sim.m)	step1	1	-
	step2	1	-
	step3	1	-
	step4	1	-
Battery current limit (controls EC charge)	ibatlimit	-25	A
Load current limit (controls EC charge)	iloadlimit	-20	A
Number of series connected EC's	Ns	10	-
Number of parallel connected EC's	Np	1	-
Maximum unit voltage	V_max_per_cap	2.5	V
Minimum unit voltage	V_min_per_cap	0.5	V
Series Resistance	Rs	0.0008	$\Omega$
Leakage Resistance	Rp	1000	$\Omega$
Charge protection constant	c_cha	-100	-
Discharge protection constant	c_dch	-15	-
Unit capacitance	C	2605.522	F
EC-bank reference voltage	V_cap_ref	22	V
EC-bank initial voltage	V_init_cap	22	V
Battery SOC	SOC	0.5	-
DC/DC current limit	I <sub>max</sub>	300	A
DC/DC loss function, resistive losses	R_loss	0.0028	$\Omega$
DC/DC loss function, voltage drop losses	V_loss	1.8921	V
Measured battery VOC (10cells)	voc_real	12.95	V
Measured battery internal resistance per cell	R_per_cell	0.0011326	$\Omega$
Number of 10cell-battery units	ess_module_num	4	-

Performance parameter	Matlab-variable	Value	Unit
RMS Battery Current	RMS_Ratio	67	%
Power loss in main battery	W_loss_ratio	41	%
Total energy efficiency	Energy_efficiency	81	%
Charge Control	ch	83	%

Simulation of *Size I* system with passive balancing, 1 cycle.

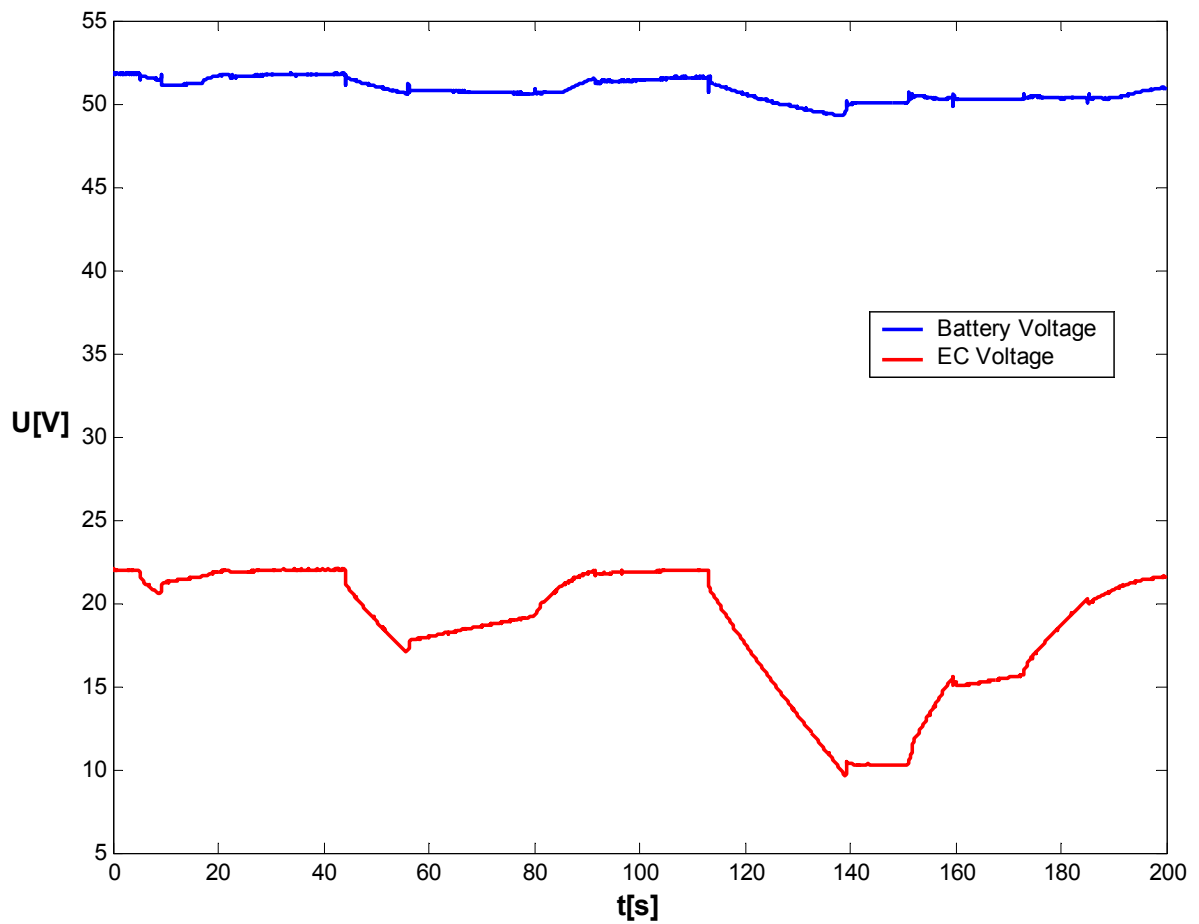
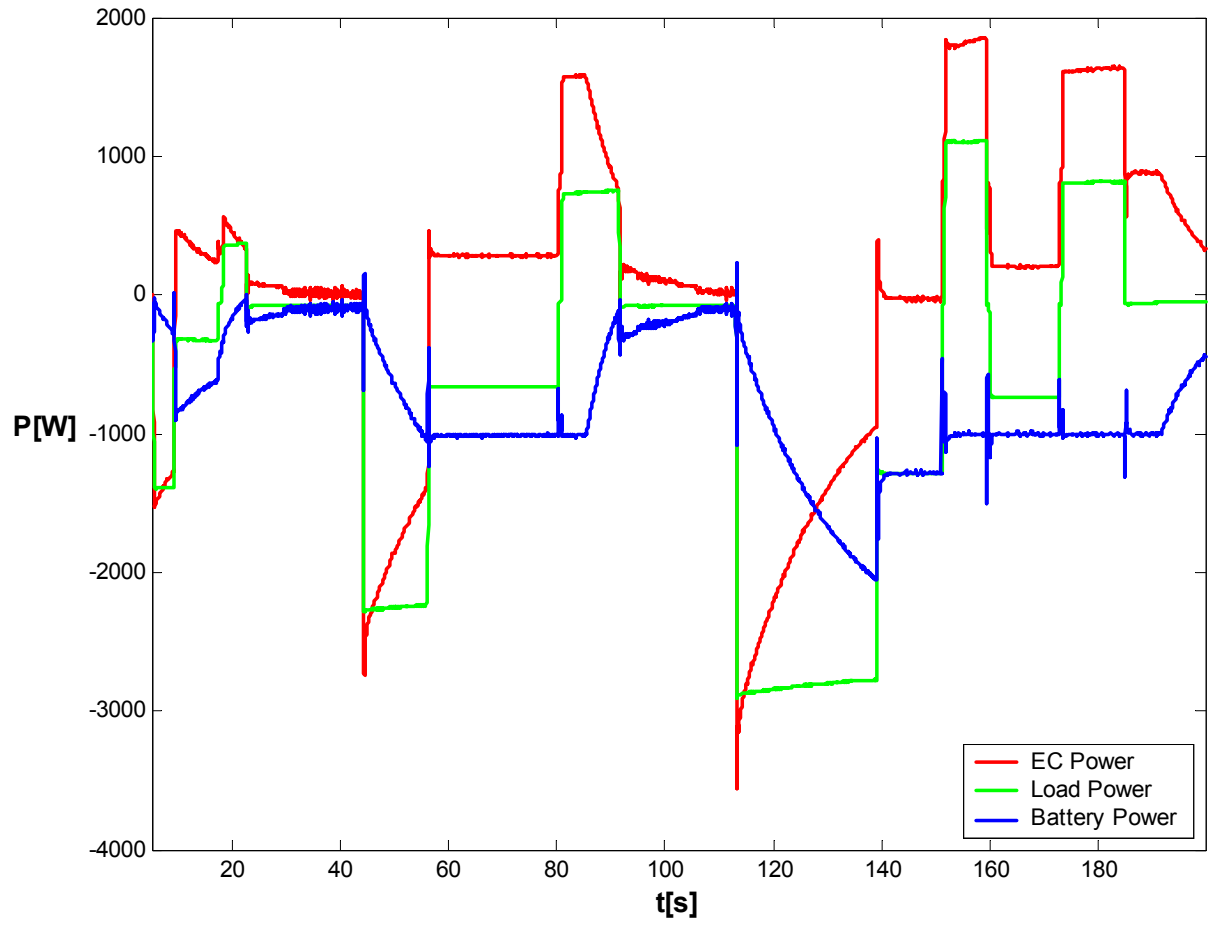


### Experimental results of *Size I* system with passive balancing, 1 urban cycle.

Parameter	Matlab-variable	Value	Unit
Load cycle	p_load	ECE15-L	-
Number of cycles	Num_cycle	1	-
Weight constant to scale load	weight_constant	-2.5	-
Rise-time of low pass filter	Risetime_load_comp	20	s
Control strategy (see init_sim.m)	step1	1	-
	step2	1	-
	step3	1	-
	step4	1	-
Battery current limit (controls EC charge)	ibatlimit	-25	A
Load current limit (controls EC charge)	iloadlimit	-20	A
Number of series connected EC's	Ns	10	-
Number of parallel connected EC's	Np	1	-
Maximum unit voltage	V_max_per_cap	2.5	V
Minimum unit voltage	V_min_per_cap	0.5	V
Series Resistance	Rs	0.0008	$\Omega$
Leakage Resistance	Rp	1000	$\Omega$
Charge protection constant	c_cha	-100	-
Discharge protection constant	c_dch	-15	-
Unit capacitance	C	2605.522	F
EC-bank reference voltage	V_cap_ref	22	V
EC-bank initial voltage	V_init_cap	22	V
Battery SOC	SOC	0.5	-
DC/DC current limit	I <sub>max</sub>	300	A
DC/DC loss function, resistive losses	R_loss	0.0028	$\Omega$
DC/DC loss function, voltage drop losses	V_loss	1.8921	V
Measured battery VOC (10cells)	voc_real	12.95	V
Measured battery internal resistance per cell	R_per_cell	0.0010375	$\Omega$
Number of 10cell-battery units	ess_module_num	4	-

Performance parameter	Matlab-variable	Value	Unit
RMS Battery Current	RMS_Ratio	70	%
Power loss in main battery	W_loss_ratio	41	%
Total energy efficiency	Energy_efficiency	81	%
Charge Control	ch	84	%

### Experimental results of *Size I* system with passive balancing, 1 cycle

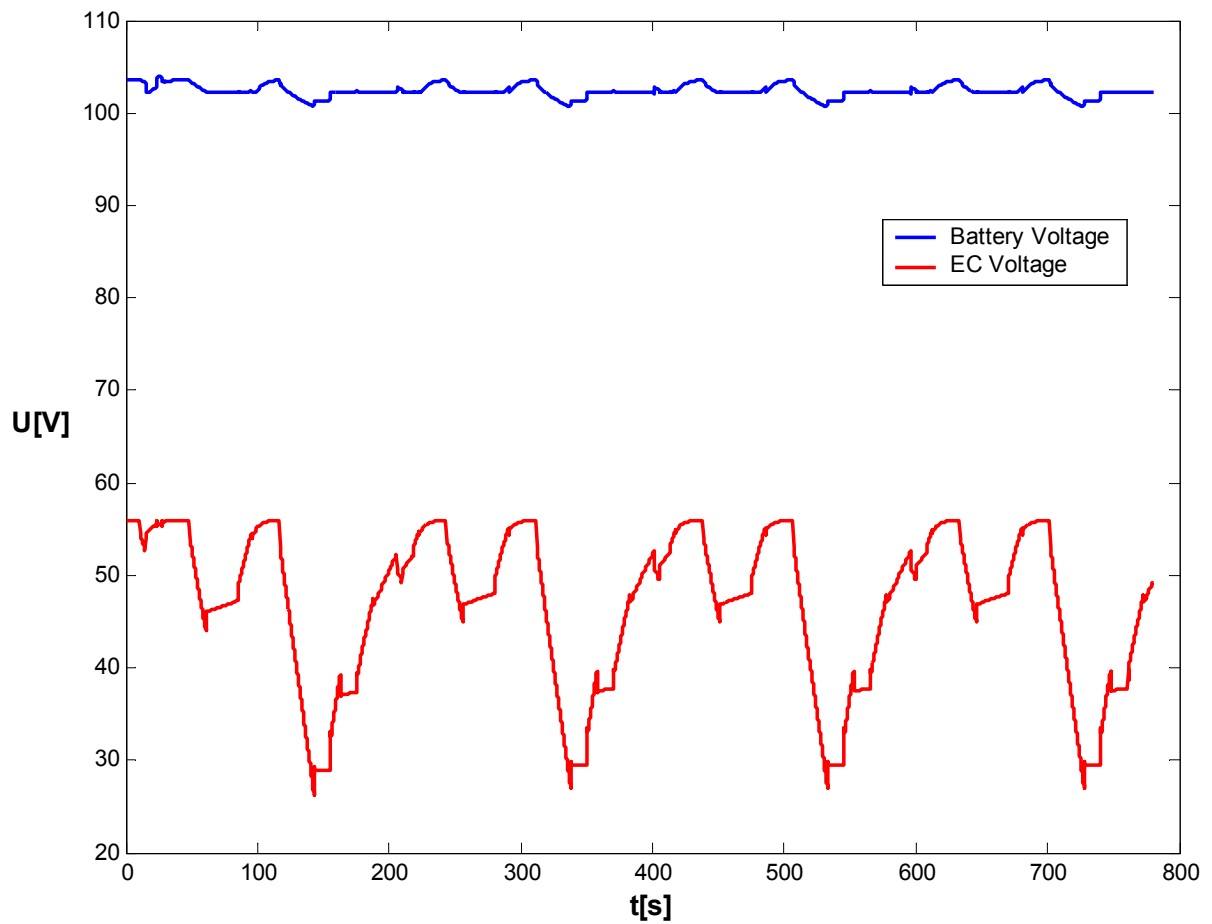
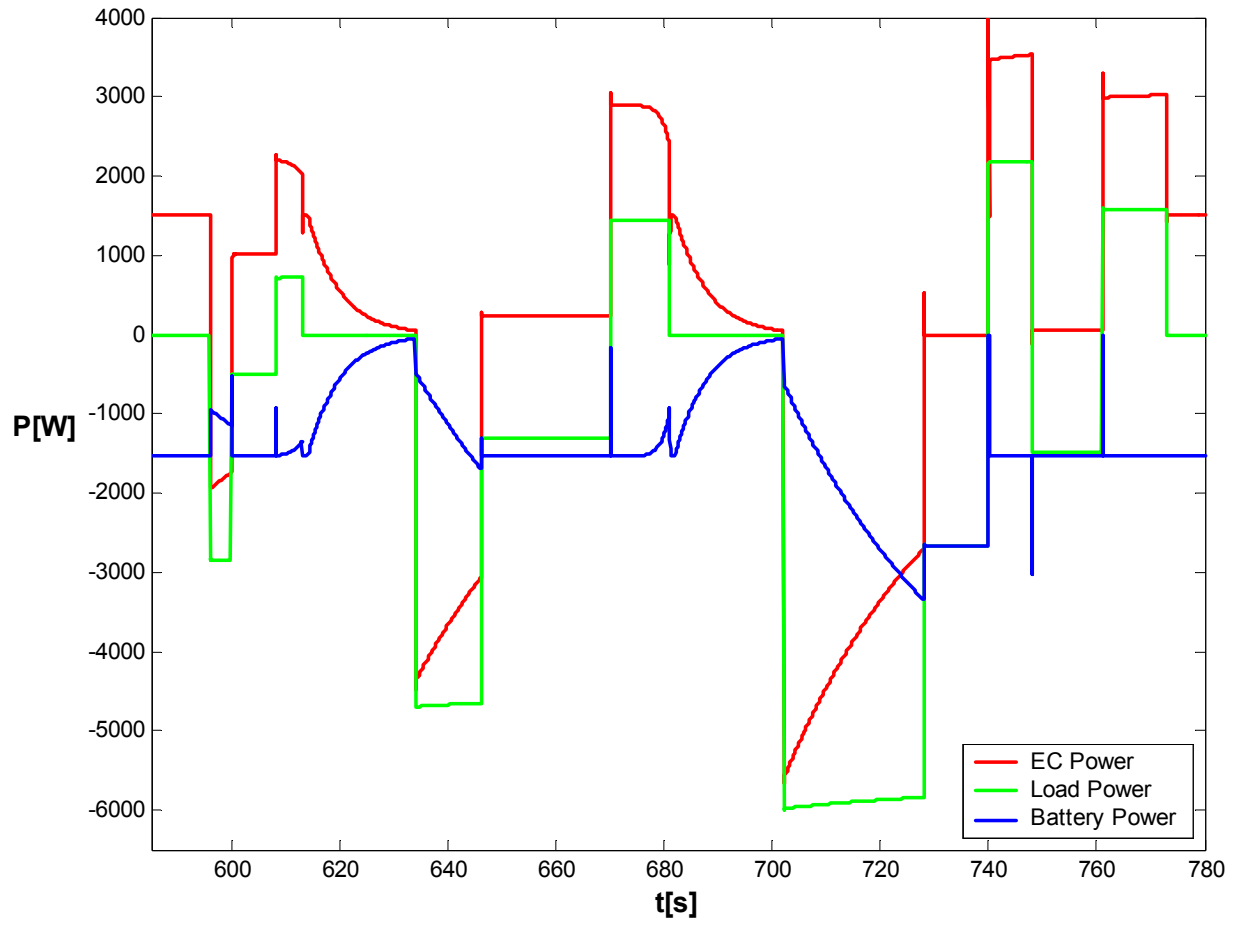


### Simulation of *Size II* system, 4 urban cycles.

Parameter	Matlab-variable	Value	Unit
Load cycle	p_load	ECE15-L	-
Number of cycles	Num_cycle	4	-
Weight constant to scale load	weight_constant	-2.5	-
Rise-time of low pass filter	Risetime_load_comp	35	s
Control strategy (see init_sim.m)	step1	1	-
	step2	1	-
	step3	1	-
	step4	1	-
Battery current limit (controls EC charge)	ibatlimit	-25	A
Load current limit (controls EC charge)	iloadlimit	-15	A
Number of series connected EC's	Ns	28	-
Number of parallel connected EC's	Np	1	-
Maximum unit voltage	V_max_per_cap	2	V
Minimum unit voltage	V_min_per_cap	0.5	V
Series Resistance	Rs	0.00089	$\Omega$
Leakage Resistance	Rp	1000	$\Omega$
Charge protection constant	c_cha	-100	-
Discharge protection constant	c_dch	-15	-
Unit capacitance	C	2700	F
EC-bank reference voltage	V_cap_ref	56	V
EC-bank initial voltage	V_init_cap	56	V
Battery SOC	SOC	0.5	-
DC/DC current limit	I <sub>max</sub>	300	A
DC/DC loss function, resistive losses	R_loss	0.0178	$\Omega$
DC/DC loss function, voltage drop losses	V_loss	0.3821	V
Measured battery VOC (10cells)	voc_real	12.95	V
Measured battery internal resistance per cell	R_per_cell	0.0010375	$\Omega$
Number of 10cell-battery units	ess_module_num	8	-

Performance parameter	Matlab-variable	Value	Unit
RMS Battery Current	RMS_Ratio	57	%
Power loss in main battery	W_loss_ratio	30	%
Total energy efficiency	Energy_efficiency	90	%
Charge Control	ch	84 84 84 84	%

Simulation of *Size II* system, 4 cycles.

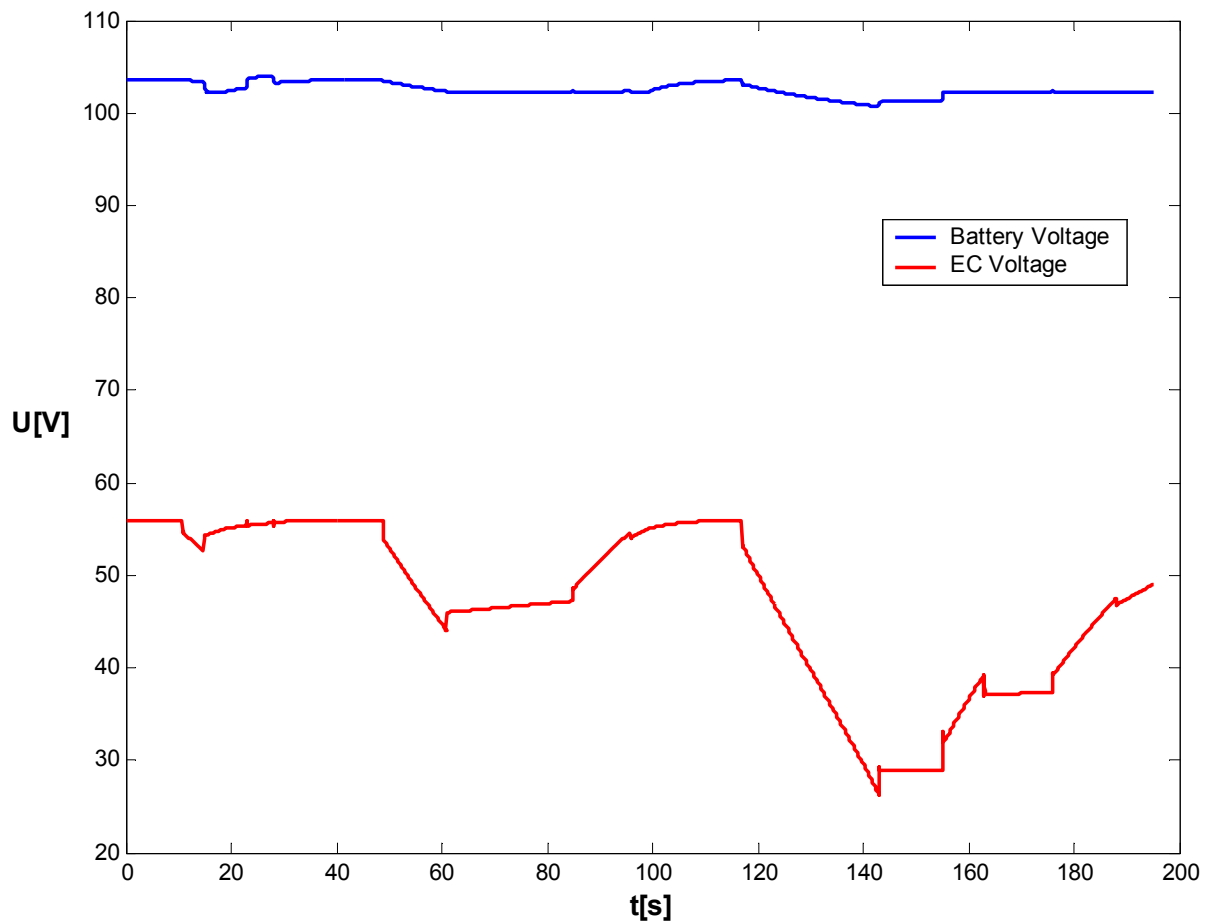
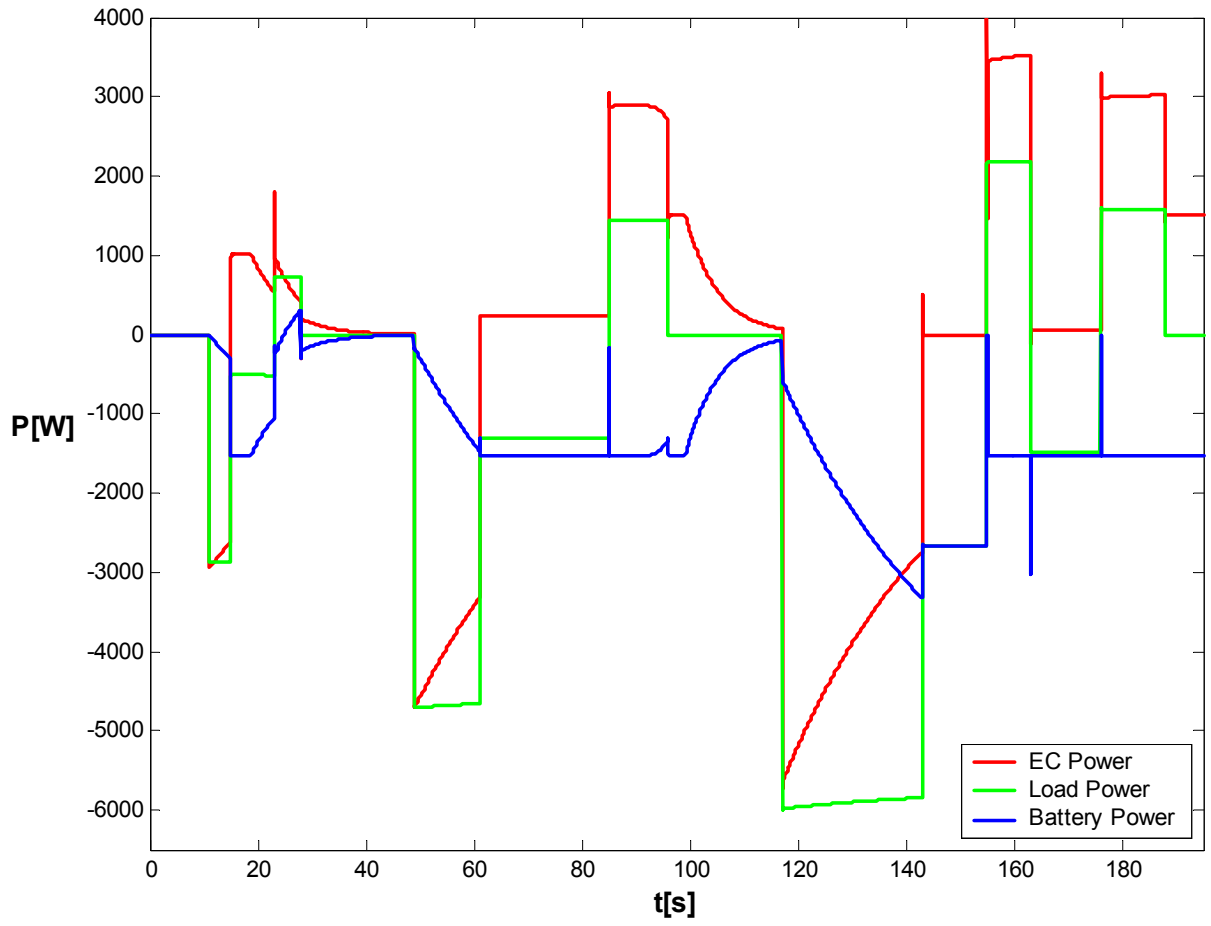


### Simulation of *Size II* system, 1 urban cycle.

Parameter	Matlab-variable	Value	Unit
Load cycle	p_load	ECE15-L	-
Number of cycles	Num_cycle	1	-
Weight constant to scale load	weight_constant	-2.5	-
Rise-time of low pass filter	Risetime_load_comp	35	s
Control strategy (see init_sim.m)	step1	1	-
	step2	1	-
	step3	1	-
	step4	1	-
Battery current limit (controls EC charge)	ibatlimit	-25	A
Load current limit (controls EC charge)	iloadlimit	-15	A
Number of series connected EC's	Ns	28	-
Number of parallel connected EC's	Np	1	-
Maximum unit voltage	V_max_per_cap	2	V
Minimum unit voltage	V_min_per_cap	0.5	V
Series Resistance	Rs	0.00089	$\Omega$
Leakage Resistance	Rp	1000	$\Omega$
Charge protection constant	c_cha	-100	-
Discharge protection constant	c_dch	-15	-
Unit capacitance	C	2700	F
EC-bank reference voltage	V_cap_ref	56	V
EC-bank initial voltage	V_init_cap	56	V
Battery SOC	SOC	0.5	-
DC/DC current limit	I <sub>max</sub>	300	A
DC/DC loss function, resistive losses	R_loss	0.0178	$\Omega$
DC/DC loss function, voltage drop losses	V_loss	0.3821	V
Measured battery VOC (10cells)	voc_real	12.95	V
Measured battery internal resistance per cell	R_per_cell	0.0010375	$\Omega$
Number of 10cell-battery units	ess_module_num	8	-

Performance parameter	Matlab-variable	Value	Unit
RMS Battery Current	RMS_Ratio	55	%
Power loss in main battery	W_loss_ratio	27	%
Total energy efficiency	Energy_efficiency	90	%
Charge Control	ch	84	%

Simulation of *Size II* system, 1 cycle.

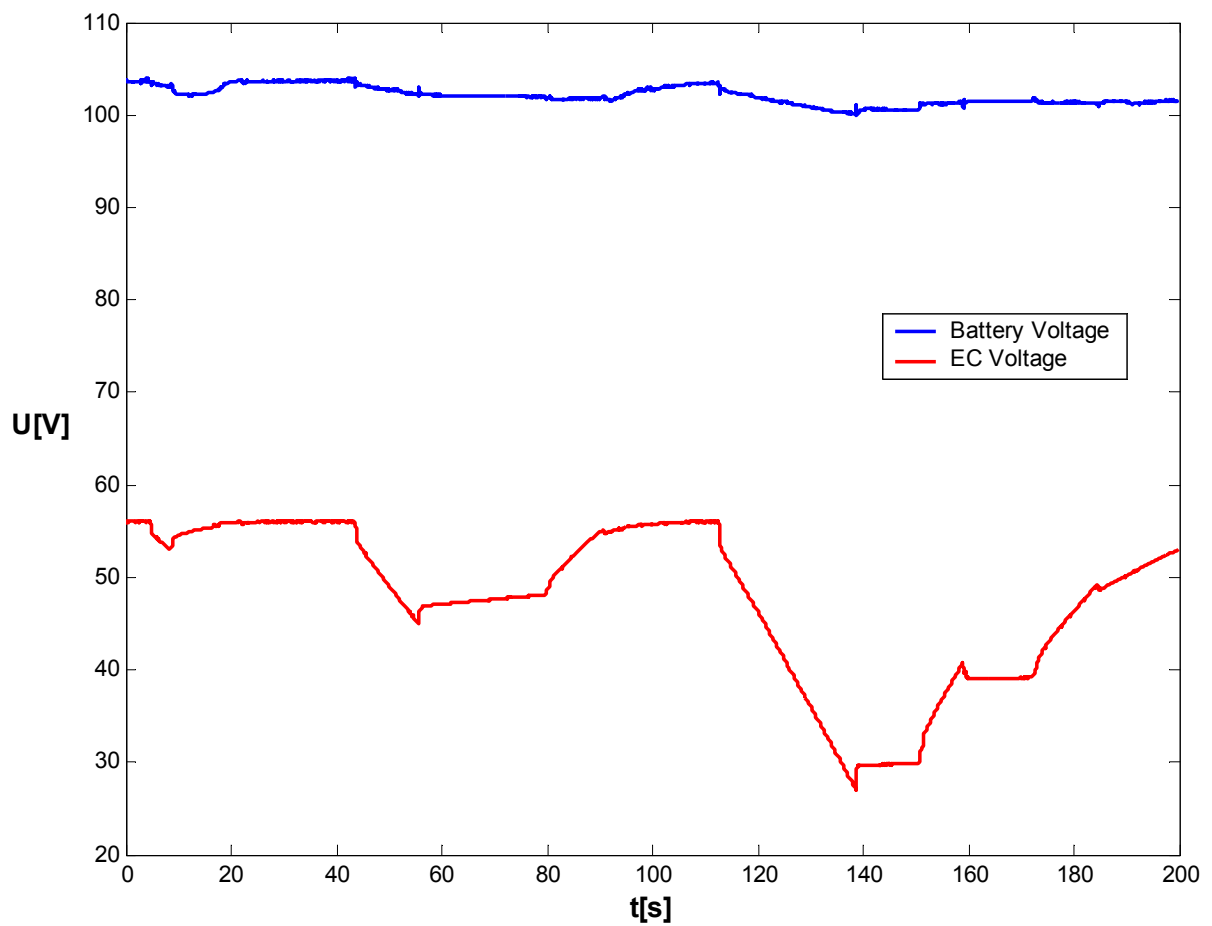
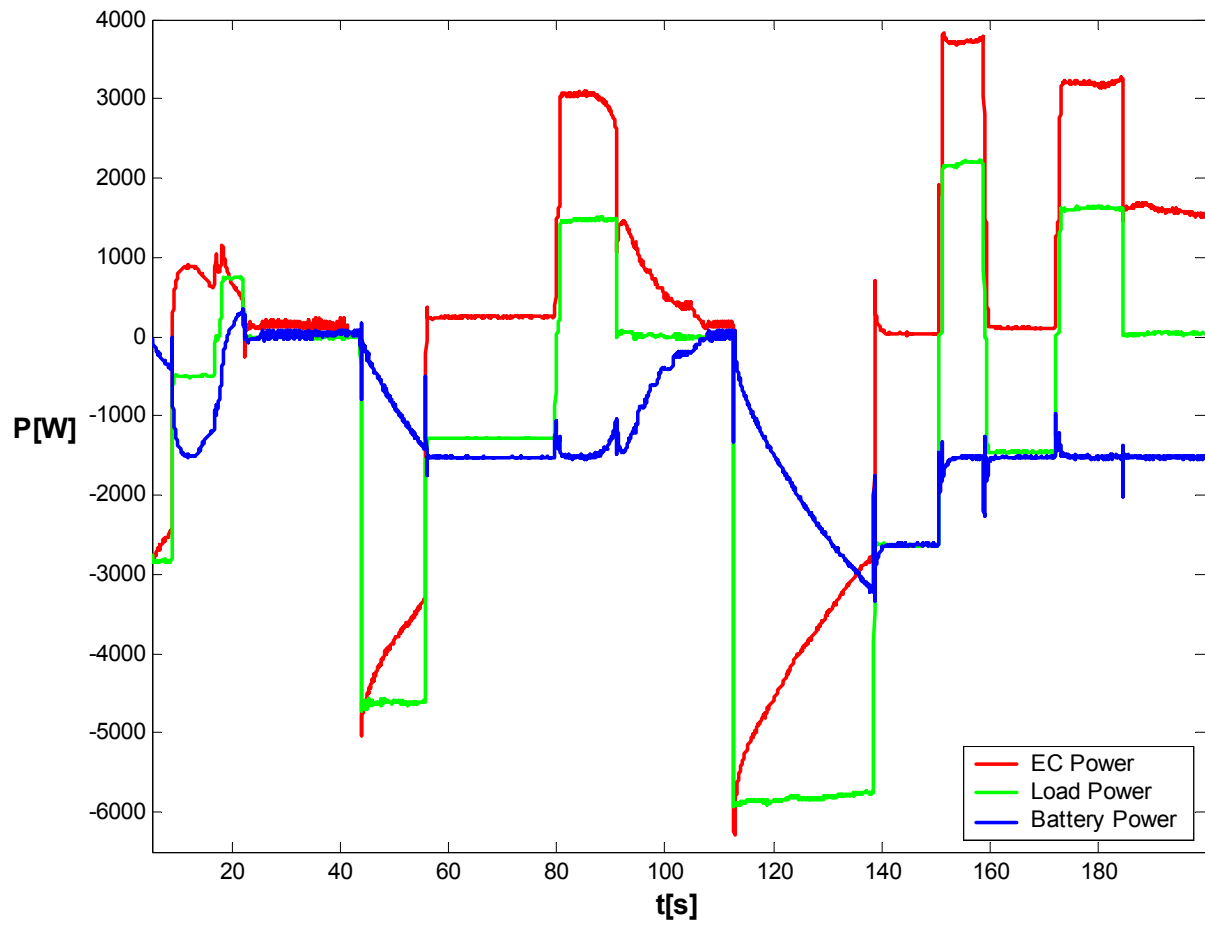


**Experimental results of *Size II* system, 1 urban cycle.**

<b>Parameter</b>	<b>Matlab-variable</b>	<b>Value</b>	<b>Unit</b>
Load cycle	p_load	ECE15-L	-
Number of cycles	Num_cycle	1	-
Weight constant to scale load	weight_constant	-2.5	-
Rise-time of low pass filter	Risetime_load_comp	35	s
Control strategy (see init_sim.m)	step1	1	-
	step2	1	-
	step3	1	-
	step4	1	-
Battery current limit (controls EC charge)	ibatlimit	-25	A
Load current limit (controls EC charge)	iloadlimit	-15	A
Number of series connected EC's	Ns	28	-
Number of parallel connected EC's	Np	1	-
Maximum unit voltage	V_max_per_cap	2	V
Minimum unit voltage	V_min_per_cap	0.5	V
Series Resistance	Rs	0.00089	$\Omega$
Leakage Resistance	Rp	1000	$\Omega$
Charge protection constant	c_cha	-100	-
Discharge protection constant	c_dch	-15	-
Unit capacitance	C	2700	F
EC-bank reference voltage	V_cap_ref	56	V
EC-bank initial voltage	V_init_cap	56	V
Battery SOC	SOC	0.5	-
DC/DC current limit	I <sub>max</sub>	300	A
DC/DC loss function, resistive losses	R_loss	0.0178	$\Omega$
DC/DC loss function, voltage drop losses	V_loss	0.3821	V
Measured battery VOC (10cells)	voc_real	12.95	V
Measured battery internal resistance per cell	R_per_cell	0.0010375	$\Omega$
Number of 10cell-battery units	ess_module_num	8	-

<b>Performance parameter</b>	<b>Matlab-variable</b>	<b>Value</b>	<b>Unit</b>
RMS Battery Current	RMS_Ratio	56	%
Power loss in main battery	W_loss_ratio	26	%
Total energy efficiency	Energy_efficiency	93	%
Charge Control	ch	85	%

Experimental results of *Size II* system, 1 cycle.

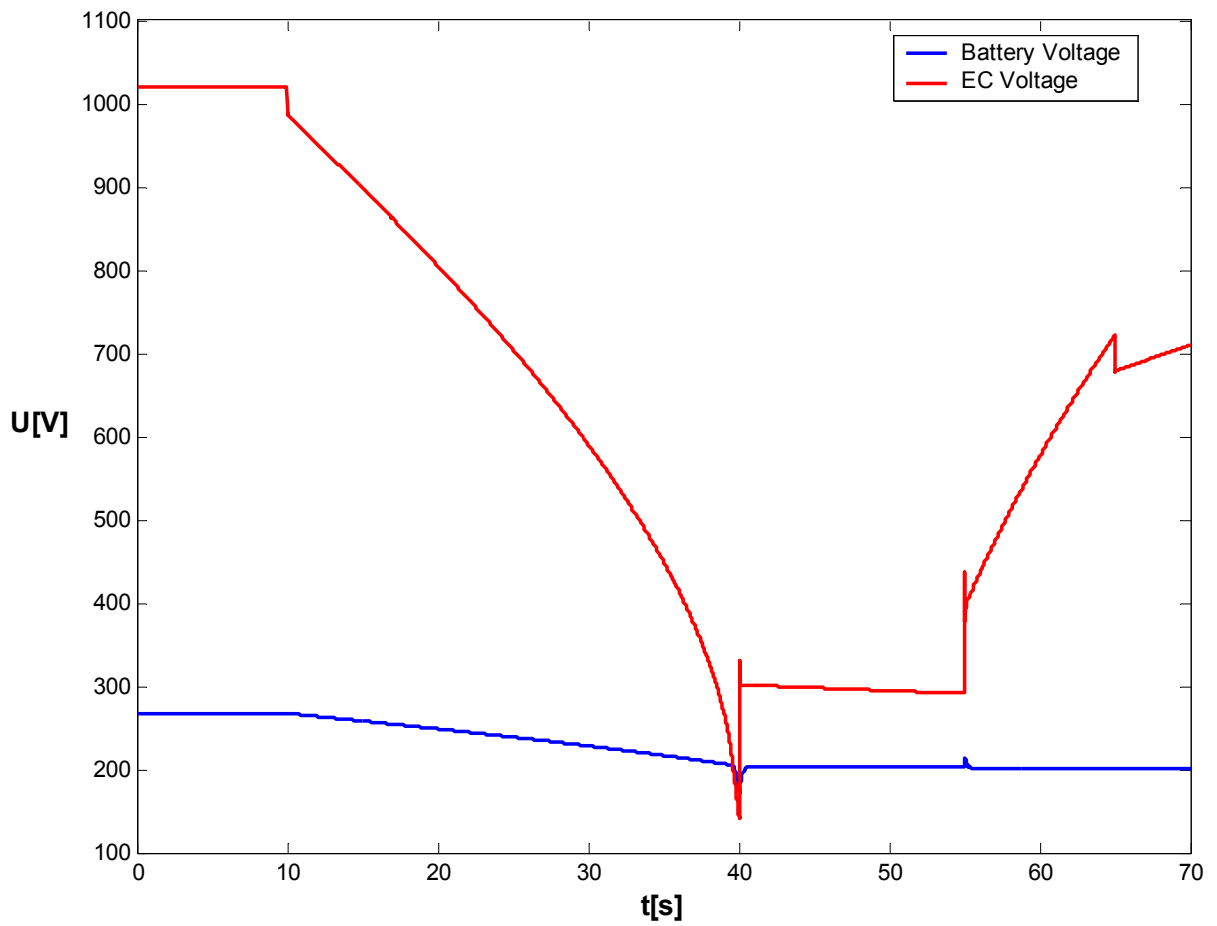
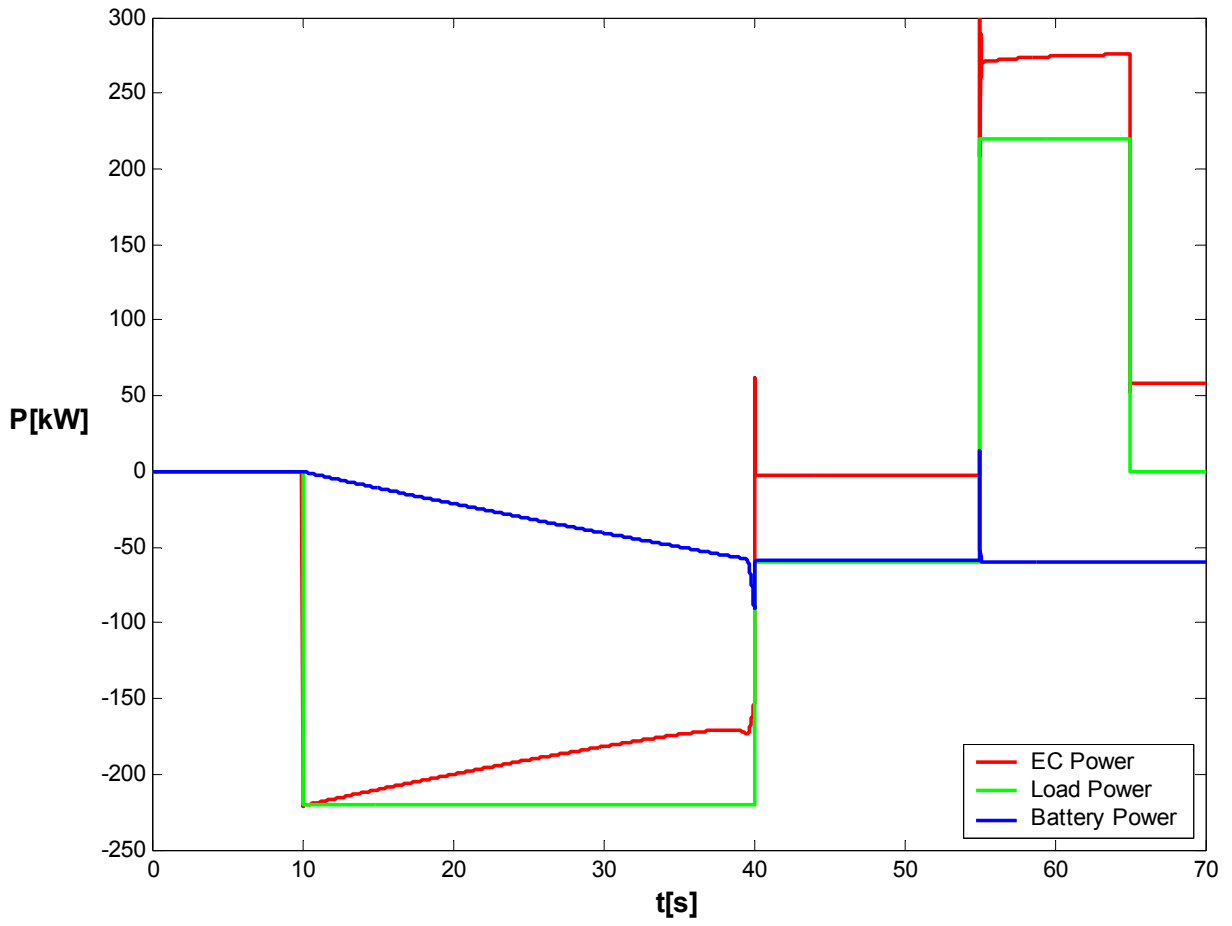


### Simulation of *Size III* system, NiMH batteries, maximum current 5C.

Parameter	Matlab-variable	Value	Unit
Load cycle	p_load	Bus test cycle	-
Number of cycles	Num_cycle	1	-
Weight constant to scale load	weight_constant	-	-
Rise-time of low pass filter	Risetime_load_comp	100	s
Control strategy (see init_sim.m)	step1	1	-
	step2	1	-
	step3	1	-
	step4	1	-
Battery current limit (controls EC charge)	ibatlimit	-55.65	A
Load current limit (controls EC charge)	iloadlimit	-53	A
Number of series connected EC's	Ns	380	-
Number of parallel connected EC's	Np	1	-
Maximum unit voltage	V_max_per_cap	2.7	V
Minimum unit voltage	V_min_per_cap	0.1	V
Series Resistance	Rs	0.0004	$\Omega$
Leakage Resistance	Rp	1000	$\Omega$
Charge protection constant	c_cha	-50	-
Discharge protection constant	c_dch	-2	-
Unit capacitance	C	5000	F
EC-bank reference voltage	V_cap_ref	1026	V
EC-bank initial voltage	V_init_cap	1026	V
Battery SOC	SOC	0.6	-
DC/DC current limit	I <sub>max</sub>	850	A
DC/DC loss function, resistive losses	R_loss	0.0178	$\Omega$
DC/DC loss function, voltage drop losses	V_loss	0.3821	V
Measured battery VOC (10cells)	voc_real	13.275	V
Measured battery internal resistance per cell	R_per_cell	0.0011326	$\Omega$
Number of 10cell-battery units	ess_module_num	20	-

Performance parameter	Matlab-variable	Value	Unit
RMS Battery Current	RMS_Ratio	-	%
Power loss in main battery	W_loss_ratio	-	%
Total energy efficiency	Energy_efficiency	75	%
Charge Control	ch	-	%

Simulation of *Size III* system, NiMH batteries, maximum current 5C.



## Appendix C ECE15-L Power Profile and Bus Test Cycle

The first part of the ECE15-L driving cycle (Figure 1) consists of 4 identical *Urban Cycles*, referred to as the “*Urban Part*”. The *Urban Cycle* is presented in Table 1 and Figure 2.

In the city bus example, another driving cycle is used, referred to as the *Bus Cycle*, presented in Table 2 and Figure 3.

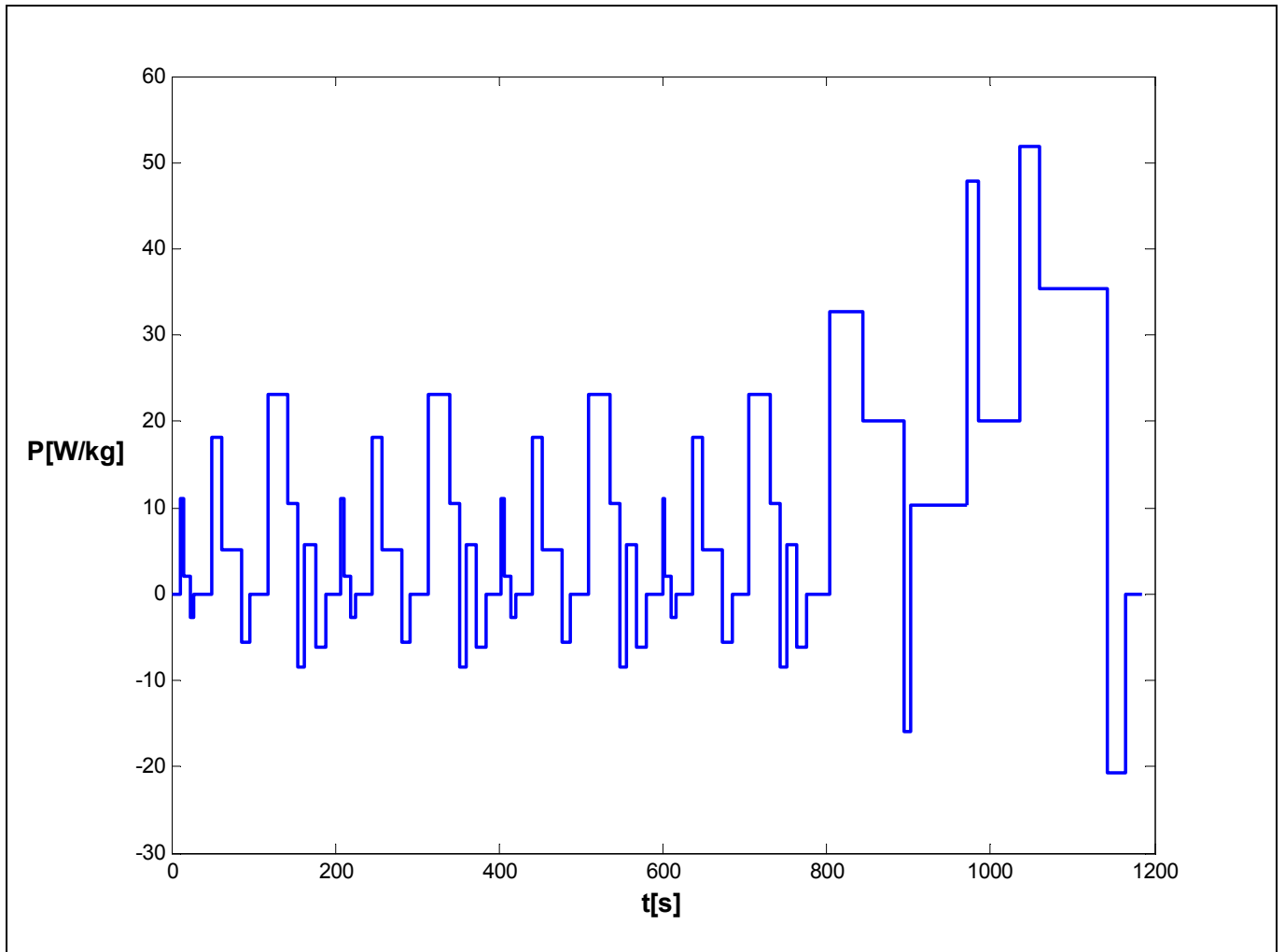
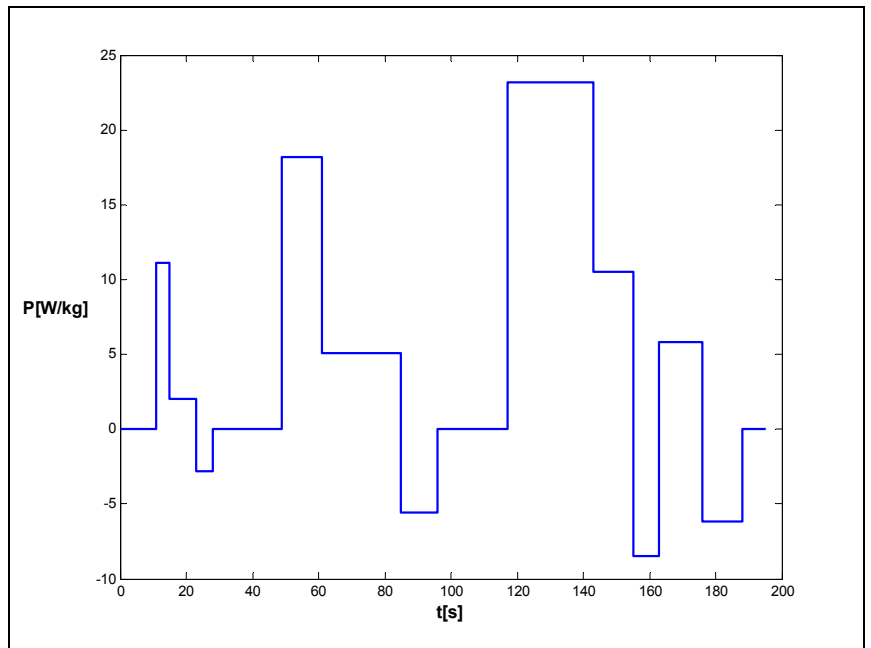


Figure 1 ECE15-L Power Profile.

**Table 1 Urban cycle.**

Time (sec)	Specific Power (W/kg)
0-11	0
11-15	11.1
15-23	2.0
23-28	-2.8
28-49	0
49-61	18.2
61-85	5.1
85-96	-5.6
96-117	0
117-143	23.2
143-155	10.5
155-163	-8.5
163-176	5.8
176-188	-6.2
188-195	0



**Figure 2 ECE15-L power profile: urban cycle.**

**Table 2 Bus cycle.**

Time (s)	Power (kW)
0-10	0
10-40	220
40-55	60
55-65	-220
65-70	0

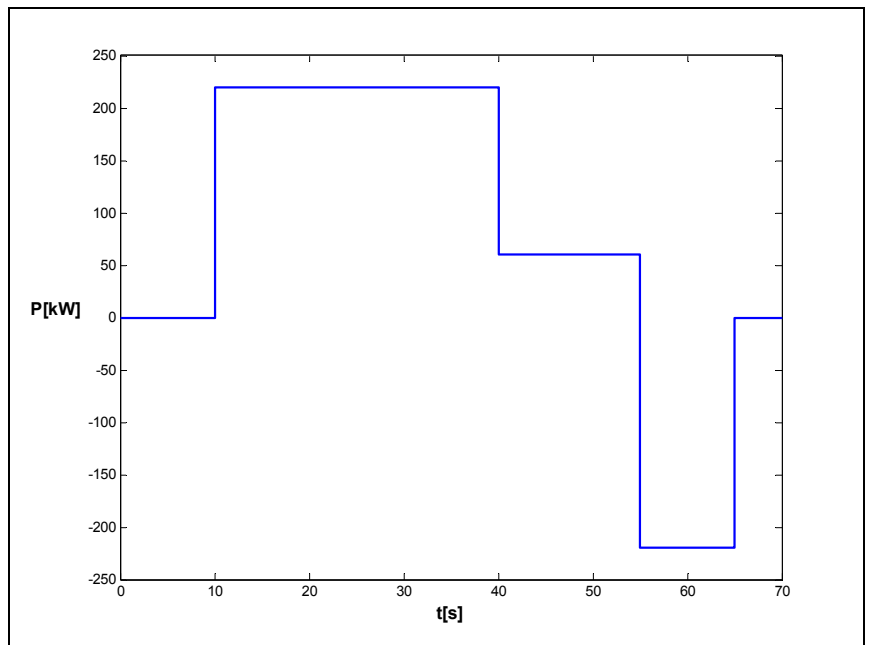
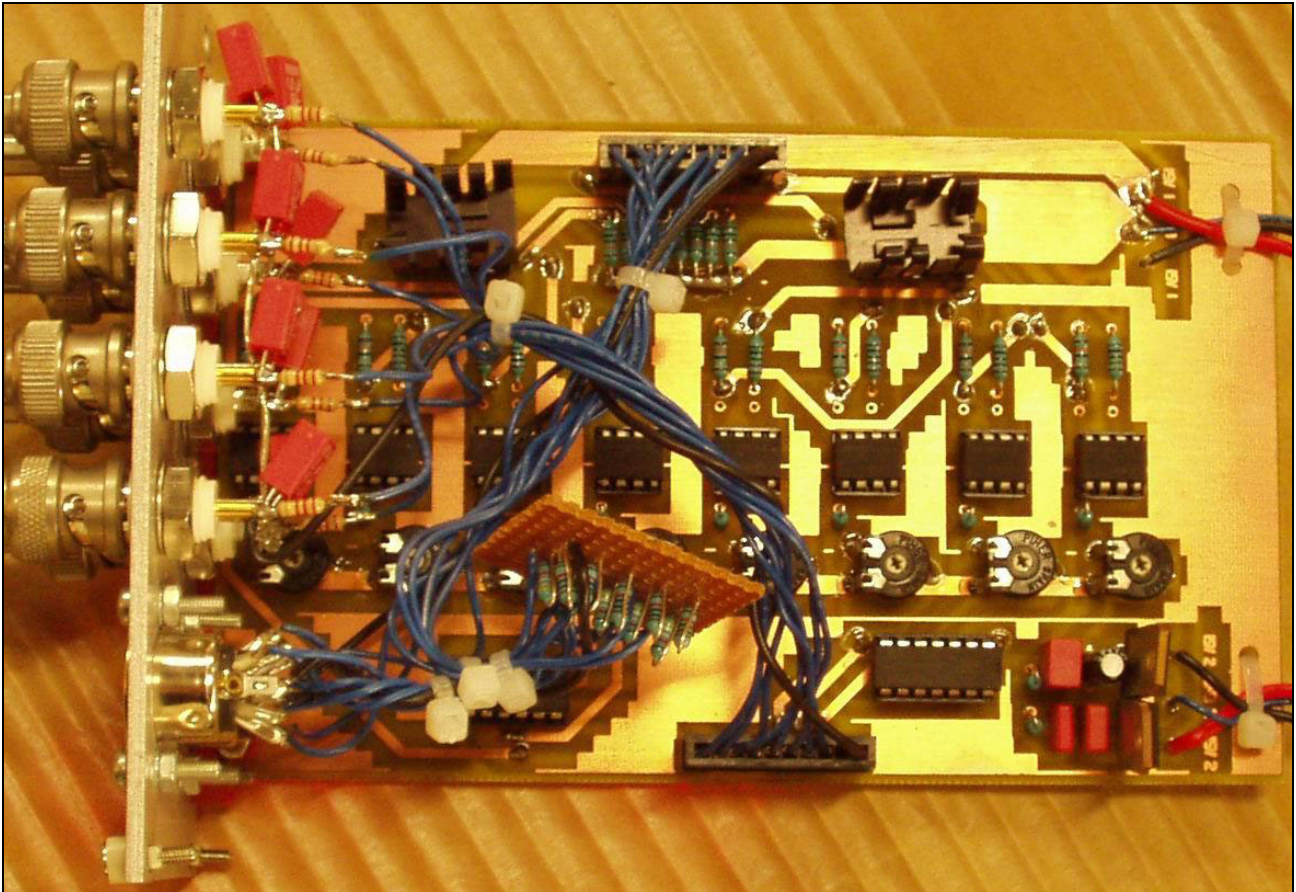


**Figure 3 Bus test cycle.**

## Appendix D Optocoupling Card, LEM Modules and Calibration

### Optocoupling Card



#### Specifications:

Number of channels	8	-
Input connector channel 1-3	DIN5	
Input connector channel 4-8	DIN7	
Output connector channel 1-8	BNC	
Power supply connector	Cables	
Input voltage range	$\pm 10$	V
Output voltage range	$\pm 8$	V
Power supply	$2 \times \pm 15$ 500	V mA
Input impedance	100	k $\Omega$
Output impedance (without filter)	3	$\Omega$
Output impedance (with filter)	2.2	k $\Omega$
Rise time (square wave input)	10	ms
Output RC-filter cut-off frequency	450	Hz

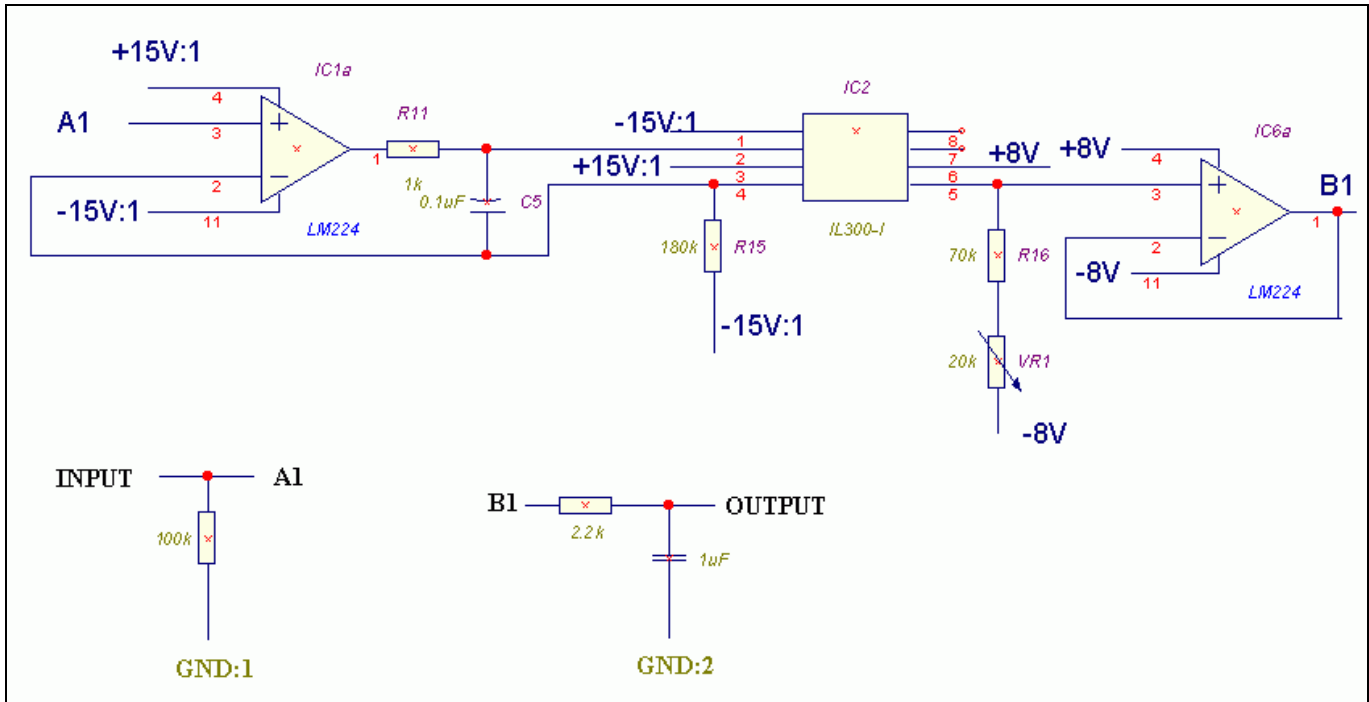


**Figure 1 Schematics**

The circuit is based on the analogue optocoupler IL300 from *Infineon*<sup>®</sup>. It consists of one drive circuit, IC1a in Figure 1, and an output driver, IC6a. Both drivers are LM224. The second power supply, marked  $\pm 8V$ , is obtained from the second  $\pm 15V$  supply and 7808/7908 voltage regulators. A 100k bias stage is applied at the input for protection. The filtering is performed directly at the output with a 2k2/1µF RC-filter. Full documentation, like schematics and pcb-layouts, are included in the attached CD. The optocoupling card was manufactured by the authors using etching technique on a 2-sided standard 100x160mm board.

**Notes:**

To reduce noise, the capacitor C5 can be added at the input amplifier. High frequency noise is greatly reduced. In this project, a 0.1µF capacitor was used. Noise performance was promising, but problems were encountered when the optocoupling card was used in the real laboratory set-up. In the low frequency region up to approximately 20Hz, the operation was satisfactory. At mid frequencies (20Hz-1kHz), the overall amplification was increased. This results in that signals with noise or ripple in this frequency region was significantly amplified over the level the system was calibrated for. In the high frequency region (>1kHz), amplification was, as expected, low. An approximate sketch of the frequency response of the optocoupling card is presented in Figure 2.

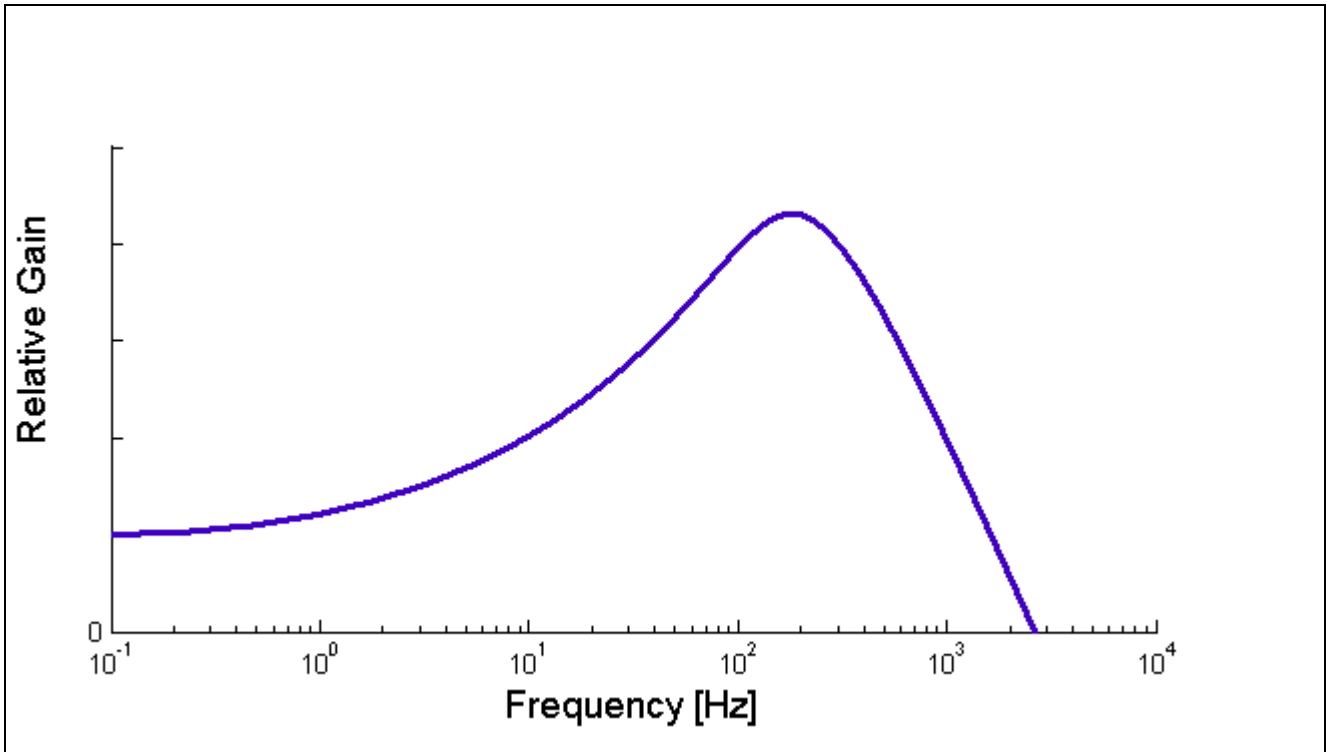


Figure 2 Frequency response with C5

The solution for this problem was to remove the C5 capacitor. The noise level was increased, but the overall performance was still satisfactory. The final frequency response is shown in Figure 3.

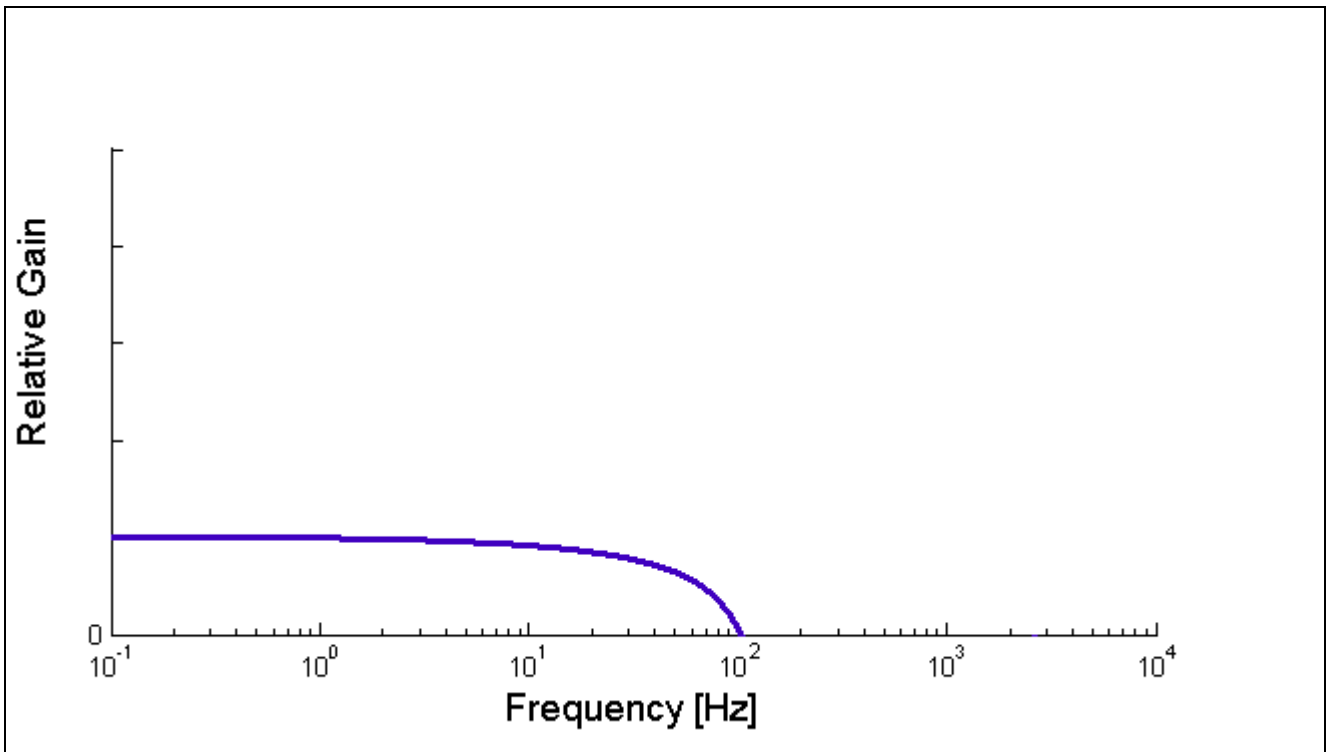


Figure 3 Frequency response without C5

## PCB layouts

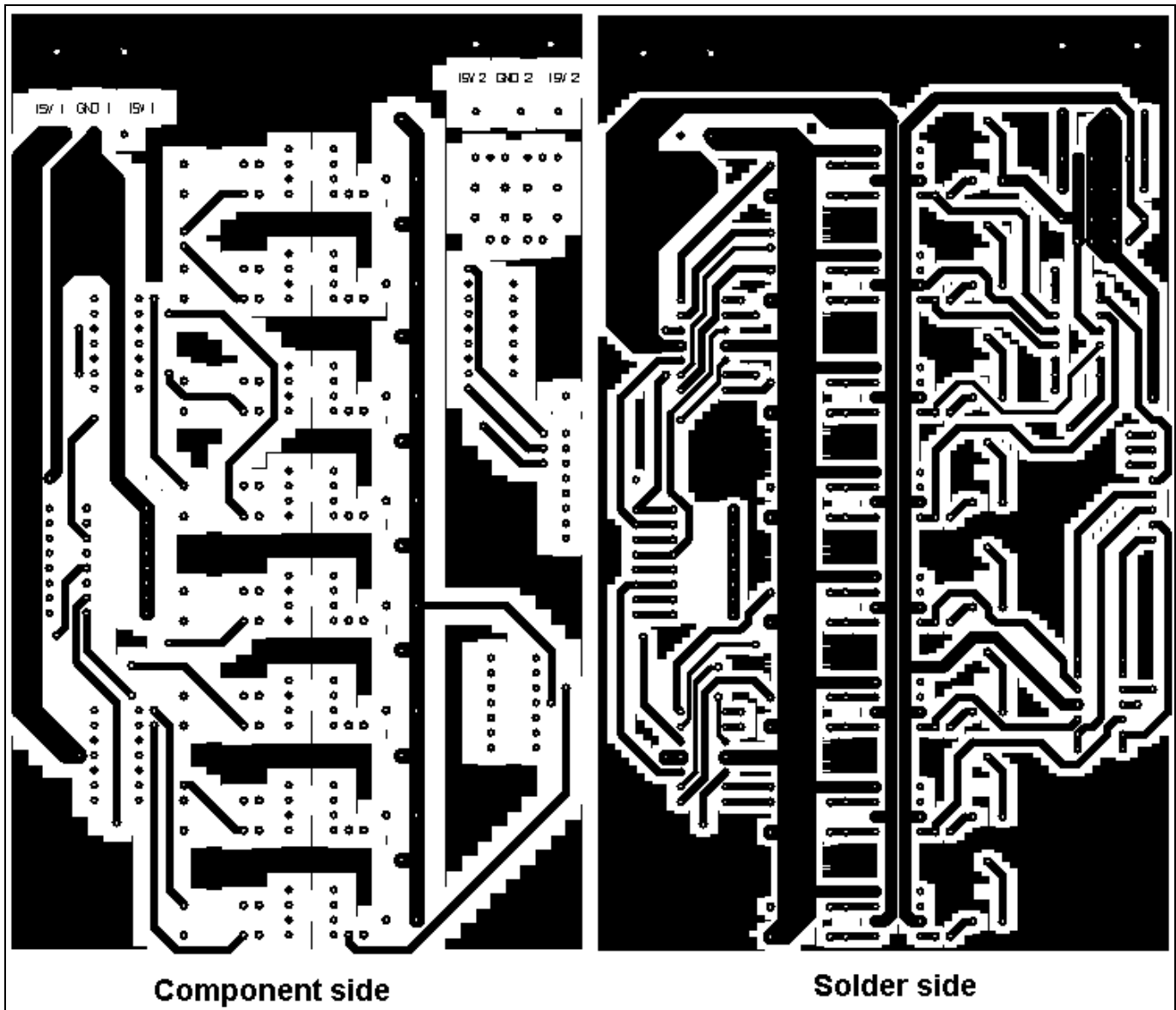


Figure 4 PCB-layouts

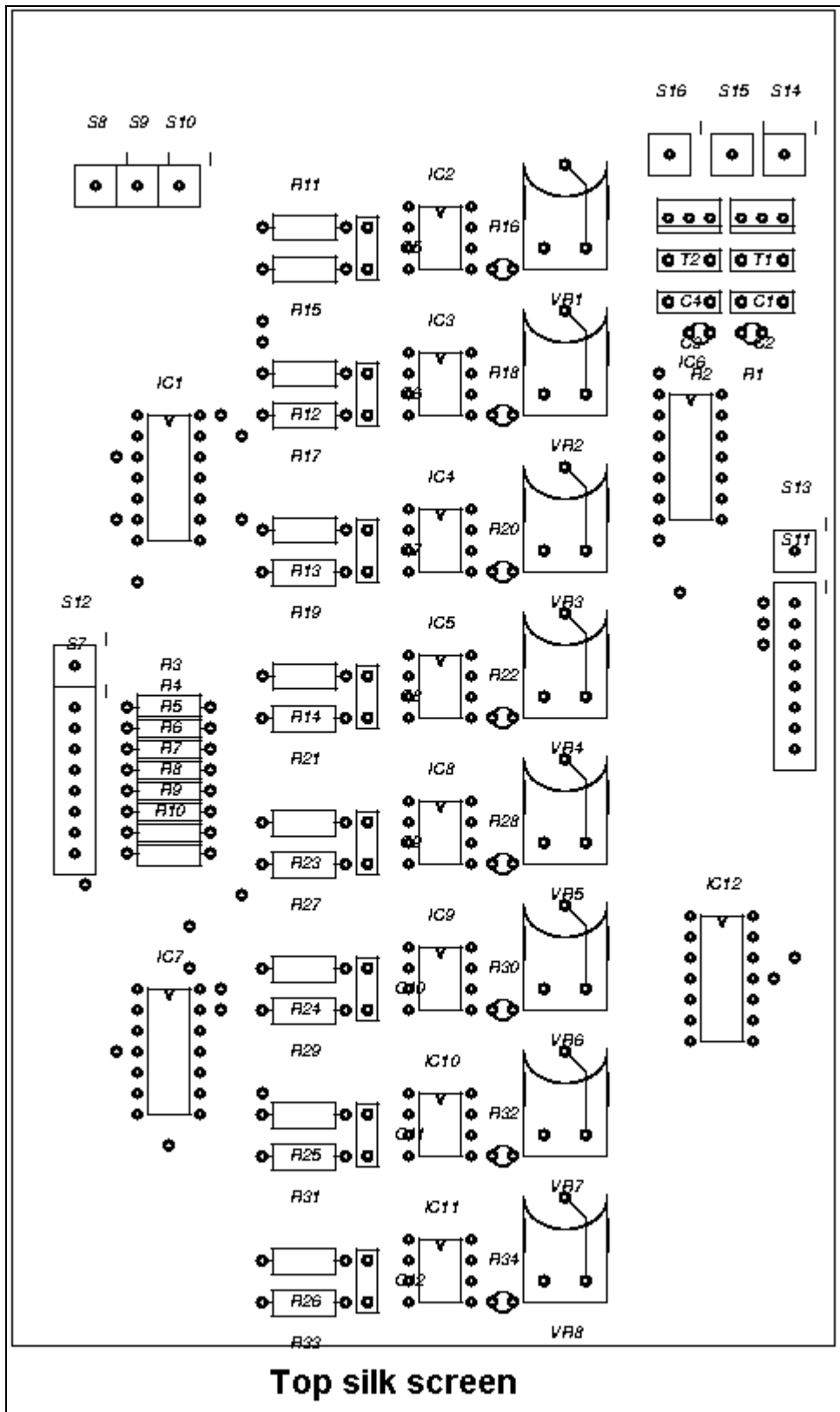


Figure 5 Components

## LEM Modules

The LEM modules used in current measurements must be equipped with an external circuit to produce proper output signals. The value of the main resistance “R2” in Figure 7 is calculated from the maximum current to measure and the maximum output voltage.

Specifications:

Type	LT 300-S	-
Rated current	300	A
Ratio	1:2000	-
Internal resistance	35	$\Omega$
Battery- and load current LEM		
Main resistance, R2	94	$\Omega$
Maximum input current	$\pm 150$	A
Maximum output voltage	$\pm 7$	V
EC-current LEM		
Main resistance, R2	47	$\Omega$
Maximum input current	$\pm 300$	A
Maximum output voltage	$\pm 7$	V

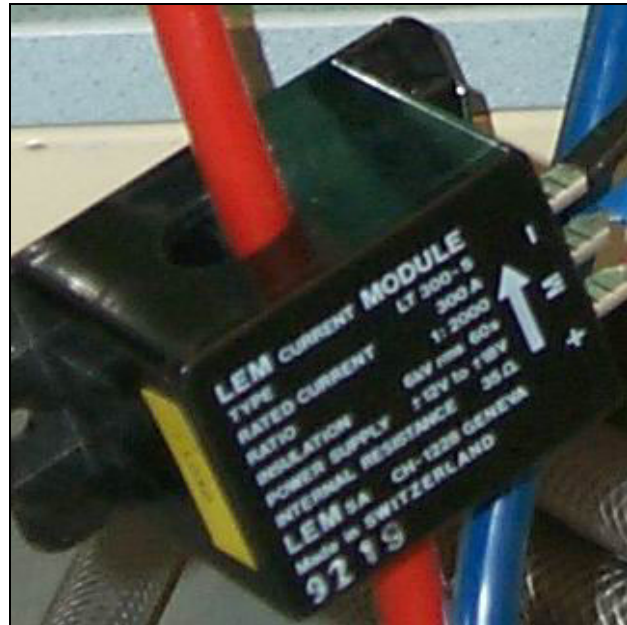


Figure 6 Photo of load current LEM

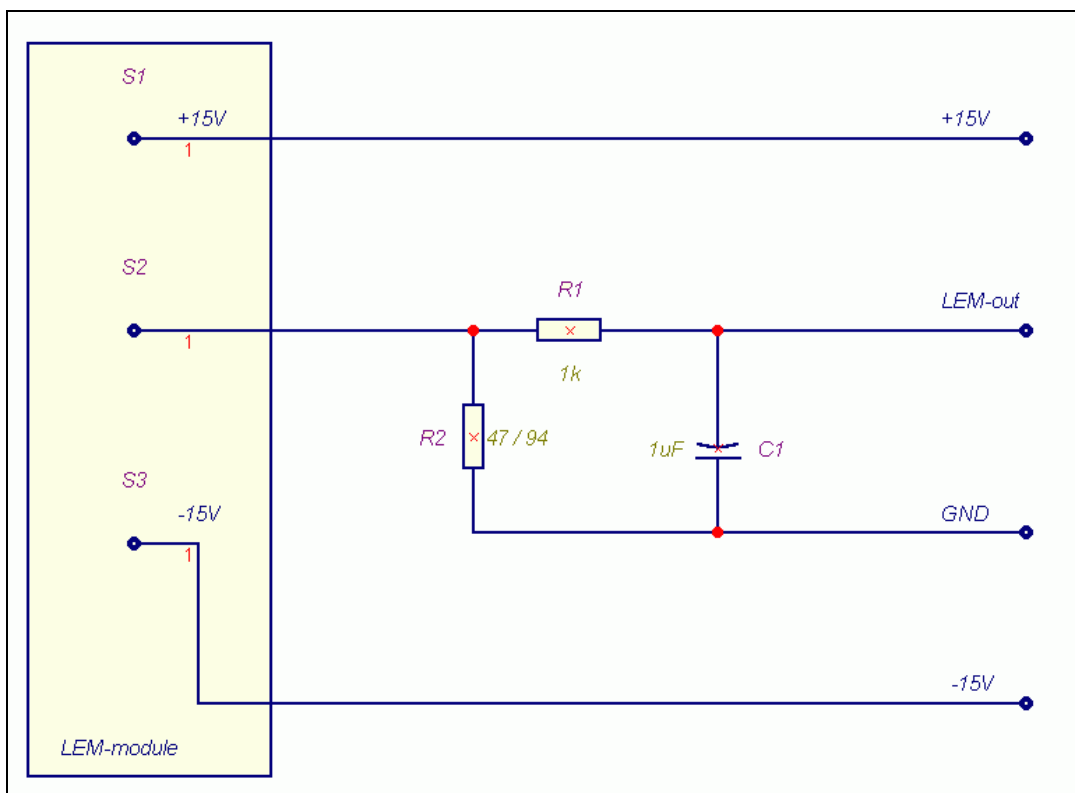


Figure 7 LEM-circuitry

## Calibration

The measure and control system must be properly calibrated in order to be used in calculations of system performance. In this project however, the focus is set on the general system behaviour and control algorithms. Therefore, the measure channels are calibrated assuming that the transfer function is linear and stable, not significantly dependent on temperature etc.

The measure and control system was calibrated using a chain-calibration method, where the linear transfer function from applied signals to presented data is calculated. For the voltage channels, approximately 10 control signals were measured using a calibrated voltmeter as reference. The current measurements were performed by supplying reference currents directly from the Digatron<sup>®</sup> thyristor converter. In the .m-file below, all measured signals and their corresponding readings from ControlDesk<sup>®</sup> are presented. These values are used in polyfit-calculatons, yielding a transfer function used in the MATLAB<sup>®</sup>/SIMULINK<sup>®</sup> model.

```
***
calib_ch.m
%Calibration 2003-09-24. (Size // system) Channel 1-3: current
%measurements. Digatron Unit 1 used as reference.
%Channel 3-8: voltage measurements. Fluke 87
%nr.210 used as reference.
%ch<nr>=[<nr> <reference value> <readings from
%controldesk>];

ch4=[4 0 0.2453
4 5.12 0.2989
4 10.41 0.3545
4 12.42 0.3756
4 15.07 0.4035
4 17.36 0.4272
4 20.05 0.455
4 22.32 0.4787
4 25.19 0.5083
4 27.98 0.537
4 30.61 0.5639
4 7.52 0.3243
4 2.561 0.272];

ch5=[5 0 0.2421
5 5.12 0.2963
5 10.41 0.353027
5 12.42 0.374023
5 15.07 0.402344
5 17.36 0.42627
5 20.05 0.45459
5 22.32 0.4785
5 25.19 0.5083
5 27.98 0.5375
5 30.61 0.564453
5 7.52 0.322266
5 2.561 0.269531];

ch6=[6 85.3 0.4908
6 90.6 0.5062
6 95.5 0.5208
6 101.4 0.5378
6 105.2 0.549
6 110.6 0.5648
6 115.8 0.5799
6 120.2 0.5929];

ch7=[7 0 0.270508
7 5.12 0.325684
7 10.41 0.383301
7 12.42 0.405273
7 15.07 0.433594
7 17.36 0.458496
7 20.05 0.487305
7 22.32 0.511719
7 25.19 0.54248
7 27.98 0.572266
7 30.61 0.600098];

ch8=[8 39.99 0.327148
8 45.5 0.373047
8 50.6 0.416016
8 52.6 0.432617

8 55.3 0.455078
8 57.3 0.47168
8 60.1 0.495117
8 54.7 0.450684];

ch2=[2 27.7500 -30.8205
2 5.0000 26.7228
2 -7.0000 63.4707
2 45.5000 -78.0789
2 12.7500 7.5648
2 -14.0000 83.5380
2 58.0000 -111.2042
2 26.2500 -26.7810
2 -21.2500 103.6913
2 14.5 3.2056
2 -15.5 87.7652];

ch3=[3 27.7500 -35.7986
3 5.0000 19.9548
3 -7.0000 56.7682
3 45.5000 -82.8303
3 12.7500 1.6787
3 -14.0000 77.1334
3 58.0000 -115.8778
3 26.2500 -31.8236
3 -21.2500 97.3679
3 14.5 -2.5214
3 -15.5 81.4015];

ch1=[1 27.7500 -31.2435
1 5.0000 -2.6782
1 -7.0000 14.8963
1 45.5000 -54.1765
1 12.7500 -12.3480
1 -14.0000 24.2250
1 58.0000 -70.2151
1 26.2500 -29.3214
1 -21.2500 33.6921
1 14.5 -14.5332
1 -15.5 26.1873];

[p4,s]=polyfit(ch4(:,2),ch4(:,3),1);
[p5,s]=polyfit(ch5(:,2),ch5(:,3),1);
[p6,s]=polyfit(ch6(:,2),ch6(:,3),1);
[p7,s]=polyfit(ch7(:,2),ch7(:,3),1);
[p8,s]=polyfit(ch8(:,2),ch8(:,3),1);
[p2,s]=polyfit(-1.*ch2(:,2),0.001.*ch2(:,3),1);
[p3,s]=polyfit(-1.*ch3(:,2),0.001.*ch3(:,3),1);
[p1,s]=polyfit(-1.*ch1(:,2),0.001.*ch1(:,3),1);
```

## Appendix E Specifications

### DC/DC converter simulated in all simulations and experiments

DC/DC converter

Maximum current	330	A
Minimum input voltage	10	V
Maximum input voltage	500	V
Maximum output voltage	650	V and $\geq U_{in}$
Maximum power	160	kW
Efficiency, typ	95	%

#### Modification of DC/DC converter

In early experimental tests of the DC/DC converter, it was concluded that this particular product was modified in an earlier Volvo project. This modification inhibited step-down operation mode. After studying the electrical schematics and dismounting the converter, the earlier modification was found: the gate signals to the step-down IGBT's was isolated and grounded. After re-modification of the circuits, the DC/DC converter was functioning in both operation modes.

### Electrochemical Capacitors used in simulations and experiments of *Size I* and *Size II*.

EC's *Size I*:

Maximum current	600	A
Maximum voltage	2.5	V / cell
Capacitance	2600	F / cell
Number of EC's	10	-
Series Resistance	0.6	m $\Omega$ /EC
Parallel Resistance	1k	$\Omega$ /unit

Passive balancing using 10  $\Omega$  resistors.

EC's *Size II*:

Maximum current	300	A
Maximum voltage	56	V
Capacitance	2700	F / cell
Number of EC's	28	-

Active balancing using buck-boost technique.

### Electrochemical Capacitors used in simulations and experiments of *Size III*.

EC's *Size III* [12]

Maximum current	> 1680	A
Rated Current	950	A
Capacitance	5000	F / cell
Series Resistance	0.4	m $\Omega$ / EC
Weight	0.87	kg / EC
Rated Voltage	2.7	V / cell
Surge Voltage	2.85	V / cell

### **Batteries used in simulations and experiments of *Size I*, *Size II* and *Size III*.**

#### NiMH Batteries

Capacity	60	Ah
Voltage (SOC 0.5)	1.25	V / cell
Series Resistance	1.1	mΩ / cell
Energy capacity	50	Wh / kg
Power capacity	253	W / kg
Weight	1.48	kg / cell

#### Li-ion Batteries [13]

Capacity	45	Ah
Voltage (SOC 0.5)	3.6	V / cell
Series Resistance	no data	mΩ / cell
Energy capacity	150	Wh / kg
Power capacity	419	W / kg
Weight	1.07	kg / cell

### **Vehicle parameters used in the city-bus example.**

Typical values for a Volvo B7L Bus are [7]

m	18 900	kg
$C_d * A * \rho$	5.2780	-
Cr	0.007	-
$v_m$	85	km/h
$t_m$	30	s

## Appendix F Performance Parameters

### **RMS Battery Current**

In both simulations and experiments, the RMS battery current is calculated and compared to the calculated RMS load current.

$$I_{RMS} = \sqrt{\left(\frac{1}{T} \int_0^T I^2 dt\right)}$$

In MATLAB<sup>®</sup>, the RMS current was calculated using the following command

```
***  
%Reduction of RMS-current  
n_I=length(I_bat);  
RMS_I_bat=norm(I_bat)/sqrt(n_I);  
RMS_I_load=norm(I_load)/sqrt(n_I);  
RMS_I_cap=norm(I_cap)/sqrt(n_I);  
RMS_Ratio=RMS_I_bat/RMS_I_load*100;  
***
```

### **Power Loss in Battery**

This parameter is calculated from the power loss output of the Advisor battery model. The power loss is integrated numerically and compared to the case when the load current is taken from the battery alone. The calculations from experimental results are performed in the same way, using measured battery and load current.

The following command sequence is used in MATLAB<sup>®</sup> (extracted from p\_proc.m in Appendix A).

```
***  
%Reduction of losses in battery. Losses is calculated from directly in the  
%Advisor battery model  
W_loss_bat=-sum(P_est_bat.*time_step_sim);  
W_loss_bat_ref=-sum(P_est_bat_ref.*time_step_sim);  
W_loss_ratio=W_loss_bat/W_loss_bat_ref*100;  
***
```

### Total Energy Efficiency

The basic principle behind this parameter is summarised in the following equation:

$$\eta_{Total} = \frac{W_{Load}}{W_{Battery} + W_{EC}} = \frac{\int_0^T I_{Load} \cdot U_{Battery} dt}{\int_0^T (U_{Battery} - I_{Battery} \cdot R_{In}) \cdot I_{Battery} dt + \frac{C}{2N_s} \cdot (U_{EC,final}^2 - U_{EC,initial}^2)}$$

In Matlab, this calculation is performed using the following sequence. (extracted from `p_proc.m` in Appendix A)

```
***
%Total Energy efficiency. Calculated as the ratio between total energy
%absorbed by the load and the total energy delivered from the battery and
%the EC's
Total_load=sum(U_bat.*I_load).*time_step_real;
Total_bat=sum((U_bat-I_bat.*R_per_cell*ess_module_num*10).*I_bat).*time_step_real;

W_initcap=(C/Ns)*0.5*mean(U_cap(1:10)).^2;
U_capfinal=mean(U_cap(length(U_cap)-10:length(U_cap)))-mean(I_cap(length(U_cap)-
10:length(U_cap)))*Rs*Ns;
W_finalcap=(C/Ns)*0.5*U_capfinal.^2;
Total_cap=W_finalcap-W_initcap;
Total_sys=Total_bat+Total_cap;
Energy_efficiency=Total_load/Total_sys*100;
disp(['Total Efficiency = ' num2str(round(Energy_efficiency)) ' %'])
***
```

### Charge Control

To check the steady-state charge performance of the EC's, ensuring that the net energy transferred during each cycle is zero, the "Charge Control" parameter is calculated. For each cycle, the average EC voltage is calculated and compared to the initial voltage. These values are then compared to each other, to check if or when they reach a steady-state value. For example, a sequence [90 80 75 70]% means that the average value of the EC's are monotonically decreasing and not reaching a steady-state value in four cycles. In contrast, a sequence [95 89 88 88]% shows satisfactory operation, where steady-state values are reached and the level is in the upper region (where the EC's are charged).

In Matlab, the calculations are performed using the following sequence. (extracted from `p_proc.m` in Appendix A)

```
***
%Charge capacity. This parameter is the mean value of the EC-voltage
%compared to the reference voltage.
for k=1:Num_cycle
    v(k)=mean(U_cap((k-1)*195+1:k*195/time_step_real));
    ch(k)=v(k)/V_init_cap.*100;
end
***
```